1

AFIT/GE/ENG/92D-11

CEPSTRAL AND AUDITORY MODEL FEATURES FOR SPEAKER RECOGNITION

THESIS

John M. Colombi
Captain, USAF

AFIT/GE/ENG/92D-11

612225

126

Approved for public release; distribution unlimited

AFIT/GE/ENG/92D-11

CEPSTRAL AND AUDITORY MODEL FEATURES FOR SPEAKER RECOGNITION

THESIS

Presented to the Faculty of the School of Engineering
of the Air Force Institute of Technology
Air University
In Partial Fulfillment of the
Requirements for the Degree of
Master of Science in Electrical Engineering

John M. Colombi, B.S.E.E.
Captain, USAF

December 1, 1992

Acknowledgments

I wish to thank my thesis committee with their diverse backgrounds and individual contributions. Individual thanks to Dr. Steven Rogers for his unique approach and guidance. It has been said he expects and demands *nothing ...but best from you*. I truly enjoyed the material within this thesis, thanks to him. I must personally give thanks to Dr. Tim Anderson whose expertise on auditory models and whose frequent discussions and daily interactions made this thesis a pleasure. His computer and disk resources, and my allowed control over them, were invaluable. Thanks also to the other professors who lent consideration, expertise and valuable insight. I must finally thank my (usually understanding) wife Cheryl, who managed to juggle work, school and two adorable children. She will always be my inspiration.

John M. Colombi

Table of Contents

Page

Page

List of Figures

Figure Page

List of Tables

Table Page

AFIT/GE/ENG/92D-11

Abstract

The TIMIT and KING databases, as well as a ten day AFIT speaker corpus, are used to compare proven spectral processing techniques to an auditory neural representation for speaker identification. The feature sets compared were Linear Predictive Coding (LPC) cepstral coefficients and auditory nerve firing rates using the Payton model. This auditory model provides for the mechanisms found in the human middle and inner auditory periphery as well as neural transduction. Clustering algorithms were used successfully to generate speaker specific codebooks - one statistically based and the other a neural approach. These algorithms are the Linde-Buzo-Gray (LBG) algorithm and a Kohonen self-organizing feature map (SOFM). The LBG algorithm consistently provided optimal codebook designs with corresponding better classification rates. The resulting Vector Quantized (VQ) distortion based classification indicates the auditory model provides slightly reduced recognition in clean studio quality recordings (LPC 100%, Payton 90%), yet achieves similar performance to the LPC cepstral representation in both degraded environments (both 95%) and in test data recorded over multiple sessions (both over 98%). A variety of normalization techniques, preprocessing procedures and classifier fusion methods were examined on this biologically motivated feature set.

This thesis provides the first comparative analysis between conventional signal processing and neural representations on the same speaker utterances. It also provides the first classification results using a speaker corpus of non-studio quality, specifically KING. Lastly, the effects of multiple session training time for speaker recognition using an auditory model is precedent.

CEPSTRAL AND AUDITORY MODEL FEATURES FOR SPEAKER RECOGNITION

I. Introduction

1.1 Background

Accurate and robust speech recognition has evaded researchers for over four decades. The ability to effortlessly communicate with our growing computer environment has attracted a large body of research internationally. One particular aspect of this problem is automatic speaker recognition (ASR). Speaker recognition is defined as the ability to recognize individuals only by the received acoustic speech signal. The technologies which support this goal would allow identification or verification of individuals in such applications as DoD surveillance, forensic data, and secure facility access. Adaptation to individual speech patterns may also prove useful in improved speech processing.

1.2 Problem

This thesis will investigate the use of an auditory model as features to perform improved speaker identification, especially in degraded, noisy environments. Current proven methods use linear predictive analysis, which creates a parametric model of speech production [8, 10, 12, 13, 22, 76, 94, 95, 101, 118]. These techniques are not robust in noise since the models' inherent assumptions are violated [80]. As an alternative, an auditory model will be evaluated as a feature extraction preprocessor. The digitally sampled speech is input to the model whose output is auditory nerve firing patterns. These firing patterns will subsequently be used as multi-dimensional features. This research will provide a quantitative evaluation of experiments involving transformations, clustering, and classification capabilities of these unique patterns. A comparative examination to proven spectral and linear predictive pre-processing methods for text-independent speaker identification will be accomplished.

1.3 Assumptions

The hypothesis which underlies this research is that an auditory neural representation contains speaker dependent information, either instantaneously or through temporal patterns, as well as providing adequate resolution of this information. The human auditory system performs both types of processing. The cochlea encodes received information based on frequency analysis (frequency or place theory) as well as temporal patterns of the stimulus (temporal theory) [70, 71]. This is accomplished by the location of neurons along the basilar membrane as well as the synchronization of their firing. Current methods of speaker identification often perform a linear predictive analysis on the speech signal. This process fits a linear all-pole model to the speech production [67, 80]. However, this model, which accounts for the speakers' vocal tract and other speech production apparatus is directly speaker dependent. The frequency analysis capabilities of the auditory model may not contain the necessary resolution for speaker dependence.

1.4 Scope

The TIMIT and KING databases, as well as an AFIT recorded corpus, are used to compare and analyze proven spectral processing techniques to an auditory neural representation for speaker recognition. The primary contribution provides measures of an auditory model representation to contain speaker dependent information. The ability of these features to generalize for added noise and intra-speaker distortions will be experimentally evaluated.

1.5 Approach /Methodology

This thesis initially investigates popular Linear Predictive Coding (LPC) Cepstral processing on the DARPA TIMIT Phonetic Speech Database. Various Vector Quantization (VQ) classification techniques were evaluated to create a quantitative baseline. Varying degrees of additive white Gaussian noise added to the speech utterance were incorporated in this baseline. An auditory model proposed by Payton will be used to extract auditory nerve firing rates with the same VQ distortion metrics used for classification. These quantizers include the recursive Linde-Buzo-Gray splitting technique and various configurations of Kohonen's Self Organizing Feature Maps. This research will use the hypothesis that long-term averages of the short-term spectrum contain speaker dependent information [113]. Experimentation will investigate various temporal characteristics [114] of the speech signal using a simple difference procedure [56]. Lastly, classification fusion techniques will determine correlation of classification errors between the various features. These results will determine the measure of speaker dependent information of a neural auditory model, in conjunction with clustering analysis and artificial neural networks, to improve performance of speaker identification.

1.6 Conclusion

This thesis will first provide the significant background on this multifaceted problem. Speech and speaker recognition can include such diversive areas as signal processing, linear modeling and mathematics, physiological and psychological theories, biology, and pattern analysis. Chapter II provides an historic synopsis of key techniques examined, with a major source of information extracted from the recent International Conference of Acoustics, Speech and Signal Processing (ICASSP) proceedings. The chapter will examine the analysis of feature extraction by spectral and linear processing models, summarize vector quantization techniques and their related distortion based classification metrics for speaker identification, and lastly detail the Payton auditory model. Methodology, experimentation and results are contained in Chapters III and IV. Chapter V provides pertinent conclusions and analysis. For additional information on the human auditory periphery and its quantitative analysis, refer to Appendix A.

II. Literature Review

2.1 Introduction

Automatic Speaker Recognition (ASR) is one of many emerging technologies which will support an effortless and natural interaction with the growing computer environment. Though many techniques have publicized remarkable accuracies, they are typically limited by size of speaker populations, small vocabularies or restricted sentences, and noise-free environments (see Table 2). One model which may overcome the current limitations in noise of speaker recognizers is based on the human auditory system; such models have demonstrated improvements for speech recognition [5, 7, 37, 38]. This review examines the achievements in Automatic Speaker Recognition.

Speaker recognition is often defined in two separate categories: speaker verification (authentication) and speaker identification. Verification, the easier of the two, is a process whereby a recognizer provides a decision to accept or deny a claim of identity by an unknown individual. This is attempted solely by analysis of a speech utterance, either specific text (text-dependent) or non-prompted (text-independent) speech. Identification is the process of choosing the identity from a known population of many speakers; as well as responding appropriately to an unknown individual not contained in this set. This review will clarify the multiple classification and clustering techniques, as well as detail some of the current features extracted from the speech signal.

In a recent *I.E.E.E. Proceedings* article, C. Weinstein discusses the opportunities for advanced military applications based on speech technologies. These opportunities include military security, advanced battle management, advanced pilot cockpits and improved air traffic control training [121]. He states that current speaker recognition research is focusing on the difficult text-independent problem, with the goal of achieving higher performance in noise and communications channel degradation. Others point out that biometric features such as fingerprints, hand geometry, or retinal images can be recognized, as well as an individual's unique activities, such as handwriting, keyboard typing, or speech [72]. Results have also been reported on recognition of individuals by their face images [116, 119]. Speaker recognition can also be directly applied to speaker selection or adaptation, so as to improve *speech* recognition techniques [32]. Lastly, it has been said that humans are unable to appreciate the difficulties that speaker recognition poses for a computer, since humans comprehend speech so easily [58].

First, this review will discuss the various features often extracted from the speech signal. In the following sections, details on the current classification and clustering paradigms will be presented, focusing on vector quantization (VQ) techniques and including the popular Hidden Markov Model and Artificial Neural Networks (connectionist) paradigms. Lastly, some recent representations using auditory models for speech recognition and details concerning the Payton model are examined.

2.2 Feature Extraction

A tight coupling exists between a feature extractor and the recognizer or classifier; it is often said a good classifier has goods features. In attempting to recognize an individual using acoustic features, many current strategies for clustering are inherently based on some preprocessing of the received acoustic waveform [10].

An historic synopsis of feature extraction techniques for speaker identification is provided both by Parsons [80] and ITT [59], with references unexpectedly dating back to 1954. Such features either attempt to model the "individual differences in vocal tract anatomy" or on personal articulation habits. Parsons [80] details work by Wolf (1972) and Sambur (1975). Wolf researched spectral characteristics of nasal consonants, fricatives, and vowels, as well as pitch and vowel durations. Sambur, using the same speech database examined formant frequencies, LPC based poles, pitch and some specific temporal characteristics. Both achieved high accuracies, yet with limited speakers and "high" signal-to-noise ratios [80:Chapter 12].

In the literature, such preprocessing has included Linear Predictive Coding (LPC), mel frequency energies, line spectral pairs, cepstrum coefficients and LPC cepstrum, in addition to various polynomial expansions and derivatives over time. These have each been shown to be successful feature sets, for various speech processing applications. Table 1 provides a synopsis of speech pre-processing examined over the past twenty years.

Table 1. Feature Extraction Examples for Speaker Recognition

Feature	Author (Date)	Comments
Filterbanks	Pruzansky (1963, 1964)	100Hz - 10KHz, various averages of (and between several) filterbank outputs over time were examined [80].
Spectral Characteristics	Wolf(1972)	Nasal consonants, fricatives, vowels, pitch and vowel duration [80].
Pitch Contours	Atal(1972)	Karhunen-Loève transform on pitch contours [80].
Filterbank Correlation	Li and Hughes(1974)	Correlations among filterbank energies [80].
LPC Cepstral	Atal(1974, 1976)	Comparison to log-area ratios, correlation coefficients, LPC coefficients [8, 10].
Spectral Characteristics	Sambur(1975)	Formant frequencies, LPC Poles, pitch, some temporal patterns [80].
Formants	Goldstein (1976)	Vowels, 199 ranked features [80].
Linear Prediction	Sambur (1976)	LPC, reflection, log-area ratios, found orthogonal reflection coefficients best (least significant projections) [80].
Long-Term Statistics	Markel (1977, 1979)	Mean and standard deviation of pitch, reflection coefficients [80].
Mel Cepstral	Davis and Mermelstein (1980)	Cosine expansion of the spectrum, comparison to linear and LPC cepstral [19].
Delta Cepstral	Furui(1981)	Polynomial expansion over time [22].
Log Area Ratios	Schwartz(1982)	Examined different classifiers using spectral log area ratios [105].

Table 1. (cont'd) Feature Extraction Examples for Speaker Recognition

Feature	Author (Date)	Comments
LPC Cepstral	Oglesby and Mason (1990)	10th order LPC derived cepstral [76].
Line Spectral Pair	Liu(1990)	Several variants of LSP - Even, Odd, Mean and Difference of LSPs [62].
Mel Cepstral and LPC	Bennani (1990)	12th order LPC and Mel Frequency Cepstral, based on 24 triangular filters [12].
LPC Cepstral	Gaganelis and Frangoulis (1990)	10th order LPC [23].
Delta LPC Cepstral	Furui (1991)	LPC cepstral, first order regression every 88 msec period [69].
Delta Cepstral /Cepstral	Rosenburg (1990, 1991)	12th order cepstral and delta-cepstral coefficients, weighted using a sinusoidal "lifter" [94, 95].
Mel Cepstral	Oglesby and Mason (1991)	12 filterbanks, Mel frequency spaced [77].
Eigenvector Analysis	Bennani (1991)	LPC and Mel cepstrum covariance, mean and two eigenvectors [13].
Filterbanks	Higgins (1991)	Power output of 14 uniformly spaced frequency banks [35].
Auditory Model	Hattori (1992)	Seneff auditory model mean rate response, 40 channels [32].
Delta Cepstral /Cepstral	Tseng et al (1992)	Linear combination of cepstral and delta cepstral. Found cepstral alone performed better recognition [118].
LPC Cepstral	Savic and Sorensen (1992)	20th order cepstral derived from only 12th order LPC [101].

2.2.1 Linear Prediction Analysis When disregarding the nasal tract and associated sounds, speech production can be accurately modeled by an all-pole filter excited by either a semi-periodic impulse train or white gaussian noise. This model makes some assumptions, but provides a simplified and fairly accurate model of voiced utterances. Thus, LPC analysis creates a series of representative coefficients which can subsequently be passed to a classifier. A good review with mathematical formulations and examples of LPC is provided by Atal [9] and Makhoul [67]. These features have experienced great use in vector quantization, discriminant analysis and neural network approaches toward speech and speaker recognition. However, there is serious limitations in their use in noise, as Parsons points out,

> When the speech signal is corrupted by noise, the assumptions of the all-pole model are violated and the quality of the estimate suffers. Low signal-to-noise ratios (e.g., below 5 to 10 dB) can cause serious distortion of the model spectral density [80:page 165].

2.2.2 Cepstrum Analysis Most recent research has relied extensively on cepstrum coefficients and cepstrum derivatives. The theory behind this feature space for speaker recognition is reviewed.

2.2.2.1 Power Cepstrum The cepstrum or power cepstrum is defined as the power spectrum of the logarithm of the power spectrum of a function [16]. In 1977, Childers further describes this representation's usefulness.

> In practice the power cepstrum is effective if the wavelet and the impulse train, whose convolution comprise the composite data, occupy different quefrency ranges.

The authors use the term wavelet to denote some original signal (potentially with echoes or reverberations) and quefrency is the coinage for the units of the cepstral spectrum.

This description is directly applicable to our model of speech production. We will usually concern ourselves with short sequences of framed speech data, $s(n)$. This signal can be considered the convolution of an excitation signal, $g(n)$, with a transfer function of the vocal tract, $h(n)$. At time t,

$$s(n,t) = \sum_{k=-\infty}^{t} g(k)h(n-k) \tag{1}$$

Taking the Fourier Transform, the spectrum is as follows.

$$S(w,t) = \sum_{k=-\infty}^{\infty} s(k,t)e^{-jwk} \tag{2}$$

The inverse Fourier Transform of the log magnitude spectrum provides,

$$\log|S(w,t)| = \sum_{k=-\infty}^{\infty} c_k(t)e^{-jwk} \tag{3}$$

where $c_k(t)$ is the k^{th} cepstral coefficient at time t.

It is noted the second transform has been described as both the forward transform [16, 28, 80] as well as the inverse transform [10, 114], as shown above. However, since Equation 3 produces a real and even function, the sign of the complex exponential is irrelevant. By separating the complex exponential into real and imaginary components, this fact is evident.

$$\log|S(w,t)| \;=\; \sum_{k=-\infty}^{\infty} c_k(t)\cos(wkt) \pm j \sum_{k=-\infty}^{\infty} c_k(t)\sin(wkt) \tag{4}$$

However, the second summation, being an odd function, sums to 0 over these limits.

$$\log|S(w,t)| \;=\; \sum_{k=-\infty}^{\infty} c_k(t)\cos(wkt) \tag{5}$$

Soong [114] references that a finite order of terms can be used in a Discrete Cosine Transform (DCT) for this representation. He also remarks that since the covariance of these cepstral coefficients is diagonal dominant, they are very similar to a Karhunen-Loève (KL) Transform.

Figures 1, 2, and 3 shows the above process on a sample of speech. The samples correspond to a vowel by a male speaker [1]. In performing the second transform, in general,

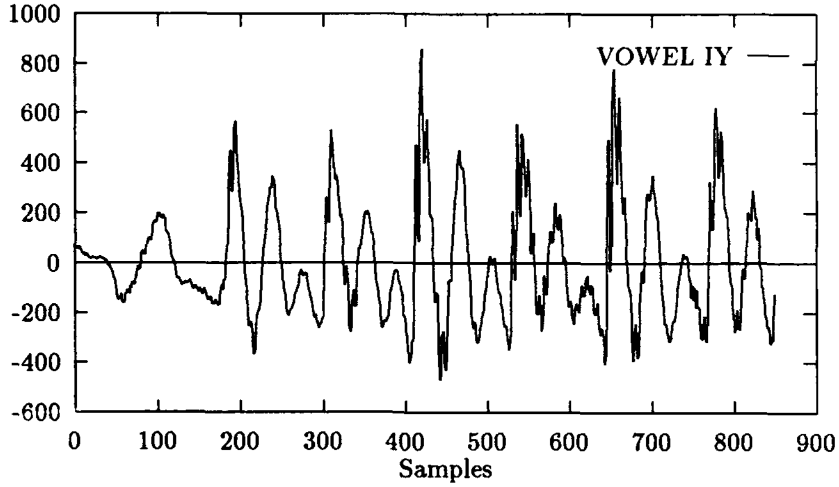

Figure 1. Sample Speech (Vowel IY, male speaker)

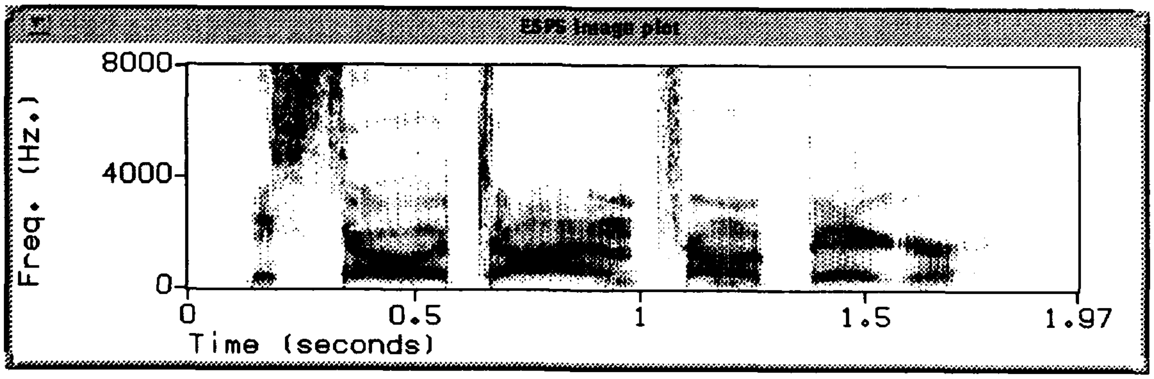

Figure 2. Sample Spectrum. The previous samples correspond to the first voiced region, at approximately 0.2 sec.

the slow moving transfer function is separated from the higher fundamental frequencies of

[1] It should be pointed out, that based on a sampling rate of 16 KHz, one can easily calculate the pitch of the unknown speaker, as shown in Figure 1. The fundamental frequency (pitch) in this waveform is approximately 140 - 150 Hz (110 samples).

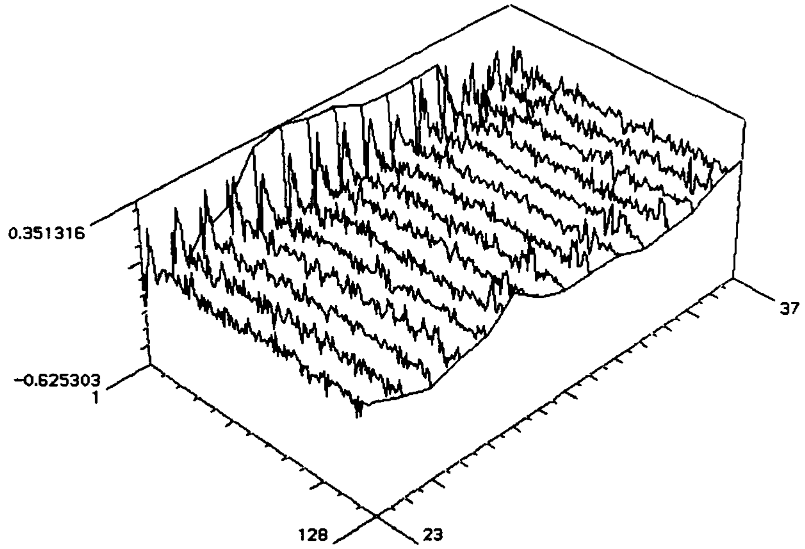

Figure 3. Sample 8th order Power Cepstrum (128 coefficients) of the referenced voiced samples. The plot shows consecutive 16 msec frames calculated every 5.33 msec during the phoneme IY.

pitch and formant within the cepstral spectrum. Also, the fundamental frequency (pitch) and the various harmonics (formants) usually present themselves dominantly in clean, noise-free speech [80]. In hardware implementations of feature extraction, often a bank of N linear bandpass filters across the spectrum will provide energy values. These can then be Fourier transformed to acquire cepstral coefficients very efficiently.

The use of cepstrum coefficients has also seen applicability in such areas as radar, sonar, marine and earth seismology, speech processing, image processing and even old audio recording restorations [16]. In general, the cepstrum serves in echo cancellation and in the deconvolution of two signals, usually some original signal and a train of impulses. This allows easy implementation toward speech processing since the cepstrum's deconvolution capability can be used to separate the impulse train of the glottis from the vocal tract transfer function. Thus, it is often used to model the vocal tract, and resonant frequencies or formants. For speaker recognition, the entire cepstral signal will be used, to extract both glottal and vocal tract information.

2.2.2.2 Mel-Scale Cepstrum This cepstral representation is considered Mel-Frequency Cepstral if the spectrum is warped before the second (inverse) Fourier transform. Additionally, if a filterbank approach is used, these bandpass filters are spaced with appropriate bandwidths according to a "mel" non-linearity. Mel or bark scale approximates the resolution of the human auditory periphery. Mel Frequencies utilize a linear scale up to about 1 KHz and logarithmic thereafter. Thus, the individual bandwidths of these filters would increase. The mel-scale can be approximated by,

$$Mel = (1000/\log(2))\log(1 + freq/1000)$$

[80] and is plotted in Figure 4. Another derivation is the bilinear transform. This transformation is referenced in Kai-Fu Lee [56], crediting Shikano's application of Oppenheim's transform. Lee describes this transform, an all-pass filter, as follows,

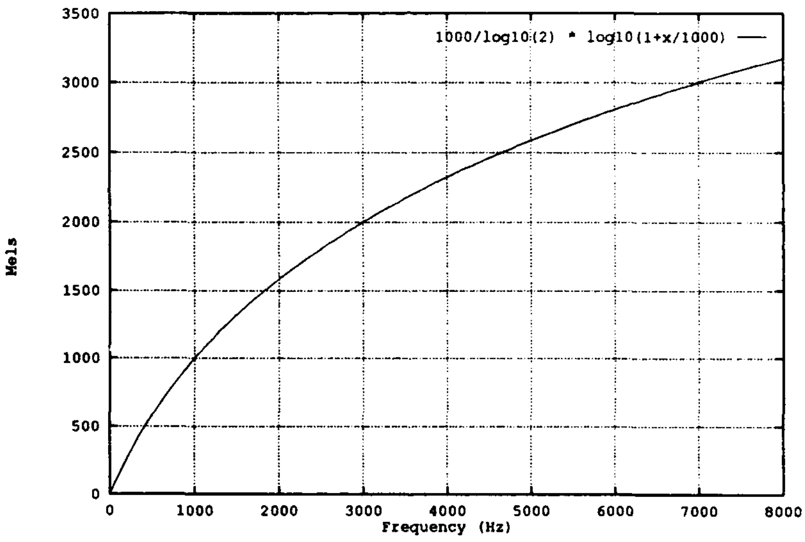

Figure 4. Mel Frequency Scale [80]

$$\begin{aligned} z^{-1}_{new} &= \frac{(z^{-1} - a)}{a - az^{-1}}, (-1 < a < 1) & (6) \\ \omega_{new} &= \omega + 2\tan^{-1}(\frac{a\sin\omega}{1 - a\cos\omega}) & (7) \end{aligned}$$

where ω_{new} is the converted warp·d frequency and positive a lengthens the low frequency axis. His SPHINX [56] spee h recognition system uses a value of .6 for a, which is comparable to the mel scale. Davis and Mermelstein [19] compared several cepstral representations for speech recognition and found Mel Cepstrum superior to linear frequency cepstral and linear prediction cepstral. A recent AFIT thesis by Rathbun [86] examined the Davis and Mermelstein representations including Mel Frequency cepstral, linear cepstral, linear predictive cepstral and various first derivatives over time of these features in two dimensions. These two dimensional representations were used in speech recognition experiments.

2.2.2.3 Complex Cepstrum The complex cepstrum, since is maintains all phase information, can be used to reconstruct the original signal, often after filtering (liftering) is performed in the cepstral domain. The complex cepstrum is defined as the inverse Fourier-transform of the complex logarithm of the Fourier-transform of the original function. The term "phase unwrapping" is used when performing this analysis. The approach in performing a logarithm on complex data is to separate the complex quantity into a magnitude and phase component phasor. A two dimensional implementation of this technique was recently documented in AFIT thesis by Lee [57] in performing VLSI image processing. This representation's usefulness for speech or speaker recognition has not been determined.

2.2.2.4 Linear Predictive Cepstrum In 1974 *J.A.S.A.* article, B.S. Atal defines the cepstrum as the inverse Fourier transform of the logarithm of the transfer function [8].

$$\ln H(z) = C(z) = \sum_{k=1}^{\infty} c_k z^{-k} \tag{8}$$

Recall that a linear predictive analysis on speech samples attempts to fit the p all-pole filter defined as,

$$H(z) = \frac{G}{1 + \sum_{k=1}^{p} a_k z^{-k}} \tag{9}$$

It can further be shown, based on this all-pole model for H(z), a recursive relation between the cepstral coefficients c_k and the prediction coefficients a_k. By taking the derivative of

(8), the cepstral coefficients can be derived by,

$$c_1 = a_1 \tag{10}$$

$$c_k = \sum_{l=1}^{k-1}(1 - l/k)a_l c_{k-l} + a_k . 1 < k \leq p \tag{11}$$

The benefit readily seen through this technique is the reduction in the feature space dimension. In using FFT or DFTs, the number of coefficients in the output is based on the order of the FFT , 2^{order}. Whereas, in Atal's method, the number would be based on the number of p poles. Parson's gives a rule-of-thumb for the number of poles p [80].

$$p = \frac{f_s}{1000} + \gamma \tag{12}$$

where f_s is the sampling frequency of the original data and γ is a "fudge constant" which is typically 2 or 3 for adding extra poles to the model for flexibility. An example of LPC cepstral is shown in Figure 5. Note the LPC representation provides the overall shape of the previous linear cepstral representation.

This feature set is found extensively in the current literature. Most often, the LPC coefficients are first obtained, then transformed to cepstral coefficients. Atal [10] had compared LPC coefficients, log area ratios, correlation coefficients and LPC cepstral and, for a limited speaker database, had shown this representation to provide better speaker recognition. Interestingly, Atal found that the Mahalanobis distance measure proved a most effective distance metric between the LPC cepstral vectors. Soong and Rosenburg [114] have shown that the higher order coefficients carry as much information as the lower order coefficients, in achieving speaker identification. Since these coefficients have numerically smaller values and provide less contribution, it was deemed appropriate to weight them based on the inverse covariance of each coefficient. This technique is known as "weighted cepstral distance." Thus, the Mahalanobis distance measure has proven effective in speaker recognition experiments.

Atal had also demonstrated that subtracting off the time averages of each coefficient can remove induced channel characteristics, caused by different recording equipment or

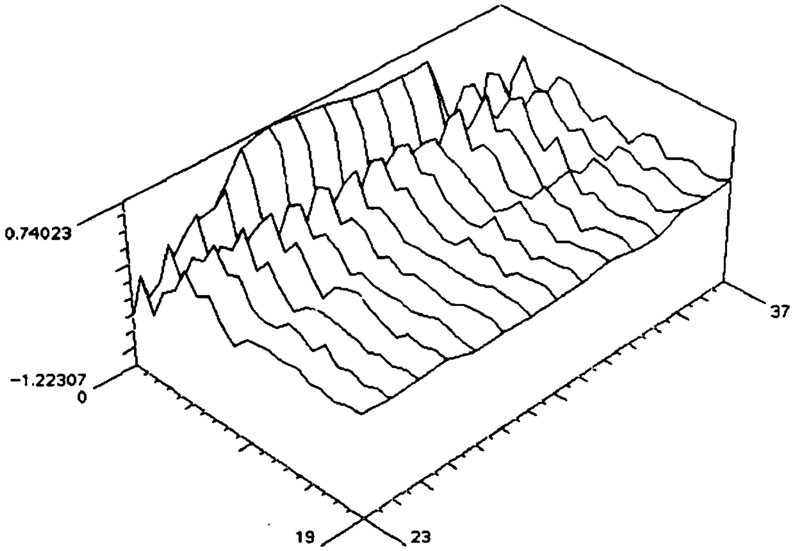

Figure 5. 20th order LPC Cepstral using. Note pertinent spectral shape information of the power cepstrum. The plot shows consecutive 16 msec frames calculated every 5.33 msec during the phoneme IY.

communications channels. One of the underlying characteristics of cepstrum analysis is that convolutions in the time domain correspond to additions in the cepstral spectrum, made possible by the log operation. Thus, transmission induced distortions (convolution in time) which are approximated as time averages of cepstral coefficients can be removed via subtraction [8].

2.2.2.5 Cepstral Expansions In signal processing, often the temporal characteristics of the signal contain useful information. This has been shown to be especially true in speech processing. One simple example is the speech spectrogram, where the horizontal formant track over time depicts various consonant vowel relations. These temporal characteristics of speech also contains speaker dependent information, for use in speaker identification. Furui [22] has shown that polynomial expansions of the cepstral time signals increase speaker identification performance. He examined time average, slope and curvature of the cepstral coefficients using a 90 msec window (9 - 10 msec frames) using the following transformation.

$$\begin{aligned} P_{0j} &= 1 && (13)\\ P_{1j} &= j-5 && (14)\\ P_{2j} &= j^2 - 10j + 55/3 && (15) \end{aligned}$$

Then, a window of 9 vectors, $c_j : (j = 1,2,\ldots 9)$, can be represented by three projection coefficients. The first order polynomial gave the greatest classification improvement.

$$\begin{aligned} a &= (\sum_{j=1}^{9} c_j)/9 && (16)\\ b &= (\sum_{j=1}^{9} c_j P_{1j})/\sum_{j=1}^{9} P_{1j}^2 && (17)\\ c &= (\sum_{j=1}^{9} c_j P_{2j})/\sum_{j=1}^{9} P_{2j}^2 && (18) \end{aligned}$$

Note, the first order can be generalize as a linear regression coefficient over the interval $2K + 1$ [56, 114]. This representation is often referred to as *delta cepstrum.*

$$r_j(t) = (\sum_{k=-K}^{K} kc_j(t+k))/\sum_{k=-K}^{K} k^2 \tag{19}$$

Soong [114] later demonstrated that transitional patterns contain uncorrelated information to that of instantaneous cepstral representations, and also showed better resistance to channel characteristics. Lee, [56] in preliminary tests for the SPHINX system, settled on only *differenced* coefficients using a 40 msec window, symmetric with $\pm\delta = 20$ msec from the current frame. The mth differenced (or delta) coefficient at time t is simply,

$$d_m(t) = c_m(t+\delta) - c_m(t-\delta) \tag{20}$$

2.3 Classification and Clustering

The end goal for Automatic Speaker Recognition is a reliable decision of an unknown individual's identity. This section details the numerous ways that classification of a speaker is currently being attempted. Classification is the process of choosing the most probable, or closest class, by the individual's features from a set of reference features or models. By grouping a set of related features to a labeled entity, one forms a class. Currently, classification can best be divided into pattern matching paradigms, model estimation techniques (such as Hidden Markov Models), and Artificial Neural Networks (ANN). This representation is depicted in Figure 6. Gaganelis and Frangoulis state a key introductory point,

> Speaker Verification systems rely often on techniques developed for Speech Recognition. Techniques like Dynamic Time Warping, Vector Quantization, Hidden Markov Modeling, Clustering and Linear Discriminant Analysis are featured in many systems [23].

The following sections will present many of these techniques for classification and clustering; however, it must be pointed out, there exhibits a great deal of overlap between all these approaches. Table 2 lists the many classification paradigms examined over the past several years.

2.3.1 Vector Quantization and Distortion Based Classification Though often used as a communications coding scheme [15], vector quantization (VQ) has proven a computationally efficient and simple scheme for pattern classification using an appropriate distortion measure. Vector quantization or clustering analysis determines the optimal representative k codewords which represent p data points. This procedure creates a codebook, A_k a finite collection of codewords, which can be used for information coding or classification Classification is performed by measuring a distortion between the unknown test speaker and the reference speaker codebooks. The optimal codebook to be created, however, relates to a particular set of criteria chosen, and in general, will present itself as an optimization problem with multiple local minima [124].

A recent article critique points out the subtle, yet important similarities between vector quantization and cluster analysis. Vector quantization, an electrical engineering concept, attempts to define the best representation or partitioning of data, often used for communications data reduction or coding. Cluster analysis is a statistical mathematics discipline which further processes the parametric details of these partitions. This thesis re-

Table 2. Classification Techniques for Speaker Recognition

Classifiers	Author (Date)	Speakers, ID %, Comments
Distortion	Atal (1974)	10 speakers, 98% identification, Mahalonobis Distance using pooled intra speaker covariance [8].
DTW	Furui (1981)	20, Dynamic Time Warp distortion measurement on fixed sentences [22].
K-means, Gaussian Estimation	Schwartz (1982)	Compared Gaussian classifiers to K-means and Mahalonobis Distance, non-parametric outperformed [105].
HMM	Poritz (1982)	Application of 5 state ergodic HMM to speaker verification [83].
VQ	Soong (1985)	First Speaker dependent codebooks, voiced and unvoiced speech [113].
VQ	Soong (1988)	2 Codebooks, 1 instantaneous and 1 temporal [114].
MLP	Oglesby and Mason (1990)	10, 92%, Backprop learning, single layer with 16 - 128 hidden nodes, Equal recognition to VQ s5.1.10.
K-means/ LVQ	Bennani et al (1990)	10, 95 - 97% [12].
HMM	Rosenburg et al (1990)	20, 98.8 - 99.1%, Used k-means to segment the utterance into acoustic segment units, also examined phonetically labeled speech [94].
HMM	Savic and Gupta (1990)	43, 97.8%, 5 HMM models representing broad classes [102].
GMM	Rose and Reynolds (1990)	12, 89%, Only 1 sec of test speech [93].

Table 2. (cont'd) Classification Techniques for Speaker Recognition

Classifiers	Author (Date)	Speakers, ID %, Comments
Binary Partition	Rudasi and Zahorian (1991)	47, 100%, TIMIT corpus, need N(N-1)/2 binary MLP classifiers.
RBF NN	Oglesby and Mason (1991)	40 , 89% true talker, different mannerisms of speech.
GMM	Rose et al (1991,1992)	10, 77.8%, Integrated noise model into GMM, GMM on Original clean speech - 99.5%.
Discriminator Counting	Higgins and Bahler (1991)	24, 80% true talker, KING corpus, multivariate gaussian, count wins/speaker summed over frames.
VQ	Matsui and Furui (1991)	9, 98.5 - 99.0 %, Voice/Unvoiced or 2-state HMM, New Distortion measure (DIM), Talker variability normalization (TVN) individually weights features.
HMM	Rosenburg (1991)	20, 96.5 - 99.7%, Whole word L-to-R HMM, text dependent (digits), compared to VQ.
Time Delay NN	Bennani and Gallinari (1991)	20, 98%, First a Male / Female TDNN, then a 10 output (speakers) TDNN using 2 hidden layers (hierarchical).
HMM, VQ, ANN	Hattori (1992)	24, 100 %, TIMIT corpus (females), Predictive NN (recurrent) within HMM, compared to VQ and MLP classifiers.
CPAM (GMM)	Tseng et al (1992)	20, 98.3% identification, CPAM - Continuous Probability Acoustic Map, mixtures of Gaussian kernels with and without HMM.
MLP	Gong and Haton (1992)	72, 89 - 100%, Trained MLP to interpolate between speaker utterances (phoneme), needs labeled speech (vowels).
VQ	Kao et al (1992)	26 (51), 93.3% (67.6), KING corpus, 11 broad class codebooks of 10 vectors, Needs labeled speech.

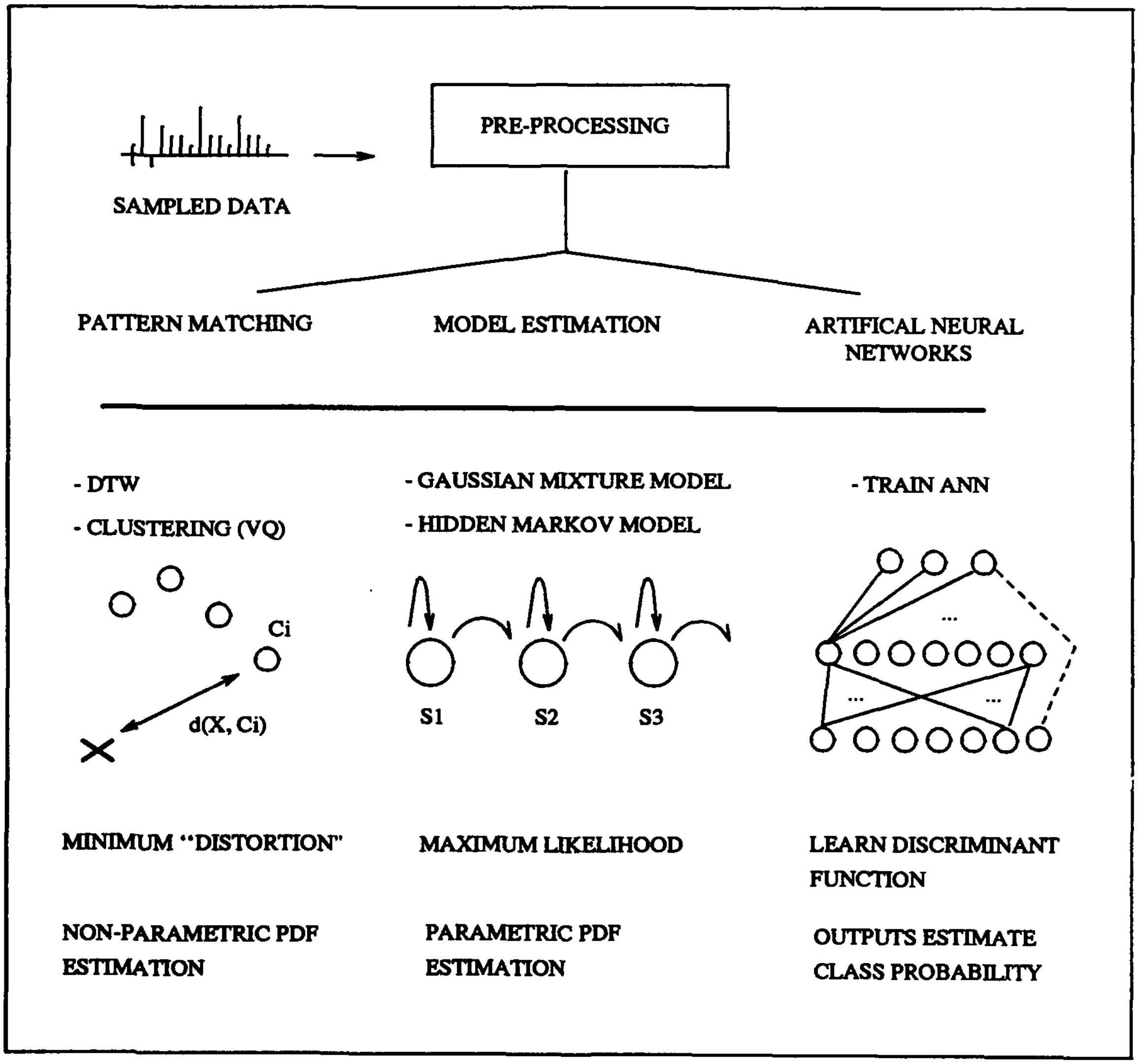

Figure 6. Speaker Recognition Classification Paradigms.

gards all techniques from both disciplines as (iterative) means to the optimal representation of the underlying probability density function of some unknown random process.

2.3.1.1 Objective Function and Necessary Criteria The objective of this quantization design procedure solves for the global minima of some objective function, typically least mean squared error. Bezdek [14] defines this distortion function as,

$$J_1(U,Y;X) = \sum_{i=1}^{p} \sum_{j}^{k} u_{ij}(\|x_i - y_j\|_I)^2 \tag{21}$$

where, X and Y are the set of training data $\{x_1, \cdots, x_p\}$ and codewords $\{y_1, \cdots, y_k\}$ respectively, U contains the membership values of each x_i to the codeword y_j, and $\| \cdot \|_I$ is typically the Euclidean norm on the X space. A vector quantizer is said to be optimal if no other quantizer has a smaller overall distortion. The two necessary conditions for optimality [126] are

1. Nearest neighbor: A training vector is mapped to the "nearest" codebook vector, based on a particular distortion metric. If the codebook contains k vectors, this mapping results in a partitioning of the input space into k regions [126, 51, 53].
2. Centroid. The codevector for a given partition is the mean or expected value of the partitions' elements.

For LBG and k-means [117], the memberships u_{ij} are defined by nearest neighbor and take on values of 0 or 1. By extending this membership to the continuous interval $[0, 1]$, fuzzy set theory is applied to clustering [14, 41, 108].

2.3.1.2 Modeling the Density Function Vector quantization produces an approximation to the continuous pdf, $p(x)$, of a variable x in R^n using a finite number of k codewords [51, 53]. Optimality of this approximation refers to minimizing an error function such as,

$$E = \int \|x - m_c\|^r p(x) dV_x \tag{22}$$

where m_c is the "best-matching" codeword and dV_x is an incremental volume in the R^n space. As previously stated, there are no closed form expressions for the placement of the

k codewords, and iterative or learning schemes are used. If $p(x)$ were known, numerical and statistical techniques could directly determine centroids, number of classes and class boundaries [21, 53]. Kohonen references the fact that the point density function of the k vectors approximates the true pdf as the ratio of data dimensionality over distortion metric increases.

2.3.1.3 The Classic Linde-Buzo-Gray Algorithm Many new clustering techniques (as well as neural techniques) compare their classification capability to the Linde, Buzo, Gray (LGB) [60] algorithm, also known as the Generalized Lloyd algorithm. This algorithm processes the training data, by epoch, iteratively splitting converged codewords. Inherently, it reduces a mean squared error objective function among all its clusters, by performing a Nearest Neighbor calculation, at each iteration. Linde et al states that no assumptions of the actual data distribution are being made, such as differentiability, and this technique is valid for discrete data. The original discussion defines techniques for a known distribution, an unknown distribution (with initial codebook) and an unknown distribution based on recursive splitting. This latter is described. For a final codebook with N codewords containing incrementally M vectors having a reconstruction error D_m, the procedure is as follows.

1. Initialize:

   - Set N; $M = 1$; Set overall distortion $D_0 = \infty$ (a large number); set iteration $m = 0$.
   - Define a conversion threshold ϵ, which defines stopping criteria for a given level.
   - Initial codebook $\hat{A}(1) = \bar{x}$ where this initial codebook contains the centroid of the training sequence.

2. Split:

   - Given $\hat{A}(M)$ which contains M codewords $\{y_i : i = 1 \ldots M\}$, split each codevector y_i into a $y_i + \delta$ and a $y_i - \delta$, where δ is defined as "a fixed perturbation vector".
   - $M = 2M$.

3. Nearest Neighbor Partition:

   - For training set $\{x_j : j = 1 \ldots p\}$, perform a Nearest Neighbor calculation, like k-means, by determining the minimum distortion partitions or clusters $\{S_i : i = 1 \ldots M\}$. These sets contain the training vectors such that $x_j \in S_i$ if $d(x_j, y_i) \leq d(x_j, y_l) \forall l \neq i$.

- Calculate distortion over entire training set.

$$D_m = \frac{1}{p}\sum_{j=1}^{p} \min_{y\in \hat{A}_m(M)} d(x_j, y). \tag{23}$$

4. Check Convergence:

   - If $(D_{m-1} - D_m)/D_m \leq \epsilon$, stop with $\hat{A}_m(M)$ being the final converged reproduction codebook for the current level. Else, $m = m + 1$, Go to Recompute Centroids.
   - If $M = N$ Stop. Else, Go to Split.

5. Recompute Centroids: Recalculate the centroids as the mean of the current partitions, S_i. The authors [60] write this as,"Find the optimal reproduction alphabet."

$$y_i = \frac{1}{|S_i|}\sum_{x_i\in S_i} x_i \tag{24}$$

More recently, competitive learning approaches have been developed which allow a codebook to learn on-line, as training data is presented [53]. Such examples include adaptive k-means, competitive learning schemes, and specifically the self-organizing feature maps by Kohonen [44, 49, 50, 51].

2.3.1.4 Generalized Competitive Learning Competitive learning systems are usually feedforward multilayer neural networks [53]. These networks adaptively quantize the pattern space spanned by some random pattern vector x [53]. In competitive learning, a series of processing elements or nodes each defined by their weight (synaptic) vectors compete to become the "winner", and subsequently become updated. A node wins the competition for an input x if its synaptic vector m, is closest to x, usually in Euclidean distance, than all other vectors. This closest vector gets modified in the direction toward the input x, by some scaled amount. Each synaptic vector m_j represents local regions about m_j [53].

In order to create Kohonen's spatial ordering of the nodes, a neighborhood concept was developed, such that a winning node and the surrounding neighbors on a lattice are updated toward the training point. This neighborhood concept also complicates the proof of convergence for SOFMs, except in the simplest of cases. However, it is also thought that this capability may aid in the convergence to non-local minima [126].

2.3.1.5 Kohonen Learning Rule A Kohonen lattice for a two dimensional output space is shown in Figure 7. Typically a two dimension output map is used, yet other output mappings may prove more desirable [50]. In fact, the choice of output dimension can be based on quantitatively defining neighborhood preservation [11]. Each node is assigned a reference vector m_i and the input vector x is presented to all nodes. The best-matching unit or winner c at iteration t is determined by,

$$||x(t) - m_c(t)|| = \min_i ||x(t) - m_i(t)|| \tag{25}$$

The learning rule proceeds as follows,

$$\begin{aligned} m_i(t+1) &= m_i(t) + \alpha(t)[x(t) - m_i(t)] \; \forall \; i \in N_c(t) \\ m_i(t+1) &= m_i(t) \; \forall \; i \notin N_c(t). \end{aligned} \tag{26}$$

Here $N_c(t)$ is the neighborhood size around the winning node c at iteration t, with $\alpha(t)$ determining the learning rate at time t. Kohonen often describes these as linear monotonically decreasing functions. Interestingly, the neighborhood function could exist as a continuous function of relative lattice distances. A typical choice could be gaussian [11]. Since learning is a stochastic process, where the vectors x are random vectors, the algorithm should iterate through a very large number of steps, on the order of 100,000 [50]. A hueristic for iterations is more than 500 times the number of nodes [50, 91]. Ranges for α have been given as beginning near unity and dropping to .1 in the first 1000 iterations, followed by many iterations (10,000) with α below .01 [50].

The update rules can be chosen from a linear schedule, a hyperbolic schedule or exponentially [124]. However, many parameters must be chosen, often adhoc, such as update schedule, total iterations, occurrence of resets and the decision to implement a conscience [91, 126]. A supervised modification to Kohonen's learning algorithm results in the Learning Vector Quantization algorithm (LVQ). LVQ requires an initial guess at the

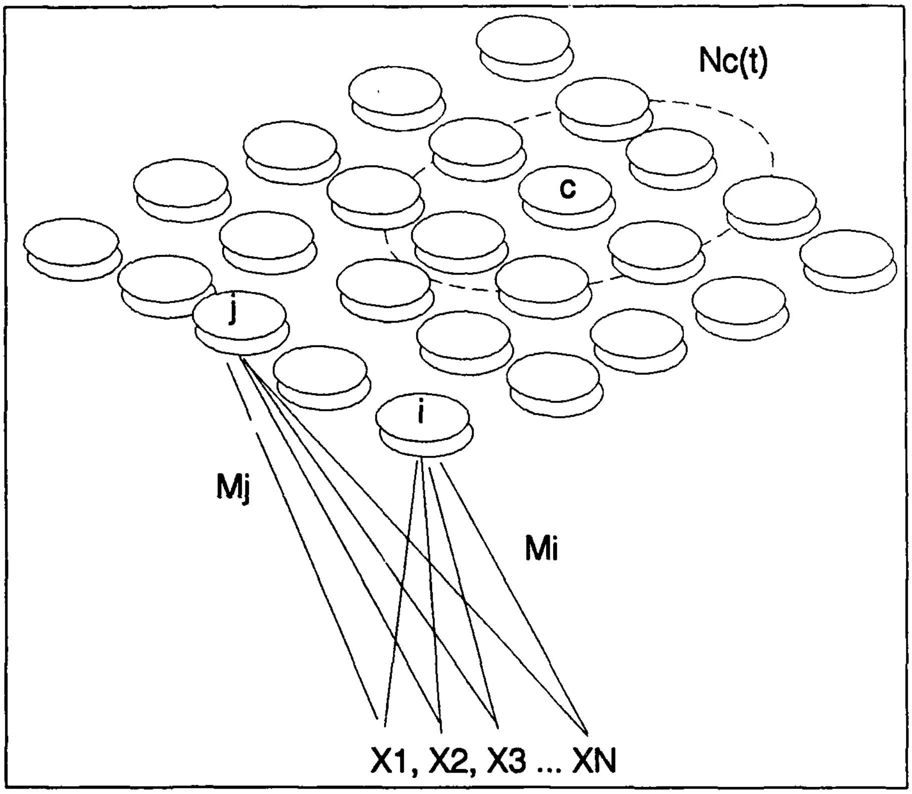

Figure 7. Kohonen 2D Lattice. This representation of the output space map shows the n-dimensional input training vector x, two node locations (weights) m_i and m_j, with some winning node, labeled c (center). At some iteration time t, there exists some neighborhood about the winner, $N_c(t)$.

codebook, and then attempts to more efficiently define the boundaries between classes, using a supervised scheme with labeled data. Kohonen, himself, suggests first using a Kohonen feature map to create a broad distribution of codevectors, then use LVQ to "fine tune" the map [51].

The learning vector quantizers (LVQ) should be used if "the self-organizing feature map is to be used as a pattern classifier [52]." Kohonen further expands the goals of LVQ in that, for classification, only decisions made as class borders count. LVQ attempts to create "near-optimal" class borders in terms of Bayes decision theory. Kohonen points out [75] that only LVQ1 and LVQ3 are self-stabilizing with continued learning; LVQ2 optimizes only relative distances of codebooks vectors around class borders, and may not truly define the actual class boundaries. Another important aspect of LVQ is that the vector quantization does not reflect the underlyıng density functions.

2.3.1.6 Conscience Let the input space be divided into k decision classes or partitions $D_1 \ldots D_k$. Each has an associated class probability $p(D_i)$ which integrates the unknown probability density $p(x)$ over the local region D_i [53]. Then if all $p(D_i) = 1/k$, a uniform partition exists. DeSieno [20] developed a modification to the "Kohonen learning" rule to specifically perform a better approximation to the underlying probability density function by insuring uniform partitions were created. This work was motivated by earlier Rumelhart and Zipser (1985) research indicating that it was possible for nodes to never win, when using a competitive learning rule. However, both the earlier research and DeSieno's experiments used a null neighborhood, including only the winner. This could be considered general competitive learning and not Kohonen learning, where spatial ordering and topology preserving characteristics are inherent. Kohonen noted that a valuable characteristic for a trained SOFM was to have each node win the competition with equal probability. DeSieno added a bias term to the Kohonen competition equation, Equation 25, based on the frequency of winning. Let p_i represent the win rate for node i, defined as number of wins (hits) divided by number of iterations (presentations) of data, h/t. DeSieno presented an iterative calculation of this rate which also is impartial to "fluxuations in the data." Let y_i be the "activation" for the nodes where

$$\begin{aligned} y_i &= 1, \text{ if } \|x - m_i\|^2 \leq \|x - m_j\|^2 \ \forall\, j \neq i \\ y_i &= 0, \text{ otherwise.} \end{aligned} \qquad (27)$$

The win rate is then

$$p_i(t+1) = p_i(t) + B[y_i - p_i(t)] \qquad (28)$$

where $0 \leq B \leq 1$. If one substitutes simply h/t in the above equation for p_i, B should monotonically decay as $1/(t+1)$. Desieno uses a value of $B = .0001$. The competition process now introduces a bias term b_i in determining a winner c,

$$\|x(t) - m_c(t)\| - b_c = \min_i \|x(t) - m_i(t)\| - b_i \qquad (29)$$

where this difference of fairness term b_i is,

$$b_i = C(1/k - p_i). \qquad (30)$$

The constant C represents the bias factor and determines the distance a losing node can achieve before entering the solution [20]. DeSieno used a C = 2.5; this thesis typically relates this value to the spread of the data, such as using the standard deviation of the training set [96].

Rogers and Kabrisky [91] discuss a modification without incorporating this bias term. Nodes are removed from competition when their win rate is greater than a threshold, inversely proportional to number of nodes, k. Thus, nodes must satisfy

$$p_i \leq \beta \frac{t}{k} \qquad (31)$$

to compete, where t is the current iteration and β is the conscience factor $1 \leq \beta$. The larger values of β results in less conscience; nodes "don't feel guilty about" winning much more than others. As an example, a β of 1.5 is considered a lot of conscience; whereas a value 5 is very little.

2.3.1.7 Statisticaı Clustering Analysis The discipline of statistical pattern analysis provides both parametric and non-parametric means of determining an unknown function probability density. Inherently, the two approaches discussed (LBG and Kohonen) attempted to obtain the optimal solution to the LMS objective function. Many of the concepts presented in this section are parametric approximations or kernel generalizations of these previous approaches. All the probability theory specifically applied to non-supervised clustering is provided in the book *Pattern Recognition: A Statistical Approach* [21] and can also be found in Tou and Gonzalez [117].

The basic statistical re^cognition problem is to decompose a mixture probability dens˙ty function (pdf), $p(x)$, into an appropriate number c of class conditional pdfs.

$$p(x) = \sum_{i=i}^{c} P_i p(x|w_i) \tag{32}$$

Devijver and Kittler [21] point out,

> When the class-conditional distributions are parametric of a known form, the unknown parameters of the distributions can be estimated from the data by well-known mixture decomposition techniques [21:pg 383].

The usually assumed parametric distribution is the multivariate gaussian. These authors describe various analytical approaches toward acquiring these class probabilities. However, the assumptions are based on marginal pdfs, where unimodal analysis can be performed. This is referred as mode separation. Though not always valid, the authors point out using a Karhunen-Loeve (KL) expansion before this mode separation can be used. The possibility ‹:xists that multiple modes may still overlap in the transformed KL eigenvector axes.

A statistical alternative to the direct parametric approach is clustering the data inıo homogeneous partitions, based on "similarities." The similarities are based on distance or distortion measures. When comparing clustering to the above parametric procedure, often data found in the same cluster would be associated within the same gaussian mode with the overall pdf, $p(x)$, Equation 32. Statistical clustering procedures include dynamical (iterative) approaches and hierarchical algorithms.

The k-means algorithm performs a nearest neighbor calculation using k arbitrary clusters, and calculates the centroids (means) of these partitions. The algorithm terminates whenever the algorithm converges. However, this representation of cluster mean can be extended to generalize more sophisticated models. Let a cluster Γ_j be represented by some kernel K_j, defined by a set of parameters V_j. Next, let (y, K_j) be a measure of similarity (distance metric) between a vector y and the cluster represented by K_j. Natural choices for K include normal distributions defined by mean and covariance as well as Karhunen-Loeve expansions of the original cluster patterns. On the other hand, the hierarchical approach begins with all data points as clusters and merges similar ones iteratively.

The authors [21] emphasize that non-supervised classification methods should be applied with great care. Such "practical problems ...as scaling of the axes, metric used, similarity measure, clustering criteria, number of points in the analyzed set, etc." will all greatly affect the results of the analysis. Other insights include these dynamic clustering methods usually being "computationally very efficient", yet the "chosen model rarely reflects the true probabilistic structure of the data. In such situations, the dynamic clustering algorithm can give rise to an unrealistic grouping of data."

2.3.1.8 Distortion Metrics A number of distortion metrics have been developed both in the mathematics community [14][21:pg 232][80:Chapter 7] and specifically for speech processing [29]. These include Minkowski, Euclidean, Chebychev, Quadratic and nonlinear, as well as Itakura-Saito Distortion and Itakura Prediction residual. This thesis will examine those types meaningful for speech (cepstral) representations, such as Euclidean distance and more specifically, squared distance,

$$d(x, m_i) = (x - m_i)^T (x - m_i) \tag{33}$$

and also the Quadratic,

$$d(x, m_i) = (x - m_i)^T R (x - m_i) \tag{34}$$

where R is a positive definite scaling matrix. Typically this can be the full covariance of the data set, or approximated by the diagonal elements if diagonal dominant. Also, R

may be a weight such as the squared index, i^2. This is known as root power sum (RPS) distortion. However, an outstanding issue will be the appropriate distortion metric for auditory features. If the assumption can be made that the human auditory periphery is merely doing a spectral analysis, then appropriate distortions can be chosen.

Another related concept is the probabilistic distance. For statistical pattern recognition (and for any recognition problem), the analysis of feature choice is important. A measure of class separability based on the complete probabilistic structure of the classes can be related as a "distance" between class pdfs. Similarly, the concept of probabilistic dependence can be examined. Several measures exist for determining separability of features based on class densities. Such measures include Chernoff, Bhattacharyya, Matusita, The Divergence, Patrick-Fisher and Lissack-Fu [21:pg 257-258]. However, this analysis currently cannot be extended beyond two class problems. Due to the numerical calculations and required estimates of the probability density functions, other simpler criteria exist where non-parametric density functions exist. These probabilistic separability measures (still only useful for two class problems) are efficient for parametric pdfs, and consideration can be made on parametric approximation of unknown non-parametric pdfs. For example, a gaussian mixture model may be fit to a data set.

2.3.1.9 Other Quantizer Designs Simulated annealing (SA) techniques and several variations have demonstrated experimental results superior to LBG [124, 127]. Simulated annealing is the process that relates optimization strategies to the annealing or cooling of molten metal. The solutions for this problem can be extended to any optimization problem, which attempts to minimize some objective function. Zeger et al [126, 127] compare the analysis of simulated annealing to that of LBG and Kohonen learning paradigms. These authors extended the Kohonen neighborhood concept using a "soft-competition" algorithm.

For the past several years, vector quantization techniques have demonstrated high recognition accuracies. Currently, Hidden Markov Model techniques are being researched extensively and compared to VQ results. Some studies have shown 50% improvements over Dynamic Time Warping and comparable results to Vector Quantization using both discrete HMMs [95] and continuous ergodic HMMs [68].

2.3.2 Hidden Markov Models/ Gaussian Models Hidden Markov models are extensively being documented in the current literature. Whereas pattern matching techniques, like DTW and Vector Quantization, create templates which represent the training data, an HMM creates a model of the training data. These models are characterized by a Markov process of state transition probabilities, in addition to a stochastic process of output probabilities. Initially, ergodic HMMs were researched, yet left-to-right models have been shown to be applicable and successful to speech processing. Lastly, Hidden Markov models can be implemented with either a discrete or a continuous output probability density function (pdf). In the former case, a vector quantization approach is often used to create a finite representation alphabet for each state, with associated probability distribution for each codeword. In the continuous approach, a probability density function, like a gaussian, is used for the output pdf for each Markov state. A good review on Hidden Markov Models is provided in Rabiner [84] and Rabiner and Juang [85]. This section will summarize recent HMM initiatives and recognition accuracies.

Only a few experiments have been reported on speaker recognition using a Hidden Markov Model. Poritz provided the initial work for speaker verification using a 5 state ergodic HMM [83]. Interestingly, it turned out that the 5 states naturally represented 5 broad classes of speech: voicing, silence, nasals, stops, and frication. His results showed 100% recognition for a small 10 speaker database using text-dependent training.

Rosenburg, Lee, Soong et al [95] examines talker verification using a whole word HMM. Their vocabulary consists of continuous digits for a 20 speaker corpus, speaking with error rates of 3.5% and .3% given for 1.1 and 4.4 seconds of test speech respectively. In this paper, the authors propose that the successes of speaker-independent word and subword HMMs for speech recognition can be applied to speaker-dependent talker verification tasks. The models use a 10 state continuous left-to-right HMM with a Gaussian mixture defining the output pdf. The mixtures contain M components (ranging from 1 to 9) which are estimated by clustering the utterance into various segments or states and clustering the training data into M clusters. A Viterbi algorithm derivative, referred to as the Viterbi frame-synchronous search, is used to provide maximum likelihood scores. DTW word templates are compared with a final score created by a concatenation of individual DTW word scores. Comparisons to DTW indicate 50% improvemeni by this technique.

Rosenburg, Lee and Soong's earlier work [94] provides the results of an HMM approach to talker verification using two different types of sub-word HMM data, phone-like units (PLUs) and acoustic segment units (ASUs). The database used only 20 speakers speaking only isolated digits. The authors point out that these results can only be suggestive toward text independent large vocabulary databases. The models used a 2 and 3 state continuous left-to-right HMM with a Gaussian mixture defining the output pdf. The mixtures contain M components which are estimated by clustering the utterance into various L segments and clustering the training data into M clusters. Their results are in terms of equal error rate [2] which is based on the test speaker probability against all others in the database, as a function of test time. Comparisons to earlier work by Tishby indicate that the left-to-right ASU segmentation may be superior to an ergodic model. The explanation offered is due to the greater temporal detail in a concatenation of left-to-right models. Vector Quantization perform only a few percent less, which is attributed to the lack of any temporal information in the clustering process. Overall, equal error rates are 7-8% for a .5 sec test utterance, and less that 1 % for a 3.5 sec utterance, with improvements possible by updating the models with test data.

Savic and Gupta [102] classify the speech signal based on vowels, fricatives, plosives and nasals. This approach better represents the model of the vocal tract which changes during production of these four "broad phonetic categories." A five state HMM is tested, with a Viterbi algorithm obtaining the maximum likelihood that the frame is assigned to a state (class). Their conclusions are noteworthy,

> ...the conclusion can be drawn that better performance can be achieved by representing each phonetic category by a different model, and by making the final

[2] Parsons [80] uses "equal error rate" between false rejections and false acceptance, usually plotted against some threshold.

> verification decision based on a weighted combination of scores for individual categories. Also, our results show that plosives do not have much speaker discrimination capability and hence, all classes of phonemes must not be used to make the verification decision.

Recognition errors rates of 2.32% for 43 speakers are shown. These results reflect those of a much earlier study by Poritz [83].

Most recently, Matsui and Furui [68] have provided a detailed comparison of Vector Quantization recognition performance to both discrete and continuous HMMs for both speaker identification and verification. A database of 46 speakers speaking at different rates (normal, fast and slow) was used. Identification results for the continuous HMM and VQ were comparable, about 90% to 95%. Discrete HMM performed at accuracies 5% to 18% below this. For the verification task, the VQ and continuous HMMs again were as robust at approximately 97% to 98%.

Some researchers are manipulating the Markov model itself, to increase recognition performance. Often these changes violate the Markov properties and are thus labeled Hidden Semi-Markov Models (HSMM) [36, 99]. One such change often performed is the explicit modeling of state durations separately. Huang combines both Discrete and Continuous HMMs, labeled Semi-Continuous Hidden Markov Models (SCHMMs) [36]. The author claims that this technique provides a good solution to the fine detail of continuous HMMs and insufficient training data to provide a good discrete HMM. Since a Markov process determines state transitions, conventional HMMs are weak in modeling state durations, especially for speech. This new SCHMM method, not only models the state transition and output probabilities, but also models the state duration probabilities explicitly. The definition is follows: "The probability of state duration ... $d_i(\tau)$ is the probability of taking the self-loop at state i for τ times." These parameters can be estimated from the observations, along with the other HMM parameters. Thus, the transition from state i to state j must include not just the state transition probability, but also all the possible time durations that may occur while in state i. Gu et al [30] demonstrated 1.9% to 9.0% improved recognition rates in using a bounded state duration HMM. These bounded states force a minimum and maximum duration value for each state. The authors also compare this approach to Poisson and gamma state distributions.

Another type of speaker model demonstrated in the literature uses gaussian mixtures. An article by Rose and Reynolds [92] specifically address speaker identification in noisy environments. The authors present two approaches. First, the background noise is integrated into the voice model. Thus, a noise process is added to the Gaussian Mixture Model with a maximum likelihood calculation being performed on this aggregate model. Both an additive and maximum noise model is examined. The second approach preprocesses the speech before the classification steps. This technique is based on spectral subtraction using long-term averages of filter bank energies. Database consists of conversational speech from 10 speakers over long distance channels. The author's choose a 32 probabilistic Gaussian mixture density, which have a diagonal covariance matrix. Error rate range from 38.0% to 19.4% identification, compared to the original 99.5% rate for clean speech. Clearly this shows the limitations of current methods on noisy telephone quality speaker identification. A more recent article by the authors [88] examines the modeling of both the background noise environment and the speakers separately with GMMs. In this innovative process, the likelihood of the observation sequence combines the two independent GMM models for each speaker.

2.3.3 Artificial Neural Network Classification The following methods can be considered Artificial Neural Network schemes, in that many incorporate a simplified processing element, which could be exaggerated as a real neuron. This section details current examples found in the literature on Multi Layer Perceptrons, Time Delay Neural Networks, Radial Basis Functions and other supervised learning approaches to the classification problem of speaker recognition.

Bennani [13] demonstrates a Time-Delay Neural Network (TDNN) for feature extraction and classification. The DARPA TIMIT database was tested and an average identification rate of 98% is given for 20 speakers. Preprocessing is done by 16th order LPC coefficients as the parameter space on windows of 25.6 msec. Then, each sentence is further divided into windows of 25 consecutive frames (approximately .6 sec), with this particular choice based on earlier research by Atal [10]. Speaker identity is decided though a two layer classifier. First, a Male-Female classification is accomplished. The article states, "Motivations for this modular architecture are multifold. First it has long been observed that speech spectra tend to form two clusters according to the sex of the speaker." A second recognizer chooses speakers.

A binary partioned Neural Network was recently demonstrated to be a successful strategy for ASR [98]. Each network is trained for a single person; however, it requires $N * (N - 1)/2$ classifiers for N reference speakers. The DARPA TIMIT database is used with 47 talkers from a single dialect (there are 8 American English dialects recorded on TIMIT). The LPC Cepstral coefficients were used as features (order 15). Error rates published are 0% for 47 speakers reached within eight seconds of test data. The article is quick to point out the limitations of this technique.

> (These will) classify with 100% accuracy as long as each of the Binary Classifiers performs correctly. The performance of [these] approaches, however, may degrade differently if not all the binary classifiers work perfectly.

Oglesby and Mason [77] research a Radial Basis Function Network as a classifier. A 40 speaker corpus, using only the digit set is tested. Noteworthy is that their database contains each speaker recorded in five different mannerisms: loud, soft, questioning, angry and normal. The feature space is the first 10 cepstral coefficients acquired through a 12 critical band filterbank of mel-frequency spaced filters. Results are compared to VQ using codebook sizes of 32, 64 and 128 as well as Multi Layer Perceptrons (MLP) with 32, 64 and 128 hidden nodes. Better performance is shown for Radial Basis Functions with performances of 8%, 20% and 22% for normal, angry and soft speech respectively, outperforming both VQ and MLP techniques. These unique results show the greatly varying effects of intra speaker variability, which is often neglected in the literature.

The two authors earlier [76] vary the hidden layers and number of nodes in a feedforward Artificial Neural Network. The "personalized" NN is trained active for an individual's speech including signals from other speakers. The intent of this approach is for the NN to "learn" unique characteristics of the individual. Their database contains utterances of

10 speakers from the digit set, using 10th order LPC-derived cepstral coefficients as the feature set. Comparisons are made to a Vector Quantization approach which shows VQ, for a 64 vector codebook, performs at 8% error identification. The authors perform a series of tests for a Feed Forward NN using a gradient descent training algorithm (Backpropagation). These test are conducted for a single hidden layer with 16 to 128 hidden nodes, and two hidden layers with 16 and then 32 nodes in the first layer and varying the nodes of the second layer (4 to 32). The best error rates of 8%, equal to that of VQ , was obtained with a single hidden layer of 128 nodes.

ITT recently investigated speaker verification using "discriminator counting" [35]. The concept in this article, which is a synopsis of their recent Government Final Technical Report [34], "models speaker-pair distinctions, rather than speakers themselves". Feature extraction uses power over 14 uniformly spaced frequency banks. Underlying theory uses N pair-wise discriminators voting over a time period L for the unknown speaker. Speaker is accepted if some threshold is met. Results show 80% of targets were detected, with only 2% of non-targets. This issue of out-of-class membership receives very little attention in the literature.

2.4 Payton Model of the Mammalian Auditory System

Over the last few decades, many details have been revealed on the processing mechanics of the cochlea, basilar membrane, neural transduction and higher processing centers, particularly in mammals and with complex stimuli [31, 39, 70, 100, 106, 125]. Currently, several models exist which attempt to duplicate or explain the available physiological data [17, 25, 27, 82, 109]. See Table 3. The Payton model is just one of those many available models. Many of the models differ in their approach toward basilar membrane mechanics. Several use a parallel linear filterbanks [25, 26, 27, 109, 110, 111, 112] or cascaded linear filterbanks (transmission line) [1, 63, 65, 66] approach, while others model the intrinsically complex basilar membrane displacement functions [2, 3, 82]. Jenison [39] specifically uses an appropriate filter based on stimulus level and the respective center frequencies. Some recent filterbank approachs have modeled the neural feedback mechanisms (outer hair cell effects) by changing the filterbank bandwidths based on averaged stimulus inten-

Table 3. Several Auditory Models and their Features

Author (Date)	Channels, Frequency Range, Characteristics
Ahn (1990)	20, 200 Hz - 3500 Hz, Filterbank developed by Armstrong Lab, combined with Seneff Inner Hair Cell/Synapse and GSD, modified filterbank GSD [1].
Ghitza (1986, 1987)	85, 200 Hz - 3200 Hz, Filterbanks, Ensemble Interval Histogram (EIH) analyzes threshold crossings of parallel filterbank outputs. Measure of temporal characteristics, noise evaluation. [25, 26].
Ghitza (1988)	Added feedback to EIH.
Jenison (1991)	Iso-intensity maps, create a suite of filters for each channel based on intensity of signal [39, 40].
Lyon (1986)	49, -,Multi Channel AGC, to change the filter tuning characteristics [65]
Lyon/ Mead (1988)	430, -, CMOS implementation with AGC [66].
Payton (1986, 1988)	20, 400 Hz - 6600 Hz, Composite model, BM displacement of Sondhi and Allen, IHC of Brachman [82, 81]
Seneff (1984)	32, 200 Hz - 2700 Hz, Generalized Synchrony Detection (GSD), a measure of the temporal synchrony to each CF [110, 109].
Seneff (1986, 1988)	40, 130 Hz - 6400 Hz [111, 112].
Others and Applications	Cohen [17], Kates [47, 48], Hunt [37, 38], Liu [64, 63], Patterson [6], Meddis[6], Shamma [6].

sity [27, 39, 63, 65, 66]. This allows the filtered responses to better match physiological data, by increasing the coverage under the response profiles of the filterbanks. Recent auditory models also attempt to provide both spectral and temporal synchrony information. Next, the Payton model, as well as other model comparisons, will be analyzed in as a preprocessor for feature extraction.

Payton chose to combine the best representations which were based on physiological measurements and contained the least simplifying assumptions. The overall model is presented in Figure 8. The model has been coded in 'C' [90] and logically separated into three stages. It should be pointed out that the model, in all three main stages, is required to solve simultaneous differential equations. The method used is based on the central difference approximation [3]. This technique replaces derivatives with difference equations. For example, the function $\zeta(t)$ and its first and second derivatives can be discretely approximated as follows, where T is the sampling period between discrete approximations.

$$\begin{aligned} \zeta(t) &= \zeta(n) && (35) \\ \partial\zeta/\partial t &= (\zeta(n) - \zeta(n-1))/T && (36) \\ \partial^2\zeta/\partial t^2 &= (\zeta(n+1) - 2\zeta(n) + \zeta(n-1))/T^2 && (37) \end{aligned}$$

In Allen and Sondhi's article [3], the authors note this technique provides stable equations if $1/T$ is greater than π times the highest resonant frequency. The current model uses a sampling frequency of 160 KHz.

2.4.1 Stage 1/ Middle Ear The first stage models the middle ear filtering. As mentioned, this resembles a low pass filter. The input to this stage is sampled data, representing sound pressure at the eardrum. Based on Guinean and Peake (1967), a ratio of stapes velocity to tympanic membrane pressure can be solved through circuit analysis. Figure 9 shows an example of a TIMIT Database utterance, with the transformation to stapes velocity given in Figure 10.

2.4.2 Stage 2/ Basilar Membrane The second stage of the Payton model performs the basilar membrane mechanics. Using the developments of Allen and Sondhi [2], dis-

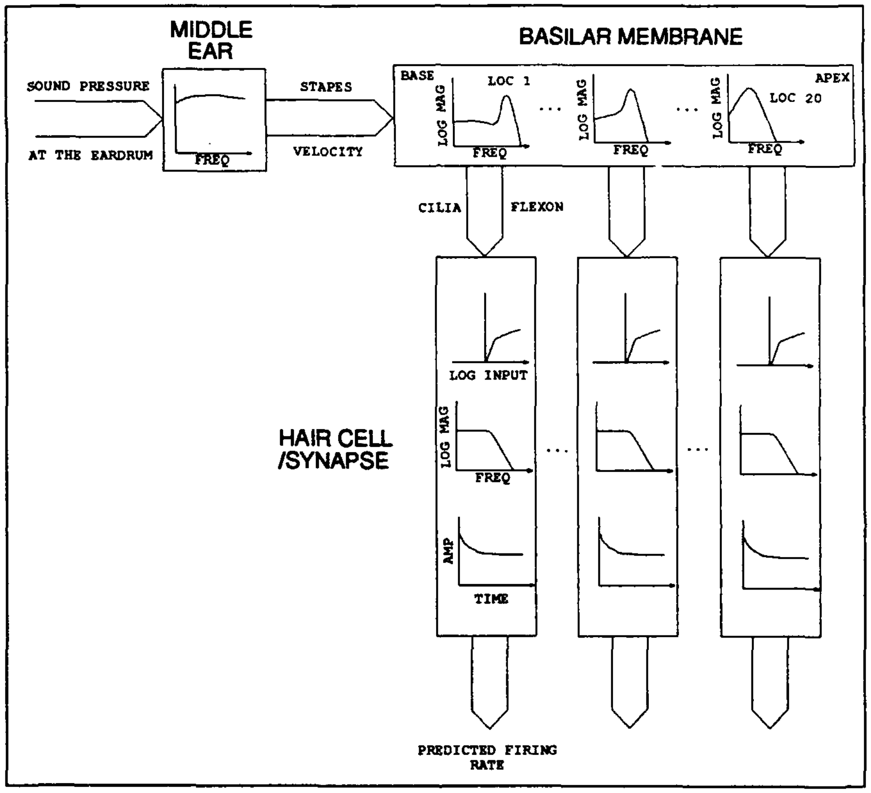

Figure 8. Composite Payton Auditory Model. The model is implemented in three stages. The first performs a low pass filtering operation creating stapes velocity. This stapes movement creates traveling waves propagating down the basilar membrane (BM). Displacement at 128 points along BM are calculated, 20 responses are then sharpened. These 20 points are input to the inner hair cell/ transduction stage, where predicted firing rates of auditory nerves are modeled [81].

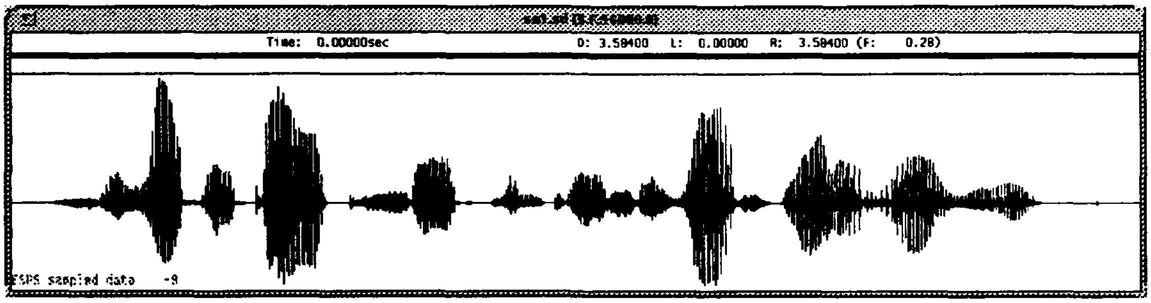

Time: 0.00000sec D: 3.58400 L: 0.00000 R: 3.58400 (F: 0.28)

Figure 9. Original sampled data from the TIMIT database, scaled by 8000. The sentence (male speaker) reads,"She had your dark suit in greasy wash water all year."

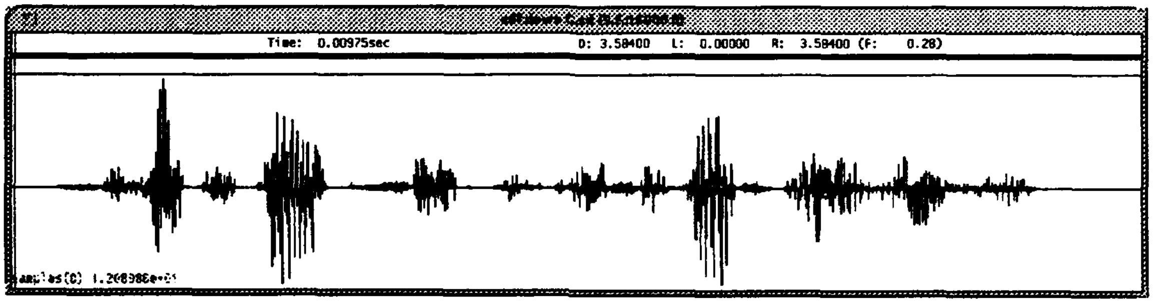

Time: 0.00975sec D: 3.58400 L: 0.00000 R: 3.58400 (F: 0.28)

Figure 10. Original sentence after First Stage of Payton Model. Sound pressure (sampled speech data) is converted to stapes velocity (microns/sec).

placement as a function of distance from the base and time is implemented. The approach is first to model the fluid pressure differential across the basilar membrane, as a function of input stapes velocity and fluid dynamics. The next step, by modeling the membrane as a three dimensional plate, is to determine the displacement of the membrane in response to this time varying pressure differential. A number of key assumptions and simplifications, however, were needed. These were,

- Cochlea fluid in incompressible, and flows in a linear fashion.
- Coiled shape did not enter into the calculations. Thus, the cochlea can be uncoiled and various symmetries monopolized in solving the differential equations.
- The coil was stationary, not expanded with fluid flow. Since the cochlea is surrounded by bony matter, this is valid:

- The height of the cochlea remained constant for each partition. This is not true. The two major stalae are neither constant nor the same, thought are generally similar.
- The cochlea partition (basilar membrane) can be modeled with a linear set of flexible plate equations. These models account for mass, compliance and damping. The authors point out this can be easily extended when physiological data is available.
- Fluid flow is two dimensional. All latitudinal (width) dynamics are assumed symmetric.

Allen and Sondhi's development does include size, stiffness, longitudinal shape, and damping of the cochlea, as well as various fluid parameters. The model can be visualized as a 2.5 cm long, .06 cm high, fluid filled rectangle with decreasing width. See Figure 11. All of these are based on physiological findings (within a cat). Again, the method on central difference was used, however, care was needed in chosing the appropriate sampling period, T, as well as the spatial period along the basilar membrane. The original Allen article solved for 256 and 512 points along the basilar membrane. Payton also used 512 points. This implementation of Payton's model, for speed efficiency, dropped down to 128 points along the basilar membrane. This is still valid to overcome aliasing [2]. The sampling period required and used was 160 KHz. The following figure shows the output of the basilar membrane model for the phoneme "IY" within the original sentence. Note the wave propagation over time. The following figure, Figure 12, shows BM data, downsampled back to the original 16 KHz, and the output of only 20 of the 128 basilar membrane locations. Recall that high frequencies are found closer to the base (toward '0'), with low frequencies at the apex (toward '19'). Table 4 relates the characteristic frequencies of these 20 locations. Basilar membrane locations correspond to .875 cm and 2.0625 cm from the base for channel 0 and channel 19, respectively.

Though all pertinent information has gone into the basilar membrane displacement analysis, the responses are not as tuned as physiological data indicates. A sharpening mechanism has been added such that slopes fall off appropriately. Liu [63] states these are typically characterized by a low frequency side slope of 6 - 12 dB/octave and a much sharper 50 - 500 dB/octave above the best frequency . This effect removes overlap between loca-

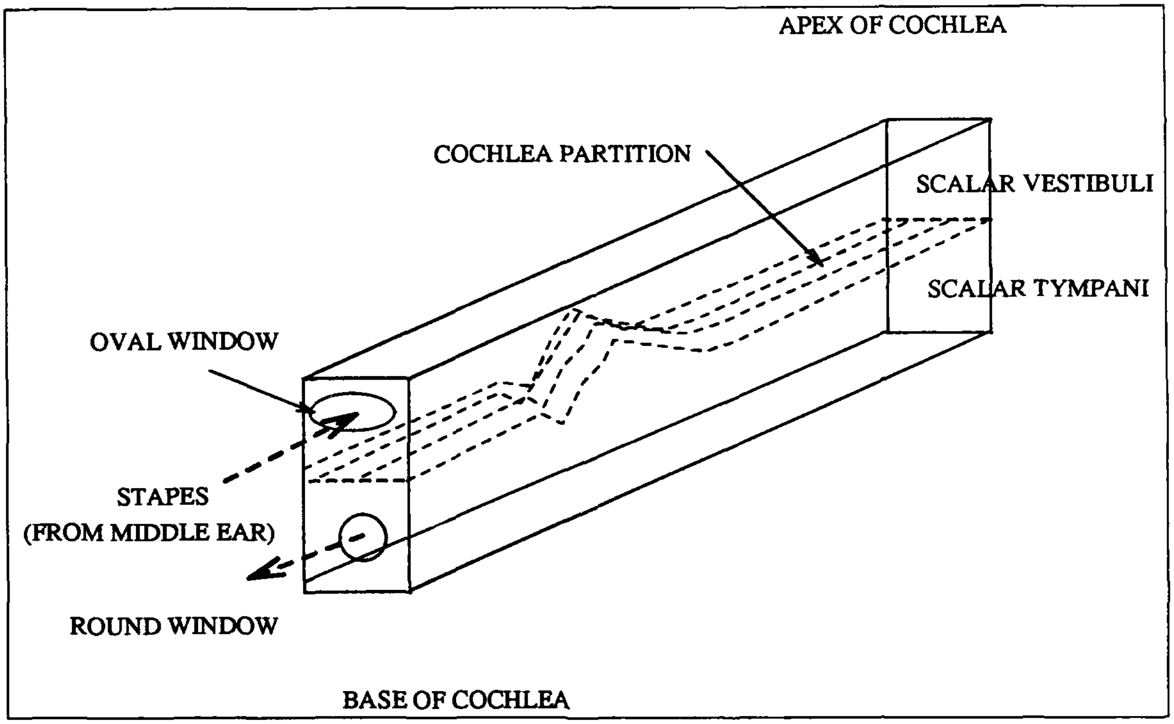

Figure 11. Uncoiled Cochlea Model. The model incorporates the length, (constant) height, latitudinal narrowing size (not shown) of the cochlea partion, stiffness of BM, and fluid dynamics [81].

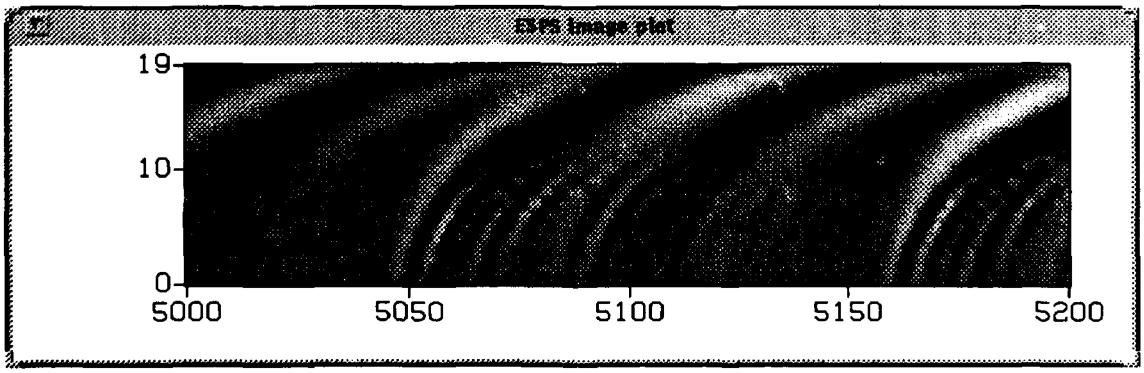

Figure 12. Original sentence through the Basilar Membrane Second Stage of Payton Model, but before second filter sharpening - Phoneme [IY].

Table 4. Characteristic Frequency of Payton Model 20 Channels.[4]

Payton Channel	Characteristic Frequency
0	6641
1	5859
2	5117
3	4492
4	3906
5	3398
6	2969
7	2617
8	2265
9	1992
10	1719
11	1484
12	1289
13	1133
14	977
15	820
16	703
17	586
18	508
19	430

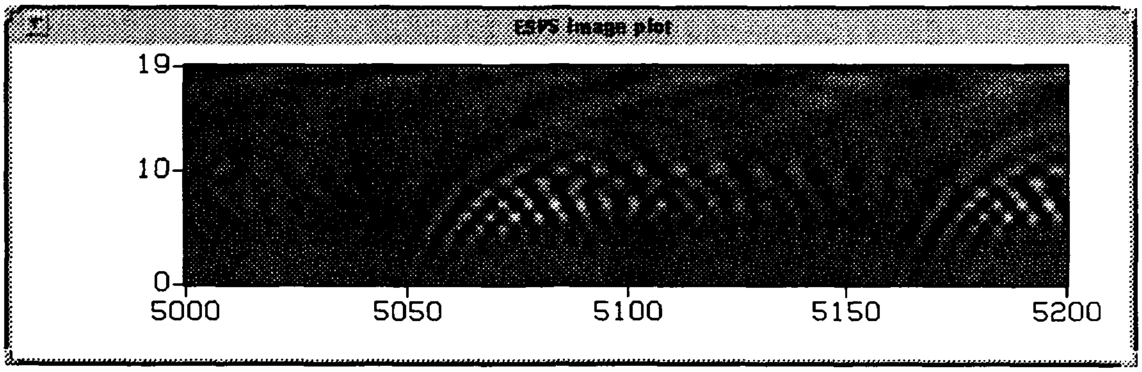

Figure 13. Original sentence through Basilar Membrane Sharpening Mechanism, a second filter with a zero placed below, and a pole placed just above the characteristic frequency - Phoneme [IY].

tions, and the emphasis in key frequencies can be recognized. The Payton method consists of a second filter with parameters developed by earlier researchers, based on physiological data. It is theorized that mechanical interactions between the inner and outer hair cells may cause this sharpening. This bank of second filters consists of a zero, above one octave below the center frequency, and a highly underdamped pole just above the best frequency. The same phoneme of the basilar membrane figure has been sharpened using the second filter and shown in Figure 13. Note the pronounced bands for this particular phoneme, where the sharpening is greatest in bands 7 - 9. These correspond in Table 4 to approximately 1900 - 2600 Hz, which correlates to Parson's [80] average second formant for an adult male.

2.4.3 Stage 2 Comparisons Other models use specifically designed filterbanks whose responses mimic this displacement and sharpening [66, 112]. By cascading low pass filters, the high frequency side roll-off can be matched to physiological data [37]. A second filter, say an appropriate high pass filter, can achieve the desired low frequency side response. These models, as Hunt [37] points out, model the properties, not the mechanisms of the auditory physiology.

Recently, Jenison demonstrated how the response to high stimulus levels (say, $\geq$ 60 – 70dB for voiced speech sounds) should incorporate a much larger populous of neural firings. Refer to Appendix A, Figure 43; to note the spread of influence for the higher levels of a 1 KHz tone. The relative response of the CF = 1133 Hz channel at higher stimulus levels should include synchrony information from many channels, as much as several octaves away [39]. This is in contrast to Sachs and Young having used only local synchrony information, within a 1/2 octave from the center frequency [125].

2.4.4 Stage 3/ Inner Hair Cell Transduction/ Synapse Lastly, the model performs the non-linear mechanical to electrical transduction. Several functions occur within this final stage. These include the following.

- Half Wave Rectification.
- Amplitude compression.
- Non-linearity saturation.
- Various Adaptation.

Payton uses the developments of Brachman (1982) in this last stage. The input signal from the sharpening mechanism is first halfwave rectified based on cell potential biased toward the positive direction of BM movement. It is also log scaled. This function also contains a "sloping saturation". The following equations were Payton's changes to the original Brachman model, in order to process arbitrary stimulus signals. She defines $stim_{dB}$ at time i on the basilar membrane as,

$$stim_{dB}(i) = 20\log[stim(i) + off], \; stim(i) + off > zero \quad (38)$$

$$stim_{dB}(i) = 20\log[zero], \; stim(i) + off \leq zero \quad (39)$$

where $zero$ is a small number to prevent illegal log operations and off was added to allow reduced neural firing during the negative half cycles of the stimulus (recall phase synchrony). This insures that $stim_{dB}$ remains small up to a threshold, off.

Next, a static nonlinearity is performed, based originally on Zwislocki (1973). First, define

$$Bin(i) = 10^{(stim_{dB}(i) - atten)/noise} \quad (40)$$

then, the rate of firing at time i is determined by,

$$rate(i) = sat[1 - e^{-\sqrt{Bin(i)}}]. \tag{41}$$

Here, *sat* is the saturation firing constant and *atten* and *noise* were constants introduced by Zwislocki. If $Bin(i)$ is a very large, corresponding to large BM displacements or large $stim_{dB}$, then $rate(i)$ approaches *sat*, or saturation firing. Likewise, small stimulus levels, dependent on off causes *rate* to approach a spontaneous rate. The "sloping saturation" occurs when $stim_{dB}$ reaches an ad hoc level S_o. An example of the saturation for a high spontaneous firing neuron, calculated from the Payton model is shown in Figure 14.

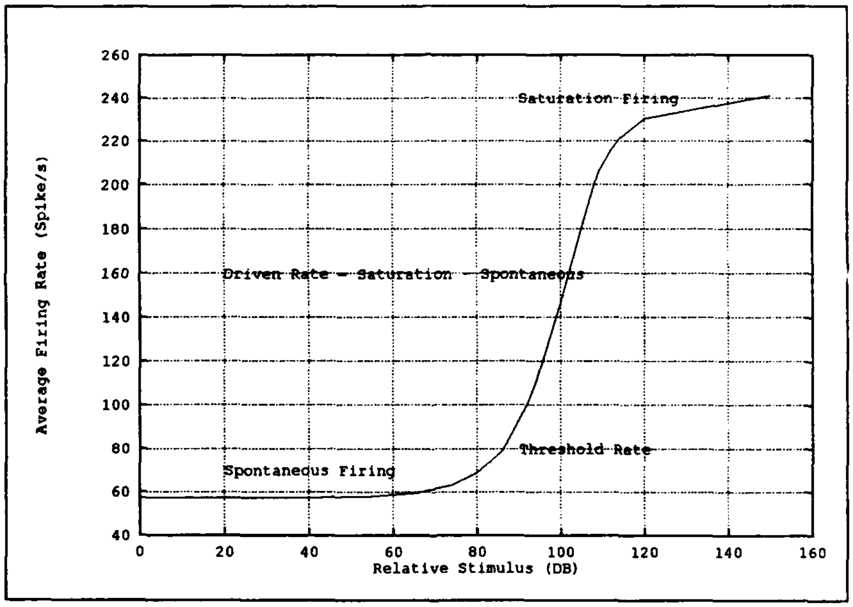

Figure 14. Neural Firing Range. This graph depicts typical responses for a high spontaneous rate, low threshold neuron, such as modeled by Payton.

This *rate* signal is low pass filtered, based on synchrony roll-off found by Brachman (1980). The filtered output defines the number of immediate reservoir sites active for the adaptation process.

Many attempts at modeling the neurotransmitter release, at the inner hair cell synapse, have been reported [33]. Payton uses Brachman original concept of three cascaded reservoirs or stores. This is depicted in Figure 15. It is currently thought that the

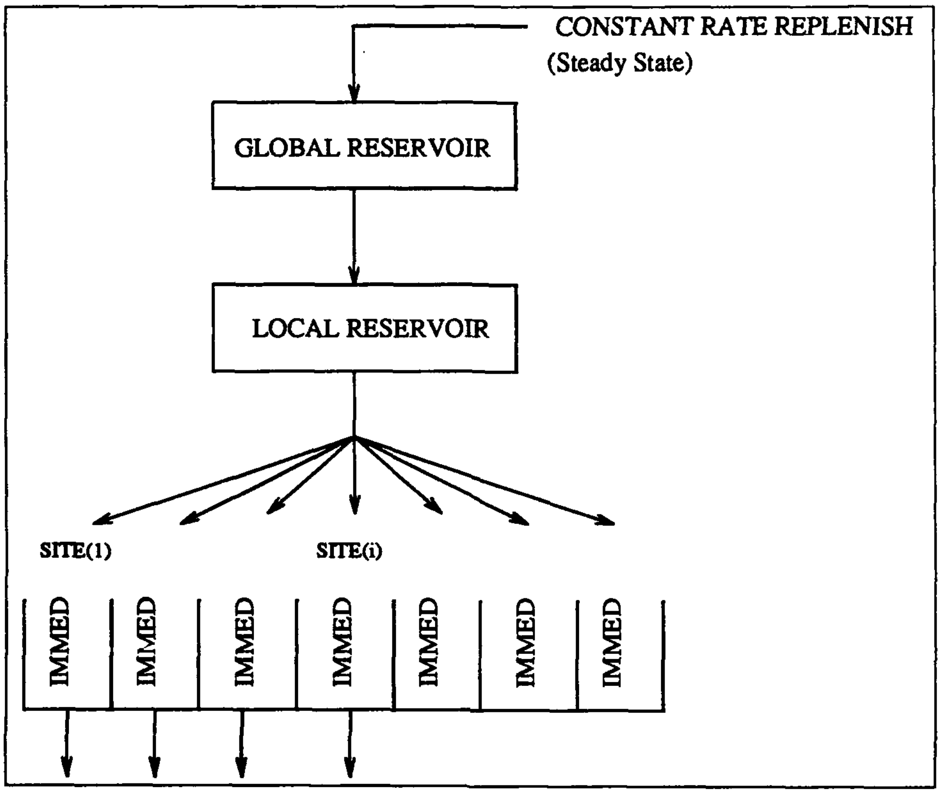

Figure 15. Payton implementation of Brachman (1980) Reservoir Scheme of "Neurotransmitter" release. Each maintains a different concentration flow equation contributing to different adaptation times for neural spike generation [81].

neurotransmitters are released based on various individual pools, local pools and global pools, and consistly are being "used" and replenished. Adaptation occurs when neurotransmitters are "used-up" faster than replenished. The concentration change equations for the immediate (n), local (L) and global (G) stores are presented.

$$
\begin{aligned}
v_I \partial c_n / \partial t &= -k_I c_n + k_{LI}(c_L - c_n) &(42)\\
v_L \partial c_L / \partial t &= -\sum_{n=1}^{m\_sites} k_{LI}(c_L - c_n) + k_{LI}(c_G - c_L) &(43)\\
v_G \partial c_G / \partial \iota &= -k_G(c_G - c_L) + k_{ss} &(44)
\end{aligned}
$$

These v's correspond to volumes of the stores, the c's correspond to site and store concentrations. The many variable k's are the various *permeability* coefficients. Note the overall functions of these concentration changes are simply scaled gradients, between any two levels of stores. So, the change of the global store will be the k_G scaled difference between the current global store and the local store concentrations. The added k_{ss} corresponds to the constant rate of replenishment for the global store. Each individual immediate site concentration, c_n, is changed separately from the others. Also note in the second equation, the local store has both a negative term, related to outward flow to all *m_site* immediate sites, and a positive term which adds concentration from the global store.

The probability of an action potential, as a function of time, is proportional to the amount of substance released by the immediate stores. Thus, the overall output of this stage is the estimated firing rate of the auditory nerves at the specific 20 locations. The following figure, Figures 16, represents the final model output.

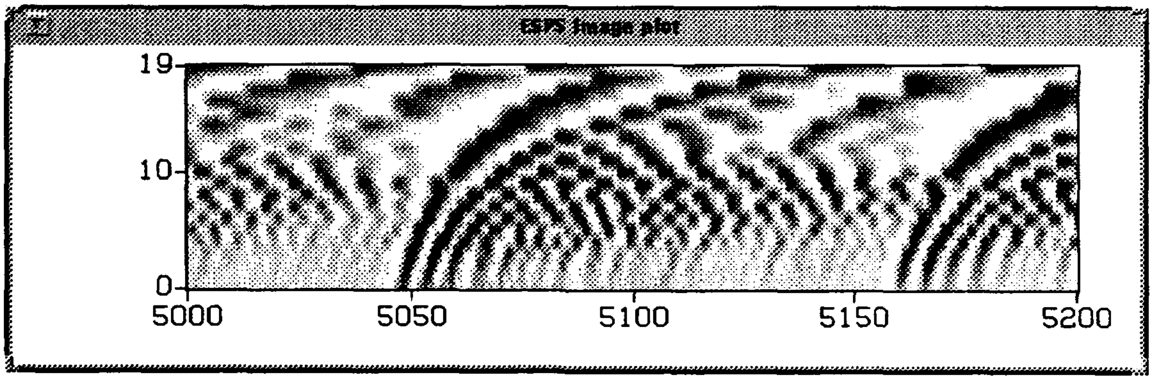

Figure 16. Original sentence after Final Transduction Stage of Payton Model - Phoneme [IY].

As a comparison, the spectogram of the original sentence is shown with the auditory representation for the entire utterance. See Figures 17 and 18. The correlation of these two spectral representations is high, in terms of formant trajectories over time.

2.4.5 Stage 3 Comparisons Many other models have similar components with their respective inner hair cell/ transduction stage. Most models [63, 112] incorporate some

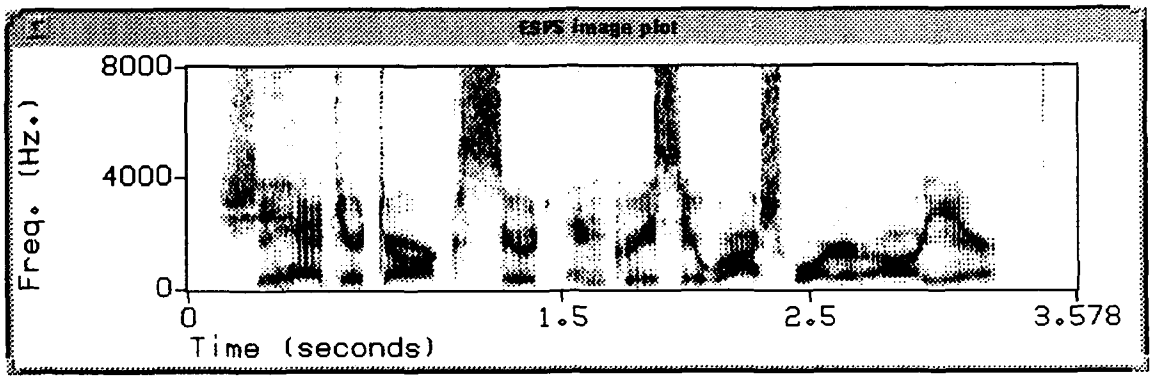

Figure 17. Original sentence Spectogram, using 256 point DFT, window size 16 msec, frame rate 5.33 msec.

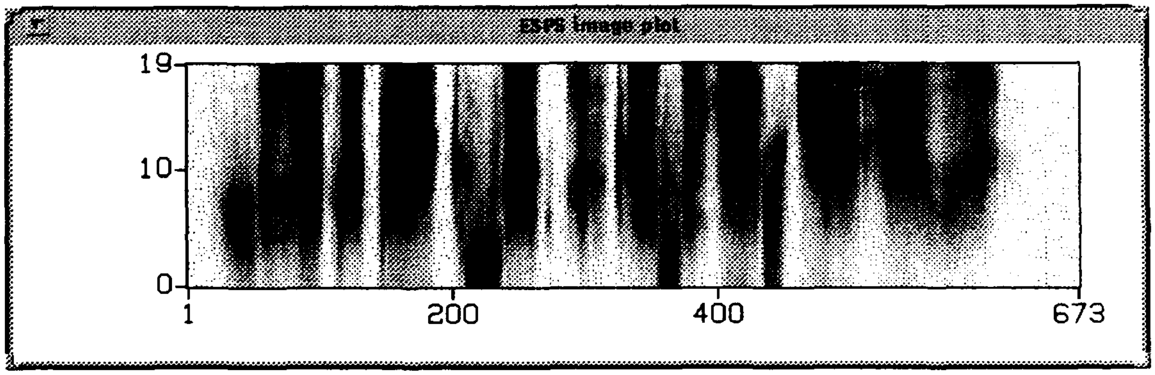

Figure 18. Original sentence after Final Transduction Stage of Payton Model, averaged with a window size of 16 msec and a frame rate 5.33 msec.

"growth limiting function" such as a non-linearity to model the saturation effects [82]. Each implements some form (multiple) of adaptation [112]. Meddis [33] reviewed eight reservoir based models, each differing on number of (cascaded) stores and varying replenishment schemes. Also, the similar application of low pass filtering to reduce synchrony for higher frequencies has been used in other models [110]. While other models have only achieved characteristic responses which correspond to the physiology, Payton has specifically tied each model subcomponent to physiological function and experimental data available, where possible.

2.4.6 Payton Analysis A number of issues are presented, based on other model representations reviewed, and the desired application of this model. These primarily include resolution and choice of frequencies. Currently, the frequency range of the Payton model is 400 Hz to 6600 Hz. Her experimentation on synthesized vowels gave her the opportunity to choose the appropriate first formant (F1). Typically, adult males have their first formant well below 400 Hz. Her choice of F1 for the phonemes $/a/$ and $/\epsilon/$ were 714 Hz and 595 Hz respectively. Likewise, the highest center frequency extends to 6600 Hz, whereas the fourth formants in her experimentation only extend to 3094 Hz. It can be noticed in the time averaged plot of the entire example sentence (Figure 18) there is very little activity on the higher channels. Tests which examine high frequency synchrony loss may use this information. However, for speech processing where formant structure may be important, a better range of frequencies may be needed. Typically, other models use frequencies ranging from 200 Hz up to around 4 KHz.

The model also chose not to implement the last stage of Brachman's original developments in the inner hair cell/ transduction section. This would have allowed the creation of neural spike trains, which could subsequently be used for synchrony evaluation. Currently, the neural firing output estimates are output from the model which can be time averaged over frames or directly input to a classifier. In order to create a spike train, some statistical distribution for interspike intervals may be assumed. This thesis will directly use the instantaneous neural spike rate information.

Lastly, whether 20 channels will provide enough resolution to accurately determine speakers needs to be addressed. If the higher frequency channels are providing little information, this reduces the effective feature space to less than 20 dimensions, say 15. Neural feature saliency (as well as spectral saliency) would be very useful information for speaker identification research. Other auditory models have primarily evaluated filterbank approaches with number of channels ranging from 20 [1] up to 85 [25], and up to 480 found in silicon models [66].

Regardless of these implementation specific details, research has shown great successes in using an auditory model preprocessing for speech recognition, especially in degraded, noise induced environments. Most importantly, each aspect of the various stages had physiological motivations for design choices. Consequently, the Payton model performs successfully in matching numerous physiological experiments, such as the following: stapes displacement/ velocity, basilar membrane motion, neural saturation curves, synchronization index (measure of phase synchrony to particular frequencies), average rate for synthesized vowels, as well Sachs and Young (1979) ALSR measurements. Next, Chapter V will examine the use of these neural firing patterns in several clustering algorithms to perform speaker identification.

2.5 Conclusion

Speech and speaker recognition has attracted a large body of research. However, not all problems have been solved. This chapter initially reviewed the "typical" feature extraction preprocessing for speech recognition. Much prior research has determined the most effective acoustic parameters for characterizing speakers [59]. The LPC and LPC cepstral features are often used since they form a compact representation and are relatively insensitive to stimulus level and some long-term signal distortion. For clean voiced speech, the LPC model provides an extremely efficient representation. However, the LPC coefficients will not model speech production in noise as well as for some "noisy" and nasal phonemes. Much research has provided many derivatives for the cepstral coefficients in maximizing their ability to perform recognition. Various improvements have included transitional characteristics, inverse covariance weighting, time-average subtraction as well as linear combinations of cepstral representations. However, low signal-to-noise ratios will still greatly effect these voice model techniques. Noise preprocessing techniques, such as spectral subtraction, assumes the noise is uncorrelated with the speech signal [80]. Liftering is another technique used for cepstral, which deemphasizes both low and high order cepstral coefficients, most often corrupted [42].

Classification techniques continue in vector quantization designs, artificial learning and training paradigms as well as techniques based on fuzzy set theory, and stochastic models. Hidden Markov Models (HMMs) are the predominate research topic in speech recognition. A few reports have provided results on the application of HMM to speaker recognition, comparing discrete and continuous models, and ergodic and left-to-right models to traditional pattern matching classification approaches. These models currently are showing promising results in various limited demonstrations, yet often compare their results to VQ methods. However, the performance of these, as well as artificial neural network techniques, in degraded environments has not been reported.

Human auditory representations have been created for two differing purposes. The first is to further explain and gain understanding of the human physiology. The second is to use these models as an improved feature set for recognition. Humans are able to perform speech and speaker recognition adequately in increasingly noisy environments. Ideally, this process can be automated and replicated for use by an automatic speaker recognition system. Only recently have these models been used for this purpose and the published data is just emerging. Much is still not known about the level of the auditory nerve, and these higher brain functions may be the key to speech and speaker recognition.

III. Methodology

3.1 Introduction

This chapter provides the methodology of experimentation, including database extraction, Entropic ESPS cepstral and Payton model preprocessing, normalization, and clustering schedules and parameters. The two primary speech databases used in this thesis were TIMIT and KING. Additionally, recordings have been collected at AFIT of ten speakers over ten sessions (days) recording both rich phonetic sentences and their full names. This shall be referred to as the "AFIT corpus."

A selected portion of the DARPA TIMIT Acoustic Phonetic Continuous Speech Database [74] was used to examine current well-established techniques for initial tests. Ten speakers, seven male and three female, from different dialects were available, each speaking ten sentences recorded during a single session. These sentences are sampled at 16 KHz and encoded linearly using 16 bits. The measured SNR, using the TIMIT header for noise power estimation ($\sim$ 2000 samples of silence) was 36.72 dB. The TIMIT sentences are classified into three types:

- *SA* - 2 Dialect sentences,
- *SX* - 5 MIT Phonetically balanced sentences,
- *SI* - 3 TI contextually varying sentences.

The latter two types contain sentences different for all speakers. The specific speakers chosen, as the following graphs will indicate, were mcmj, medf, mhpg, mmhw, mprt, mrtk, mjls, fccm, fcrh and fedw. These 100 sentences were also phonetically labeled with phoneme label and broad classification. These broad class labels include VOWEL, SILENCE, FRICATIVE, LIQUID-GLIDE, NASAL and PLOSIVE-STOP.

The KING database contains both a wideband and narrowband recording of 51 speakers containing natural conversational speech on several topics. Each speaker was recorded at 10 separate sessions, each session containing approximately 60 seconds of recording (about 30 seconds total speech). The narrowband recording used in this thesis is sampled at 8 KHz, 8 bits per sample. The first 26 speaker were recorded in San Diego, CA with much better quality than the last 25 speakers. These were recorded in Nutley, NJ [1]. Due to varying recording equipment causing drastic recording quality differences after session 5, sessions 1 - 5 are experimented separately from sessions 6 - 10. Often KING researchers reference experiments according to this "the great divide." As a comparison to the TIMIT corpus, the utterance in sessions 1 - 5 have an average S+NNR of 14.75 dB, with a corresponding SNR of 14.54 dB, using silence (low probability of voicing frames) as noise levels.

3.2 Feature Extraction

Initially, if the database is resident in binary form, a conversion to ESPS must be performed. This can be accomplished by the ESPS **btosps** utility. For compressed data, the following sample shell is provided.

```
zcat file.Z | btosps -f 8000 -t SHORT -c "King to ESPS" - file.sd
```

In order to extract features from the speech sampled waveform, a series of "typical" preprocessing steps will be taken. These steps process the data into a form better suited for subsequent analysis and classification. These initial steps include the following.

- Pre-emphasis filtering (for cepstral)
- Window selection
- Framing

The concept of preemphasis accentuates the high frequencies components, and reduces large low frequency components in the speech signal. In human voice production, these frequencies are attenuated while speaking and this preemphasis aids in regaining the estimated original values. A typical filter used is $P(z) = 1 - az^{-1}$, where a takes on values such as .90 to .97. The optimum value, however, varies on the time varying speech sounds [80:pg 264]. The plot of $a = .97$ is plotted in Figure 19. When $a = 1$, the emphasis provided is 6dB/octave. Window selection and framing are applied after preemphasis.

[1] Both are sites of ITT Aerospace, performing under government contract [34].

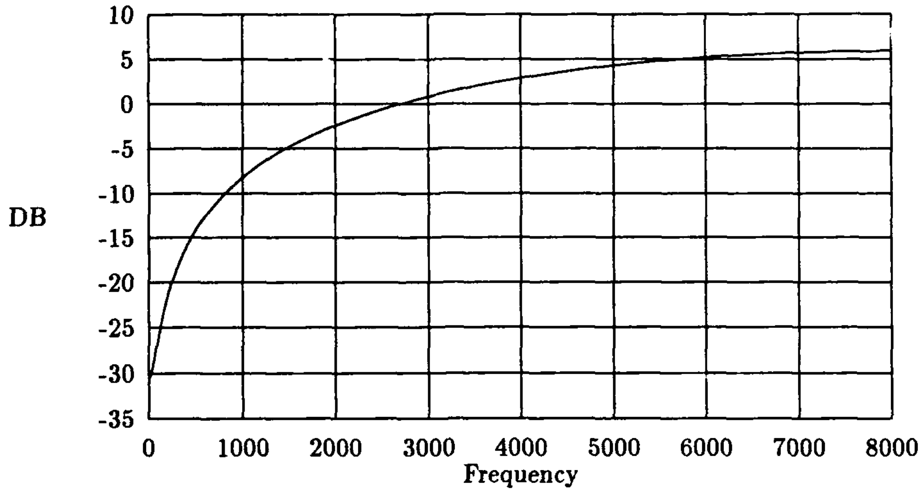

Figure 19. Preemphasis Filter

Window types available under ESPS include Rectangular, Hamming. Hanning, Cosine[4], and Triangular. The choice, if any are needed, d‹ pends on the application and the effects of window function when taking a transform, such as the DFT. Frame sizes for speech are based on assumptions of a sta ıơr ary speech signal. Typical valid assumptions for speech stationarity r.nge up to 50 - 70 msec. Lastly, a frame rate must be determined, which can be different than the frame size. This method involves stepping the frame iteratively to overcome the shortfalls associated with the window edges. Typical numbers often seen in the literature have a frame rate of one half to one third the frame length. This thesis uses a 256 sample window, and a step size of 85 samples on the TIMIT [74] database, sampled at 16 KHz. Thus, frame length is 16 msec and step size of 5.3 msec. The experimentation on the KING database, sampled at only 8 KHz, also used these same frame and step sizes, for a frame length of 32 msec and step size of 10.6 msec.

3.2.1 LPC Cepstral This thesis follows Parsons [80] rule of thumb for LPC (cepstral) order. For TIMIT, 20th order LPC cepstral coefficients were examined. For the KING database, 10th order LPC cepstral was used; however, the effects of 20 cepstral coefficients will be tested. It has been shown that cepstral order greater than LPC order has improved speech recognition [78].

The LPC Cepstral representation is easily accessible using the ESPS window command **xacf**, acoustic feature extraction. This provides an X-Window interface for the many parameters needed by the signal processing commands. Each of these features can also be obtained from the UNIX command line, or through ESPS library programming support. Such ESPS commands include **fft, fftcep** and **refcof | spectrans -m”CEP”** for representations of DFT, Cepstral(real and complex) and LPC cepstral. The method used in this thesis, uses the following pipelined ESPS utilities.

```
filter -Ppreemp_params file.sd - | refcof -P Prefcof - - |spectrans
-m "CEP" - file.cep
```

The two parameter files needed are the pre-emphasis filter coefficients and the specific LPC analysis parameters. The typical pre-emphasis is as follows.

```
# @(#)preemp_params     1.1 6/3/88 ESI
# parameter file for preemphasis with filter(1-ESPS) program
# for use with lpc analysis .. refcof or lpcana
#
float   filter_num = {1.0, -0.97}: "Preemphasis filter numerator";
float   filter_den = {1.0}: "Preemphasis filter denominator";
int     filter_nsiz = 2: "Number of numerator coefficients";
int     filter_dsiz = 0: "Number of denominator coefficients";
```

The specific choice are frame size, step size and LPC procedure is as follows.

```
# @(#)Prefcof   1.6 3/28/90 ESI
# default parameter file for refcof
int start = 1: "First point to process";
int nan = 0: "Number of points; 0 means continue to EOF";
int frame_len = 256: "Number of points per analysis frame; 0 means nan";
int step = 85: "Number or points between start of successive frames;
0 means frame_len";
string window_type = "HAMMING": "Window to apply to data": {"RECT",
"HAMMING", "TRIANG", "HANNING", "COS4"};
int order = 20: "Number of reflection coefficients to compute
per frame)";
string method = "AUTOC": "Analysis method":{"AUTOC", "COV",
"BURG", "MBURG"};
```

Spectral subtraction assumes the noise components are uncorrelated with the speech signal [80]. When using cepstral coefficients, noise effects can be deemphasized through a liftering procedure [42]. Bandpass liftering applies a raised sinusoid to the cepstral representation. The window applied is defined as follows.

$$w(k) = 1 + (L/2)sin(\pi k/L)$$

where $k : (1 \leq k \leq L)$ are the cepstral coefficient index. Juang refers to this procedure as accentuating formants of the signal. Other liftering techniques include rectangular and linear windows [42] and filtering temporal aspects of the coefficients, RASTA [46]. It has been included in the pre-precessing for speaker identification effectively [94, 95] yet, has also been shown to not improve speech classification [78].

3.2.2 Payton Model The integration of the Payton model with ESPS data structures can be accomplish through the following method. This chain of pipes demonstrates the the power of ESPS's implementation of UNIX capabilities.

```
copysd -s 4000 -d FLOAT infile.sd - | bhd - -| fast | btosps
        -f 16000 -n 20 -t FLOAT -c "Payton to ESPS" - outfile.payton
```

Taking the sampled data (.sd) file *infile.sd*, **copysd** will scale the inputs by 4000 and convert their data type to FLOAT. Typically, ESPS sampled data is SHORT integers. The **bhd** function "be-heads" the ESPS header information at the beginning of the file, leaving a

Table 5. TIMIT Energy Characteristics

	Minimum	Maximum	Average
TIMIT energy	6.87×10^4	1.93×10^6	3.91×10^5

series of raw FLOAT data samples. The single executable, **fast**, performs all Payton stages providing as output, 20 channel raw FLOAT data corresponding to auditory nerve firing rates. An ESPS header is added and this raw data is parsed into *outfile.payton*, by **btosps** - "Binary to ESPS." The number of channels (20), frequency (16 KHz) and comments are required as parameters for this final function.

It was determined that using TIMIT files directly converted to ESPS sampled data files (.sd) did not "drive" the auditory model adequately. This can be described as the model using very quiet or faint speech signals, which would barely cause neural firing above spontaneous rate. Payton references 0 dB relative to the signal strength necessary to drive a 1 KHz synapse to threshold, a firing level equal to 10% of the neurons dynamic range. The dynamic range and threshold for this neuron is shown in Chapter III, Figure 14. Various levels of a 1 KHz sinusoid, ranging from 1 Peak - 3×10^6 Peak level, were input to the model to determine the RMS values needed to obtain 0 dB. Approximately 75.5 spikes/sec (average) for the 1 KHz synapse required a 2×10^4 Peak sinusoid, with corresponding RMS energy of 2×10^8.

The subset of TIMIT utterances in these experiments ranged in RMS energy according to Table 5. Since conversational speech typically falls into 60 - 70 dB above 0 dB SPL (hearing threshold), it was determined to apply an appropriate gain to the TIMIT utterances before being input to the model. Initial experiments for phoneme recognition using a gain of 1,000 demonstrated great performance increases [6]. This thesis used a gain of 4,000 for the TIMIT utterance, placing the average RMS power at 45 dB relative to the Payton model's reference. The maximum RMS energy utterance then corresponded to a Payton model reference of 52 dB.

The issue of correct gain for the Payton model was also addressed in the KING experimentation. Since the KING sessions are separated by "the great divide", RMS

Table 6. KING Energy Characteristic; Average taken over sessions 1 - 5.

	Minimum	Maximum	Average
KING energy	2.04×10^3	4.69×10^5	5.5×10^4

energies were calculated within these two divisions separately. See Table 6 for session 1 - 5 ranges. Also, this thesis does not experiment with sessions 6 - 10. A gain of 8,000 was used before auditory model processing, resulting in a model level of approximately 42 dB.

Since the KING utterances are typically over 45 seconds long, Payton's computational complexity became an issue. The current model processes one second of speech in about 1000 seconds. A single 60 second utterance was taking upwards of 18 hours to process on a SUN SPARCstation 2. A windowing technique was performed which calculated the greatest consecutive 15 seconds of voiced speech using probability of voicing, examined at steps of 5 seconds. This used the developed **getmax_window** utility. Prior, the probability of voicing was tagged to each frame using ESPS **formant** command [79]. The Payton model could process this window in approximately five hours [2].

3.3 Clustering Methodology

Using the above feature vectors, codebooks can be created for each speaker using a series of training utterances. These do not have to been text dependent, since the clustering process will cluster individual "phonetic" sounds together. Once completed, a single multi-speaker codebook file is created by merging all individual speaker codebooks for each different size. ESPS provides the function **addclass** which appends records from one codebook file into another.

Test vectors were compared to this single multi-speaker codebook by determining the mean distortion over all frames to each individual This procedure uses **vqdst** which takes an input file of test vectors and a codebook and produces an ESPS distortion file. This ESPS utility calculates mean squared distortion. The developed utility **vq_distortion** can

[2] Armstrong Laboratory is currently porting this code onto four AT&T Digital Signal Processing chips, as well as examining code optimization strategies.

be used to calculated weighted cepstral, Mahalanobis, root power sums and dot product. Both commands create an ESPS FEA_DST type file. The command **vqclassify** will read this distortion file and present average distortions over the entire sentence and select the "winning" speaker whose codebook acquired the minimum distortion. Selected portions of the distortion file, such as source codebook and overall distortion can be easily extracted using **fea_print**, allowing further analysis of the speaker distortions in plain ASCII form.

The initial tests on TIMIT were performed training on both *sa1* and *sa2* sentences and quantizing two separate codebooks for each speaker by selecting VOWELS and non-SILENCE respectively. Varying sizes of these two codebooks were designed at rates of 4 to 9, to examine the stability of identification as a function of codebook size, Figure 20. Test sentences came from the remaining eight sentences, 5 *sx* and 3 *si* per each speaker.

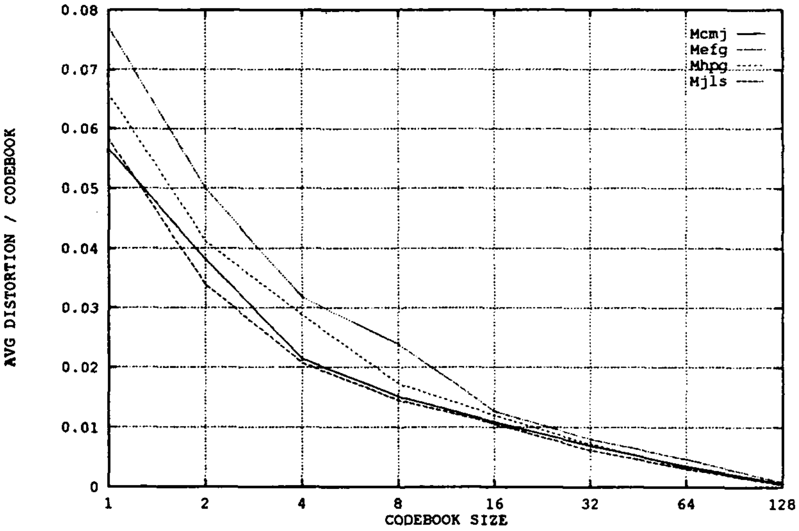

Figure 20. Four Speakers Distortiou with varying codebooks, using TIMIT vowels.

Distortions were calculated for these 80 different sentences to the two different codebooks of four sizes. These 640 total classifications resulted in 100% correctly classified. Figure 21 depicts the typical procedure used throughout this thesis.

The distortion plots in Figure 22 and Figure 23 show an example of the figure of merit between speaker dependent codebooks. The values are mean distortion per speaker

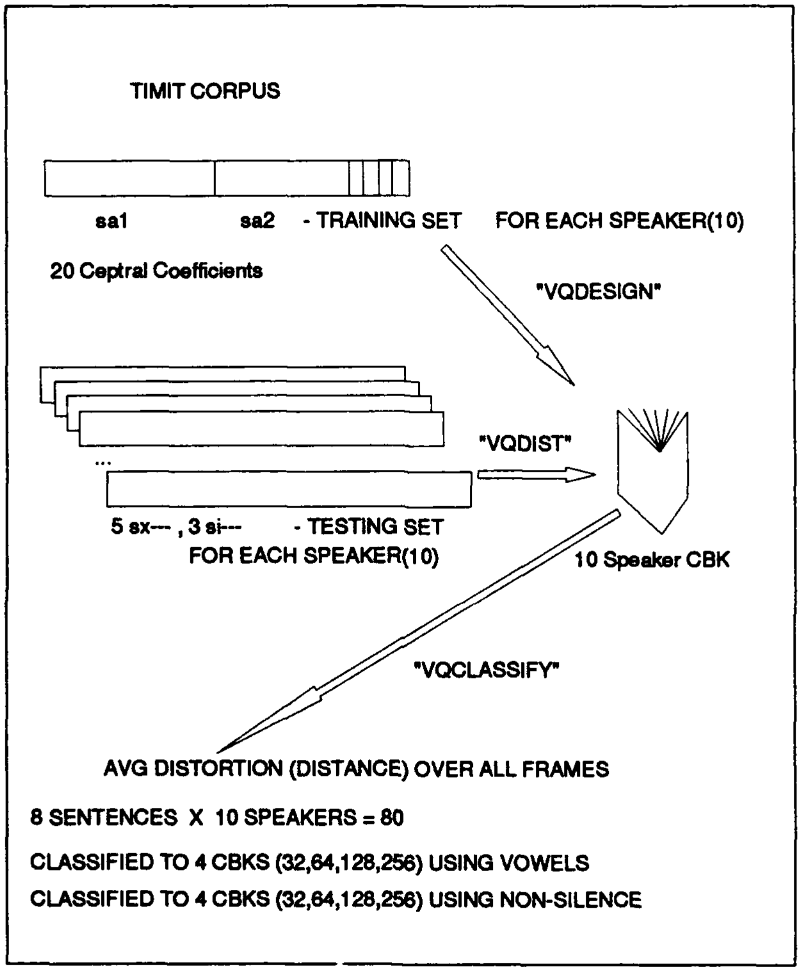
TIMIT CORPUS
sa1
sa2
- TRAINING SET
FOR EACH SPEAKER(10)
20 Ceptral Coefficients
"VQDESIGN"
"VQDIST"
...
5 sx---, 3 si---
- TESTING SET
FOR EACH SPEAKER(10)
10 Speaker CBK
"VQCLASSIFY"
AVG DISTORTION (DISTANCE) OVER ALL FRAMES
8 SENTENCES X 10 SPEAKERS = 80
CLASSIFIED TO 4 CBKS (32,64,128,256) USING VOWELS
CLASSIFIED TO 4 CBKS (32,64,128,256) USING NON-SILENCE

Figure 21. Vowel and Non-Silence Tests. This similar procedure will be used for all following tests. Combine training utterances; choose broad classification (or probability of voicing); design speaker dependent codebooks; calculate overall distortion for the test utterance using a full search through all codebooks. Minimum distortion determines classification.

codebook. The various plots are for the different size codebooks. Notice the relatively flat distortion values across speakers in Figure 22. This may be attributed to silence and high frequency noise, such as fricatives or plosives, using codevectors unproductively. Figure 23, however, shows "minimum valleys" clearly corresponding to the correct speaker, when using only vowels - high probability of voiced speech.

Codebooks of 64 vectors will be used subsequently, as well as extraction of voiced areas of the utterances for both training and testing. Typical values often seen in the literature for codebook sizes range from 32 to 256. [45, 46, 68, 113].

A figure of merit used for quantization design is quantization signal-to-noise ratio QSNR. This thesis examines this ratio to compare the effects of various quantizer parameters on overall codebook generation. If an original utterance contains N vectors x_i, quantized by $\hat{x}_i$, then QSNR is calculated as the signal power divided by the quantization distortion power [127].

$$QSNR = \frac{\sum_{i=1}^{N} x_i^2}{\sum_{i=1}^{N}(x_i - \hat{x}_i)^2} \tag{45}$$

As an example, a comparison of QSNR for quantizing TIMIT cepstral coefficients is shown in Table 7.

Table 7. TIMIT comparison of quantization distortions. TRAINING refers tc the *sa1* and *sa2* sentences, TEST refers to averaged *sx* sentences.

	male		*female*	
	TRAIN	*TEST*	*TRAIN*	*TEST*
Kohonen	12.60	8.93	9.15	9.15
LBG	12.52	8.70	9.90	8.27

3.3.1 LBG Design The ESPS command **vqdes**, provides the LBG algorithm creating codebooks of sizes 2^{rate}, where $rate = 1 \ldots 8$ due to the splitting procedure. An example of the design process with a two dimensional gaussian, standard deviation $\sigma = .5$ with mean located at $(0, 0)$, is shown in Figure 24.

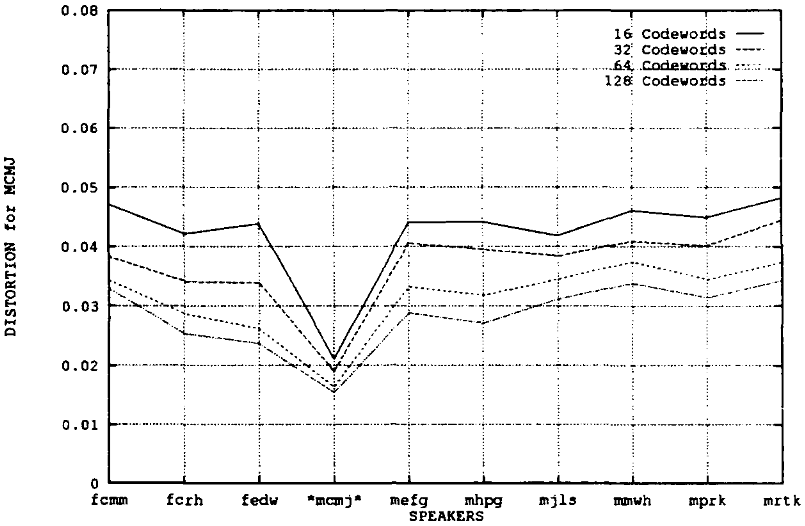

Figure 22. TIMIT speaker "mcmj" utterance showing distortions to all speaker dependent codebooks (LBG) using all speech. Note the low Figure of Merit for the winning codebook.

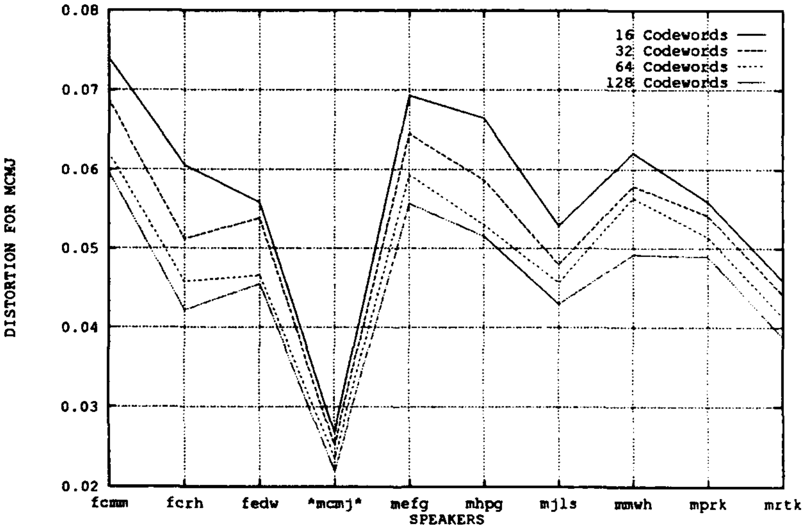

Figure 23. TIMIT speaker "mcmj" utterance showing distortions to all speaker dependent codebooks (LBG) using vowels. Note the higher Figure of Merit for the winning codebook.

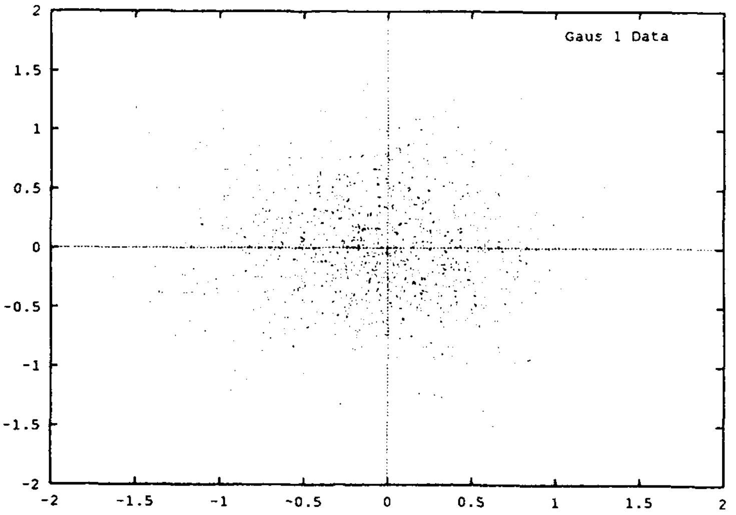

Figure 24. Gaussian Data Source, $\mu = (0,0)$ and $\sigma = 0.5$.

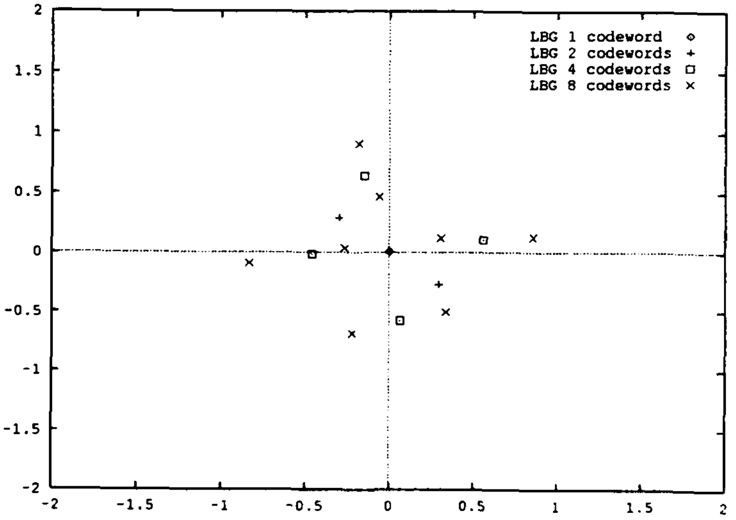

Figure 25. LBG Algorithm Quantizer Design, 1 to 8 codebooks, $\mu = (0,0)$ and $\sigma = 0.5$.

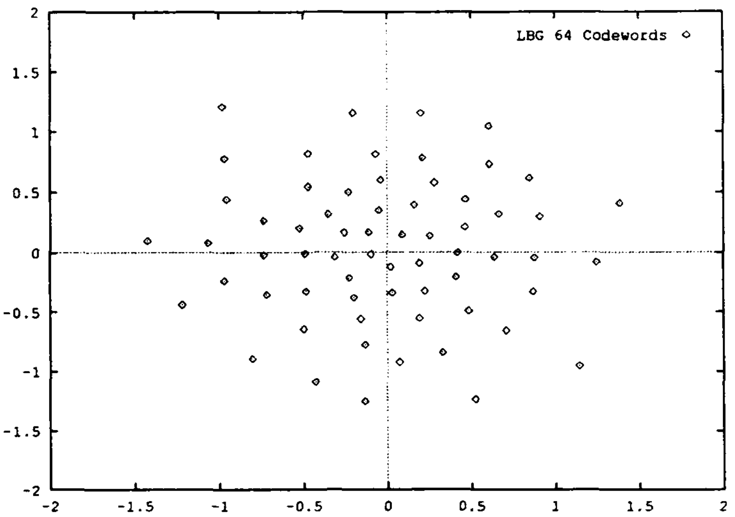

Figure 26. LBG Algorithm Quantizer Design, Final 64 codebooks, $\mu = (0,0)$ and $\sigma = 0.5$. Quantization SNR = 15.5 dB.

3.3.2 Kohonen Design Initial Kohonen tests used an 8 x 8 feature map, for fair comparisons to an LBG 64 vector codebook. The developed ESPS utility **vqdes_koh** takes as input an ESPS feature file and outputs a FEA_VQ codebook file, using a parameter file with the Kohonen design specifics. The weights were initialized uniformly to random values between -.5 and .5. The learning schedule most often used was similar to Figure 28, developed in AFIT Neural Graphics code [91]. The effects of learning iterations on QSNR is shown in Figure 27.

Examples of the various Kohonen and competitive learning paradigms, using the data set depicted in Figure 24 are shown in Figures 29, 30 and 31.

The Kohonen design, which maintains neighborhood associations, is shown in Figure 29. Qualitative analysis shows more nodes within regions of higher density. This is in disagreement with DeSieno's statement [20] that Kohonen learning often models areas of low density, though a null neighborhood was use in his experiments. It is intuitive that the neighborhood may pull many more nodes toward dense areas with increased learning in those areas.

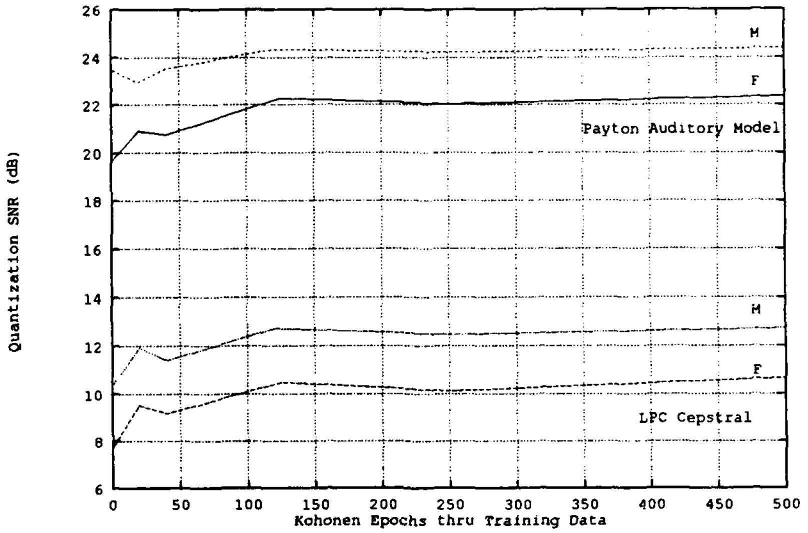

Figure 27. Kohonen learning for a TIMIT male(M) and female(F) speaker for varying iterations (epochs) for LPC cepstral and also Payton. Quantizer "learns" in the first 100 epochs then stabilizes.

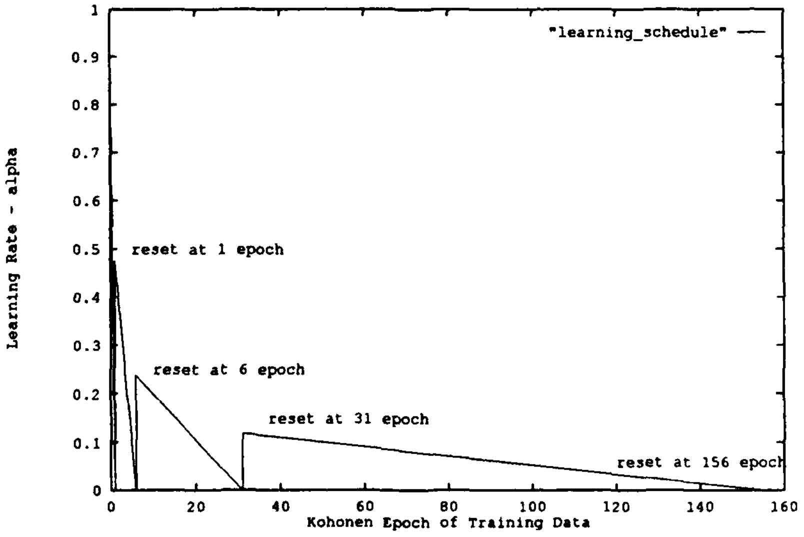

Figure 28. Kohonen learning schedule

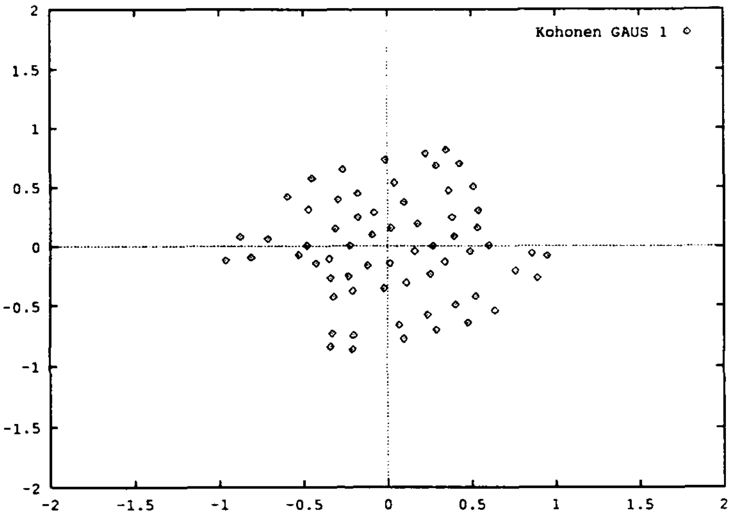

Figure 29. Kohonen Learning Algorithm run for 100 epochs, 64 codewords, for a single 2D gaussian with $\mu = (0, 0)$ and $\sigma = .5$. Quantization SNR = 11.13dB

Figure 30 demonstrates incorporation of DeSieno conscience. The value of the conscience B variable was chosen as .0001. The optimal value of B should be $1/(t+1)$, where t is iteration. Since this function decays exponentially, a value should be chosen based on iterations and training size. Though no analysis was given by DeSieno on values of the conscience variable C, an intuitive choice may be based on average standard deviation. Various values of σ, 2σ and $\sigma/2$ were examined. Slightly better QSNR were seen in this example for $\sigma/2$.

The effects of a null Kohonen neighborhood was examined (Figure 31). This competitive learning demonstrated better quantization of the training data than the basic Kohonen learning or the addition of conscience. It will be shown that this non-neighborhood preserving quantizer will demonstrate similar improved performance on 20 dimensional speech data.

3.3.3 Fusion Techniques Recent articles have addressed the analysis of combining (or fusing) various classifiers [123] as well as features themselves. Combining features often results in classification of a larger dimensional space, where problems of sparseness

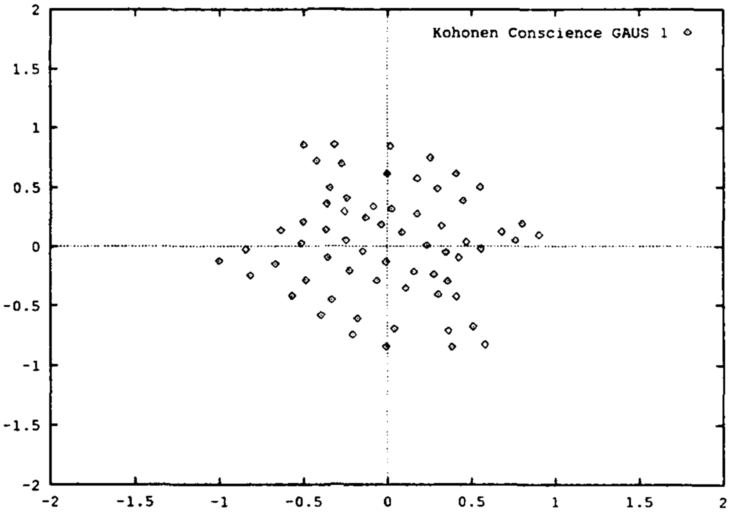

Figure 30. Same as Figure 29 with DeSieno conscience, conscience parameters B and C were .0001 and .1 respectively, for a single 2D gaussian with $\mu = (0,0)$ and $\sigma = .5$. Quantization SNR = 11.32dB.

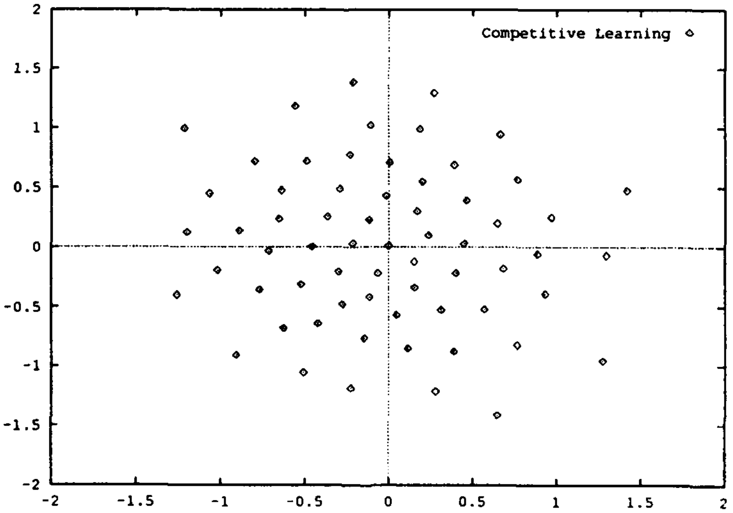

Figure 31. Kohonen / Competitive learning, 64 codewords, for a single 2D gaussian with $\mu = (0,0)$ and $\sigma = .5$.. Quantization SNR = 15.93dB.

can hinder results. Some researchers particularly strive to reduce the dimensionality of the feature space - such a technique is appropriate choice of Karhunen-Lueve or any principle component analysis. Xu [123] summaries several techniques concerning combinations of multiple classifiers. Several of these techniques were examined. For a detailed analysis on other fusion techniques, see AFIT thesis by Geurts [24].

3.3.3.1 Probabilistic Classification Currently, Vector Quantization can be used as a classifier using some given distortion metric. Since the goal is to chose the maximum likely class i, a conversion to distortions from classifier k must be converted to "post-probabilities." Xu suggests one simple procedure [123].

$$p_k(i) = \frac{1/d_k(i)}{\sum_{i=1}^{M} 1/d_k(i)} \tag{46}$$

given M different class distortions, $d_k(i)$.

3.3.3.2 Average Fusion The overall fused post-probabilities can then be averaged over all classifiers.

$$P_A(i) = \frac{1}{K} \sum_{k=1}^{K} p_k(i) \tag{47}$$

3.3.3.3 Linear Combination The individual classifiers can be combined be first appropriately weighting the post-probabilities. A similar technique was examined by Soong [114] in combining instantaneous and delta cepstral codebook distortions. This was recently seen in [118].

$$P_W(i) = \sum_{k=1}^{K} W_{k,i} p_k(i) \tag{48}$$

Soong examined the two classifier case (K = 2) combining normalized distortions.

$$d(i) = \alpha \frac{d_I(i)}{D_I} + (1 - \alpha) \frac{d_\Delta(i)}{D_\Delta} \tag{49}$$

The denominators are normalization terms which are averaged "intra-speaker distortions." These weights may be determined by the classification performance of the individual classifiers [6] or more intuitively, the figure of merit of the individual classifier distortions. This latter is examined by Geurts [24] given as

$$W_{k,i} = \rho + .1(confidence) \tag{50}$$

where $0 < confidence \leq 100$, which can be related to figure of merit. A slight modification to this weighting approach uses the inverse of figure of merit. Defining FOM for class i,

$$FOM_k(i) = \frac{d_k(i)}{\min_{j \in M}\{d_k(j)\}} \tag{51}$$

then,

$$W_{k,i} = 1/FOM_k(i) \tag{52}$$

3.4 Conclusion

This chapter provided the methodology for feature extraction, quantization, and classification. An initial examination at the recording quality of the two principle databases shows the contrasting noise levels. Also, examples of quantization distortions on a two dimensional gaussian source provided insight into the possible effects of Kohonen neighborhood. Classifier fusion techniques were introduced. All signal processing, and data manipulation were performed using Entropic ESPS functions or developed compatible utilities. The following chapter details the recognition accuracies using these quantization and fusion techniques.

IV. Experimentation/ Results

Automatic Speaker Recognition experiments were initially performed on a subset of the speaker corpus contained in TIMIT [74]. Later tests focused on the KING database [59] which provides a more realistic environment for Air Force applications [89]. Additionally, AFIT recording were taken for examination of fusion technique with facial imagery. This chapter examines the recognition results of this data using the methods defined in Chapter III.

4.1 TIMIT Experimentation

Initial TIMIT classification results demonstrated perfect identification for the ten speakers using cepstral coefficients, at codebook levels of 32, 64 ,128 and 256 and using either selected VOWELs or non-SILENCE frames. For further tests, varying degrees of additive white gaussian noise (AWGN) were added to the test utterances. This was accomplished by first creating a gaussian white noise test signal using ESPS **testsd** then added this new signal to the original. A typical command for adding an RMS level of noise to 16 KHz sampled data is provided.

```
testsd -l RMS_NOISE_LEVEL -f 16000 -t SHORT file.sd - |
addsd - file.sd noisey.sd
```

Recognition results were performed for cepstral at SNR levels of 3dB, 10dB, 15dB, 20 dB, 25dB, 30dB, and uncorrupted. Results for the two quantizers are shown in Figure 32. Each provides similar performance, showing the non-generalization of distortion-based approaches using unprocessed LPC cepstral coefficients.

For Payton, added white gaussian noise was processed on the test files at the SNR level of 10 dB only. These results are shown in Table 8 and 9 and compared to cepstral. This was expected since the training data set was not representative of the test set. Thus, both feature representations could not generalize to the added noise.

Lastly, delta coefficients [56], which have been shown to provide uncorrelated information to "instantaneous" cepstral were also extracted and quantized. A window of ap-

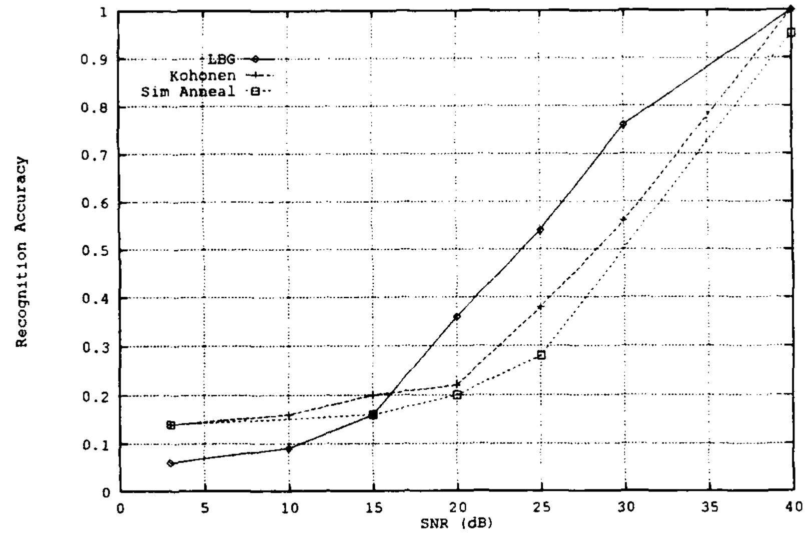

Figure 32. Recognition Performance of TIMIT LPC cepstral, using Kohonen SOFM and Linde-Buzo-Gray quantizing algorithms (Simulated Annealing design by Zeger [127] also shown.) Trained on *sa1* and *sa2* sentences, trained on *sx*.

Table 8. TIMIT Database: Speaker classification. Trained on *sa1* and *sa2*, tested on *sx*.

Classifier	LPC Cepstral	Payton Model
Kohonen	100%	76%
LBG	100%	90%

proximately 100 msec [114] (±8 TIMIT frames) was used for the delta operation. These results are shown in Table 10.

This section provided the initial procedures which will further be examined on the KING corpus. Current speaker recognition researchers prefer the KING database. The recordings are not prompted; the long distance telephone characteristics are dynamic; the recording equipment quality changed drastically after half the data base was obtained, and the multiple sessions capture varying intra-speaker distortions.

The key aspects learned from initial TIMIT experimentation are as follows. LPC cepstral, the proven technique performs perfectly (i.e. 100% classification) in clean speech. It also drops greatly in increasing noise environments. While the Payton model did good

Table 9. TIMIT Database: Speaker classification. Trained on *sa1* and *sa2*, tested on *sx* with 10dB AWGN.

Classifier	LPC Cepstral	Payton Model
Kohonen	16%	22%
LBG	9%	30%

Table 10. TIMIT Database: Speaker classification. Delta coefficients using an approximate 100 msec window (± 8 frames). Trained on *sa1* and *sa2*, tested on *sx*.

Classifier	LPC Cepstral	Payton Model
Kohonen	64%	22%
LBG	94%	66%

(90% using LBG) for clean speech, it's performance still dropped markedly. The information contained in delta (transitional) representations contains speaker dependent information. The Kohonen SOFM consistly performed below that of the classic LBG algorithm. This can probably be explained by the neighborhood process, which has demonstrated this effect on 2D gaussian data sets. Though Kohonen learning has been referenced as a means to avoid local minima, an incorrect neighborhood may "pull" nodes to more dense regions of the probability density function, resulting in poor "tail" modeling. Also, a two dimensional lattice (neighborhood structure) may not be suitable for these particular test sets. Though results not provided, supervised learning provided by Learning Vector Quantization, distorted class boundaries resulting in slightly decreased QSNR's. Since averaged distortion is used for classification, as opposed to single frame nearest neighbor, LVQ did not provide increased recognition.

4.2 KING Experimentation

4.2.1 10 Class Tests Results obtained are shown in the following tables. Table 11 will be used as the baseline performance for the 10 speaker tests. Additional quantizers using conscience and 3D Kohonen "lattice" were examined. The recognition performance did not improve greatly with these techniques. The parameters of conscience used were

Table 11. KING Database: Speaker classification. Trained on sessions 1 - 3, tested on sessions 4 and 5; 10 speakers.

Classifier	LPC Cepstral	Payton Model
Kohonen	55%	20%
LBG	80%	70%

$B = .0001$, based on DeSieno's [20] work, and a parameter C based on average standard deviation of the training vectors. The three dimensional Kohonen uses a 4 × 4 × 4 cube, with 3D radial neighborhood. The use of the incremental Kohonen learning without neighborhood will be examined and referred to as "Competitive Learning." Slight improvement over Kohonen learning has been demonstrated with this technique, shown with .95 and .5 initial learning rates. Other parameters of the Kohonen learning remained unchanged. Results are shown in Table 12.

Table 12. KING Database: Speaker classification. Trained on sessions 1 - 3, tested on sessions 4 and 5, Kohonen Modifications; 10 speakers.

Classifier	LPC Cepstral	Payton Model
Kohonen w/ Conscience	55%	25%
Kohonen 3D 4x4x4	50%	40%
Competitive (.95)	63.3%	40%
Competitive (.5)	55.0%	60%

The effect of varying probability of voicing changes recognition slightly for LBG quantization. The ESPS **formant** command, based on Secrest and Doddington's [79, 107] pitch tracking algorithm, often assigns a very small (< .1) or very large (> .9) probability of voicing value. Thus, the additional number of frames changed marginally by using low probabilities for training. These extra frames (typically on voiced-unvoiced boundaries) may have aided Kohonen's incremental learning in spreading out of dense codebook areas. See Table 13.

The effects of Payton normalization schemes and Kohonen training are shown Tables 14 and 15 respectively. Normalization did increase performance for the Payton model.

Table 13. KING Database: Speaker classification. Trained on sessions 1 - 3, tested on sessions 4 and 5. Probability of Voicing Influence on the Payton Model; 10 speakers.

Classifier	.1 PV	.3PV	.5 PV	.7 PV	.9 PV
Kohonen	40%	30%	30%	30%	20%
LBG	70%	80%	70%	70%	80%

Performing a zero mean across vector elements of auditory vectors has been seen in the literature [32].

Table 14. KING Database: Speaker classification. Trained on sessions 1 - 3, tested on sessions 4 and 5. Normalization Influence on the Payton Model.

Classifier	Remove Mean/Feature	Zero Mean Vectors
Kohonen	30%	35%
LBG	60%	85%

Table 15. KING Database: Speaker classification. Trained on sessions 1 - 3, tested on sessions 4 and 5. Kohonen Training Time Influence on the Payton Model.

Classifier	40 Epochs	120 Epochs	250 Epochs
Kohonen	20%	50%	50%

A series of delta coefficients, as reviewed in Section 2.2.2.5 were extracted from the KING instantaneous cepstral vectors. No documentation has been reported on successful use of temporal characteristics on the KING narrowband corpus. Again for cepstral, a 100 msec window was used [114], resulting in a ±4 frames in calculating the new coefficients for the cepstral coefficients. Performance increases over instantaneous cepstral were demonstrated. A series of delta windows were examined for the Payton model, shown in Figure 33. This new technique for the auditory model captures temporal firing information without specifically calculating neural pulse trains. Since it has been shown that delta cepstral contains uncorrelated information to that of instantaneous cepstral, this technique was applied to Payton. Best results are evident for the ±2 frame delta, or approximately 60 msec window.

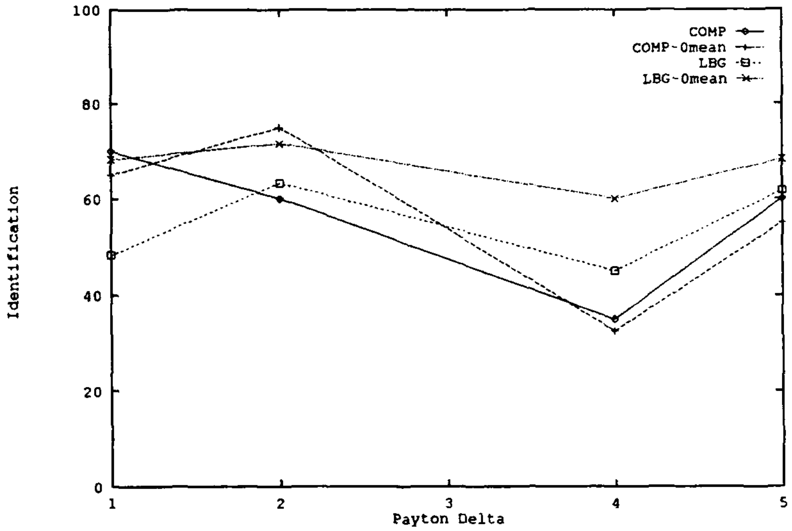

Figure 33. KING Database: Speaker Recognition using delta Payton auditory model coefficients. Shown are Competitive learning and LBG on both Payton and Payton zero-mean normalization; 10 speakers.

Normalization and liftering techniques were applied to the 10 speaker tests. A recent article [46] reported increases with liftering techniques on cepstral coefficients, both on individual vectors using bandpass liftering, and temporally over sequences of vectors using RASTA liftering. The results of bandpass liftering [42] and mean removal [8] are shown in Table 17.

Lastly, the higher frequency Payton channels were removed, since these model basilar membrane locations having characteristics frequencies greater than 4 KHz. Many other auditory models target the lower formant frequencies, thus providing greater resolution in the typical speech frequecies. These 15 coefficients (Table 18) provide comparable recognition to the best cepstral representation of 95%.

4.2.2 26 Class Tests Typically classifier performance can be expected to drop as the number of classes increase. This can be attributed to greater overlap of classes in the

Table 16. KING Database: Speaker classification. Delta cepstral coefficients using an approximate 100 msec window (± 4 frames), with various normalization. Trained on sessions 1 - 3, tested on sessions 4 and 5; 10 speakers.

Classifier	None	Zero Mean	Remove Time Average
Kohonen	25%	20%	20%
LBG	95%	90%	90%

Table 17. KING Database: Speaker classification. Trained on sessions 1 - 3, tested on sessions 4 and 5. Cepstral Normalization and BandPass Liftering procedures; 10 speakers.

Classifier	Remove Mean	Liftering
Kohonen	70%	55%
LBG	70%	75%

Table 18. KING Database: Speaker classification. Trained on sessions 1 - 3, tested on sessions 4 and 5. Effects of 15 low Characteristic Frequency Payton coefficients; 10 speakers.

Classifier	20 Payton coefficients	15 Payton coefficients
LBG	70%	95%
Competitive (.95)	40%	45%
Competitive (.5)	60%	50%

feature space; i.e. probability density function overlap of the training sets. All 26 speakers, (San Diego, CA) were quantized. Initial results dropped markedly as shown in Table 19.

Table 19. KING Database: Speaker classification. Trained on sessions 1 - 3, tested on sessions 4 and 5. Effects of ALL San Diego speakers.

	10 Speakers		26 Speakers	
Classifier	LPCC	Payton(0)	LPCC	Payton(0)
Kohonen	55%	20%	36%	40%
LBG	80%	70%	42%	44%

Often, KING researchers use over 14 coefficients on this 8 KHz database. Paliwal [78] noted that increased cepstral order over that of LPC order, though providing no new additional information, increase speech recognition performance. Twenty coefficients were examined and compared to 10 coefficients in Table 20.

Table 20. KING Database: Speaker classification. Trained on sessions 1 - 3, tested on sessions 4 and 5. Effects of number of cepstral coefficients; 26 speakers.

Classifier	10 LPCC coefficients	20 LPCC coefficients
Kohonen	36%	54%
LBG	42%	60%

This decrease in recognition can probably be attributed to the choice of voicing probability algorithm used throughout this thesis. As stated, the ESPS **formant** command is "related to the one described" by the dynamic programming pitch tracking algorithm of Secrest and Doddington [107]. Since voicing probability is a by-product of this method, higher probability regions exist only in areas with pitch, or *voiced* speech. This method neglects many other phonetics belonging to *voiced* areas such as fricatives. Therefore, a more encompassing selection algorithm would be one providing a speech/ non-speech probability estimation.

4.2.3 Fusion Results The results for combined "speaker-listener" fusion are presented in Tables 21 and 22. The Figure of Merit weighting, often provided the same results to that of average weighting. Also, the final classification correlates to the highest attainable level by the single best classifier alone. This was true for both the 10 speaker and 26 speaker tests (Table 23).

4.2.4 Speaker Verification A series of codebooks were designed to perform speaker authentication/ verification. Typically, a single speaker dependent codebook is created per speaker and thresholds are varied to evaluate verification performance. An extension to this procedure uses two separate codebooks for each individual. The first uses speaker dependent speech. The second uses speech from a set of targets. For KING, speakers 1 - 13 were used as targets, and speakers 14 - 26 were used as imposters. A similar method of testing was documented by TI [46]. The results are shown in Table 24.

The two features used, cepstral and Payton (zero mean normalization) demonstrated overall equal performance of 88% correct classifications. However, still note the exceptionally high false acceptance rate.

4.2.5 Feature Analysis The effects of normalization improved classification performance for Payton by 15%. This zero mean normalization has been seen in the literature [32] as well as performed on speech recognition experiments in AFIT theses by Stowe [115] and Recla [87]. This normalization effect on codebook generation may be explained on the basis of the Fisher ratio. The Fisher ratio (F-ratio) is a general figure of merit used for feature selection. Parson [80] describes this as "the variance of means over the mean of the variances", assuming a set of training data which can described (clustered) by class. In generalizing speaker dependent codebooks for Parson's training data, a similar Fisher ratio can be developed. This not only provides a measure of the feature representation to separate classes, but may also provide insight into the quantizer design process. Typically, the greater the F-ratio, the better the representation. This application can be described as a measure of inter-speaker class separation over the intra-speaker class compactness. The formulation is,

Table 21. KING Database: Speaker classification. Average and Figure of Merit (FOM) Fusion. Note - PAM is Payton Auditory Model, LPCC is LPC cepstral and (0) represents zero mean normalization; 10 speakers.

Classifier	Average Fusion	FOM Fusion
LPCC + PAM	80%	80%
LPCC + PAM(0)	85%	80%
LPCC + ΔLPCC	85%	85%
PAM + ΔPAM	75%	75%
PAM(0) + ΔPAM(0)	75%	70%
ΔLPCC + ΔPAM(0)	90%	90%

Table 22. KING Database: Speaker classification. Average, Figure of Merit (FOM) and Weighted Fusion. Note - PAM is Payton Auditory Model, LPCC is LPC cepstral and (0) represents zero mean normalization. WEIGHTED uses the recognition accuracy of the individual classifiers for weights in fusion; 10 speakers.

Classifier	Average	FOM	WEIGHTED
LPCC + PAM + ΔLPCC + ΔPAM	90%	90%	-
LPCC + PAM(0) + ΔLPCC + ΔPAM(0)	-	-	95%

Table 23. KING Database: Speaker classification. Average and Figure of Merit (FOM) Fusion. Note - PAM is Payton Auditory Model, LPCC is LPC cepstral and (0) represents zero mean normalization; 26 speakers.

Classifier	Average Fusion	FOM Fusion
LPCC + PAM(0)	50%	50%

Table 24. KING Database: Speaker Authentication. Trained on sessions 1 - 3, tested on sessions 4 and 5; 13 Targer speakers, 13 Imposters.

Classification	LPC Cepstral	Payton Model
False Reject	27.0%	58.0%
False Accept	11.0%	8.88%
True Accept/Reject	88.0%	88.0%

$$
\begin{aligned}
F &= \frac{\sqrt{\frac{1}{S}\sum_{s=1}^{S}\sum_{d=1}^{D}(\mu_{s,d}-\bar{\mu}_d)^2}}{\frac{1}{S}\sum_{s=1}^{S}\sqrt{\frac{1}{K}\sum_{k=1}^{K}\sum_{d=1}^{D}(c_{s,k,d}-\mu_{s,d})^2}} \qquad (53)\\
\text{where } S &= \text{number of speakers,}\\
K &= \text{number of codewords per speaker codebook,}\\
D &= \text{dimension of codewords,}\\
\mu_{s,d} &= d \text{ dimension of } s \text{ speaker mean,}\\
\bar{\mu}_d &= d \text{ dimension of global mean of all } S \text{ speaker means,}\\
\text{and } c_{s,k,d} &= d \text{ dimension of } s \text{ speaker's } k \text{ codeword.}
\end{aligned}
$$

Table 25 examines several F-ratios on the generated speaker codebooks. The increased figure of merit for the normalized coefficients is the result of a reduced denominator in Equation 53, caused by a reduced average variance per speaker. Note also that Kohonen quantization always produced a slightly higher F-ratio than LBG. This factor is due to a consistently smaller denominator, than that of LBG, possible caused by Kohonen nodes maintaining locations within relatively dense areas of the training set.

Table 25. KING Database: Speaker dependent codebook evaluation with Fisher Ratio [80]

Test Case	LPC Kohonen	LPC LBG	PAM Kohonen	PAM LBG
10 Speaker Baseline	.566	.382	.416	.260
Delta 10 Speaker	.109	.048	.055	.077
Zero Mean 10 Speaker	-	-	.475	.331
Delta Zero Mean	-	-	.104	.062
Remove Mean	.0927	.0736	.210	.091
Delta Remove Mean	.109	.048	.074	.044

Examination of the Payton and cepstral vectors and individual channels (coefficients) for speaker separability was performed; see Figures 34 and 35. Distortion histograms for individual coefficients provided little insight to class separability. The separability of speakers is evident only by averaged distortion over many frames. The goal was to account

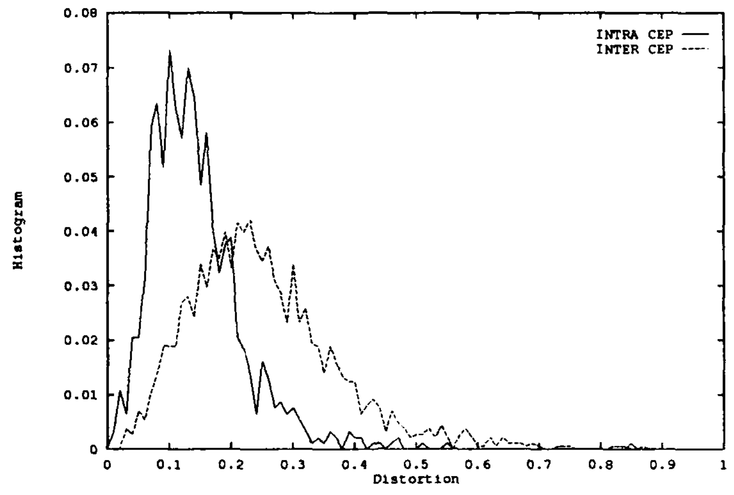

Figure 34. Cepstral Speaker Separability: KING Database: Normalized Histogram of Inter speaker and Intra speaker distortions using three speakers, over four sessions. F-ratio = 0.515

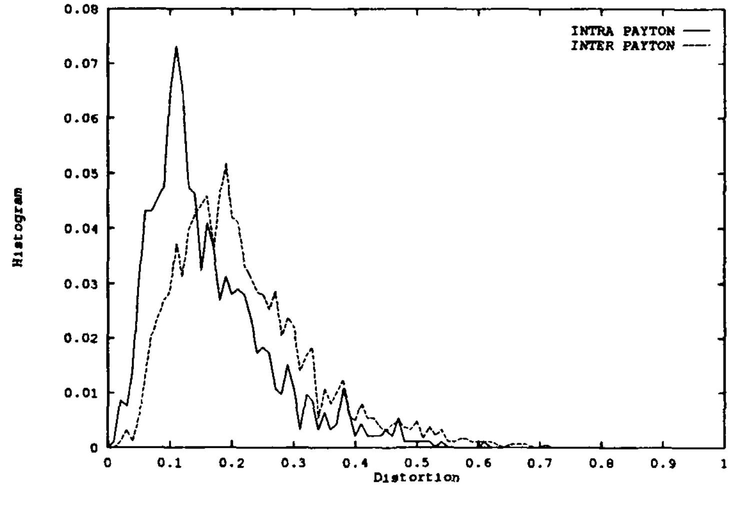

Figure 35. Payton Speaker Separability: KING Database: Normalized Histogram of Inter speaker and Intra speaker distortions using three speakers, over four sessions. F-ratio = 0.124

for potentially improved distortion metric than Euclidean. If certain coefficients could individually separate speakers, these could be used with a particular weighted metric. Overall intra-speaker and inter-speaker distortion histograms re shown for cepstral and Payton (zero mean normalized). The F-ratio between the two classes (inter-speaker and intra-speaker) is given by .515 for cepstral and .124 for Payton.

4.3 AFIT Corpus Experimentation

A concept of "user identification" is being developed which fuses the benefits of both face recognition and speaker verification. This system is envisioned to simultaneous capture facial imagery and require a name or text independent speech samples. Initial speech characterization is provided.

4.3.1 Recording Setup Training and testing was performed for both speaker identity (name) and high phonetical content sentences acquired from the TIMIT Continuous Phonetic Speech Database. A series of four prompted MIT *sx* sentences, two speaker name recording and another speaker name were recorded for ten speakers over a ten day period. The utterances were captured using Entropic Research Laboratory's ESPS pacl-age, specifically using the Ariel PRO-Port Model 656 Stereo A/D Converter. The ESPS command **s32crecord** has been used, with a 16 kHz sampling rate and 16 bit linear coding (SHORTs). A 20th order LPC analysis converted to 20 LPC cepstral coefficient was performed using ESPS **refcof** and **spectrans** functions. The speaker ames were also processes through the Payton auditory model, then mean rate response was calculated on 16 msec frames at a frame rate of 5.33 msec. Speakers are represented by codebooks created using the LBG algorithm using 64 codewords per speaker.

4.3.2 Recognition Results Identification tests were performed by training on either the phonetically balanced (PB) sentences or the speaker names (SN). Testing used either the PB, SN and also the other name utterances. These other names will be used for imposter (IM) verification. Identification results used increasing training sessions and testing on several latter days are provided in Table 26. For example, when examining the Day 6 entries, codebooks were created using all utterances recorded over 6 days, and testing consisted of utterances from Days 7 - 10. Separate codebooks were created for the PB and SN utterances per speaker. For the Payton representation, only speaker names (SN) were processed. This demonstrates how increased sessions used in training consistly improved identification. Since the PB sentences each contain rich phonetic content, it can be inferred that both diversive phonetic frames and many intra-speaker exemplars of these frames over multiple sessions increase identification accuracy. Increased multi-session training sets have also shown to increase face recognition performance, demonstrated in AFIT thesis by Krepp [54]. Note in Table 27 the performance of another's name by an imposter speaker is recognized consistently by the PB codebook, yet is often in error by the SN codebook. This is explained by the rich phonetic content of the training set, when using PB (TIMIT *sx*) sentences. These have been plotted for comparison in Figure 36.

Table 26. AFIT User Identification Database: Speaker Identification using Phonetically Balanced and Speaker Names. Trained over increasing number of days, Tested on several following days; 10 speakers.

Training Time	1 Day	2 Days	3 Days	4 Days	5Days	6 Days	7 Days
Phonetically Balanced	91.87	94.16	96.25	97.5	98.75	99.16	100.0
Speaker Names	92.85	98.33	97.5	95.0	100.0	98.33	97.5
Speaker Names (Payton)	76.50	92.30	96.32	97.41	98.95	98.75	98.33

Table 27. AFIT User Identification Database: Speaker Identification using other names. Trained over increasing number of days, Tested on *several* following days. Same test procedures as Table 26. Other Name (Imposter) recordings were tested on both the PB and the SN codebooks; 10 speakers.

Training Time	1 Day	2 Days	3 Days	4 Days	5Days	6 Days	7 Days
Imposter on SN	30.0	63.3	45.0	40.0	64.0	67.5	70.0
Imposter on PB	87.5	96.7	100.0	100.0	100.0	100.0	100.0

Speaker verification was performed using the method of "Me" and "Not Me" codebooks outlined in Section 4.2.4. Verification was performed for the Speaker "skr" SN codebook while testing on utterances by all 10 subjects stating "skr"'s name. Tests were examined over codebooks designed using increasing training session for the cepstral coefficients only; see Figure 37. Figure 37 demonstrates how the PB sentences provide better verification (0% false reject, 1.66% false accept) than speaker names (6.6% false reject ,11.1% false accept) after 5 training sessions. Also, the imposters using speaker names, even over multiple training days, show more variance in testing accuracy than the phonetically balanced sentences.

4.4 Conclusion

This chapter investigated the use of TIMIT, KING and AFIT recorded databases and the effects of both traditional and neural feature representations using both LBG and Kohonen quantizer design algorithms. The following chapter provides analysis of these results and provides overall conclusions.

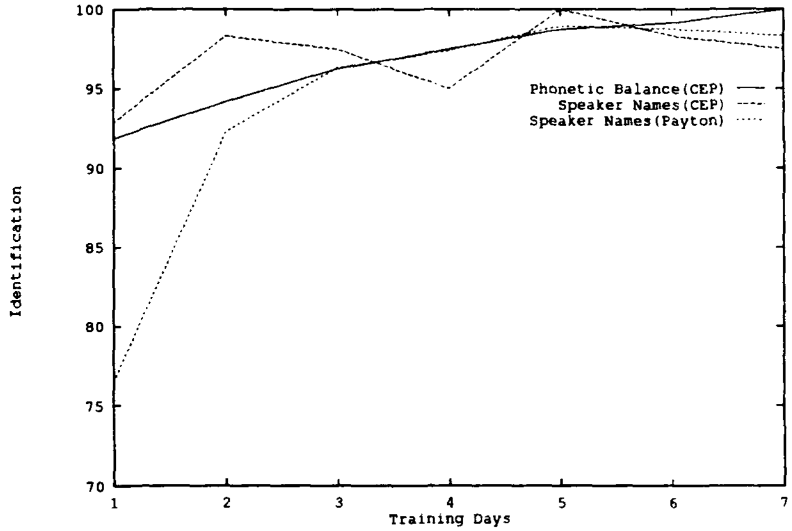

Figure 36. Recognition over increasing training sessions for the AFIT corpus.

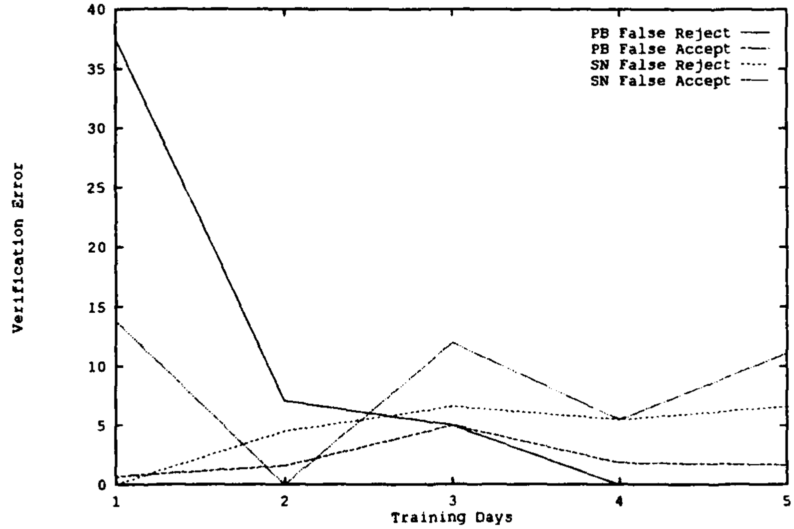

Figure 37. Verification Error over increasing training sessions for the AFIT corpus using cepstral coefficients.

V. Conclusions/ Final Analysis

This thesis compared the current proven LPC cepstral representation to features provided by the Payton auditory model, on a variety of speech databases. Recognition accuracies were compared using Linde-Buzo-Gray and Kohonen Self Organizing Feature Map quantizer designs. The final comparative analysis, overall, is that the two representations achieved similar results. For example, in 10 speaker KING tests, equal accuracies of 95% can be achieved. Similarly, for the AFIT corpus, both representations for speaker name identification achieved upwards of 98% recognition. The reduced recognition of the Payton model on TIMIT by 10% may be the highly efficient representation of LPC cepstral in clean conditions. Several noteworthy conclusions have been theorized during this effort concerning specific aspects of the quantization design, normalization techniques and preprocessing techniques and Payton auditory model implementation.

5.1 Quantization Design/ Classification

Kohonen SOFM consistently provided inferior recognition accuracies than that of LBG. Also, competitive learning demonstrated slightly better recognition results to that of Kohonen. This became evident after much "trial-and-error" experimentation of Kohonen parameters, as well. Kohonen conscience and a 3D Kohonen lattice provided no improvement, and these techniques also currently require a similar adhoc approach to parameter choice. Similar performance in comparing Kohonen with LBG (and other neural quantization technique) was demonstrated by Wu [122].

Past AFIT research by Recla and Stowe [87, 115] only investigated recognition by using the feature map neighborhood preservation qualities. These authors incorporated the speech trajectories through the Kohonen feature map with dynamic programming techniques for speech recognition. Since, overall distortion was used for speaker recognition in this thesis, neighborhood preservation was not beneficial or required. The desired quantizer design was the optimal non-parametric model of the training speech.

Quantizer design is a simple non-parametric approach to modeling the underlying probability density function of the speaker training data. It was recently reported by

Lippmann [61] that many parametric, neural and non-parametric approaches to class pdf estimation provide similar results. The underlying differences are peripheral, such as speed, memory, training time, testing time and storage requirements. Thus, a number of other techniques could have been tried and performance should have been similar. The TIMIT tests clarified the inability of this technique to generalize in added white gaussian noise (AWGN), with recognition rates dropping from 90 - 100% for Payton and cepstral in clean representations to below 30% in 10 dB AWGN. Payton did provide nearly twice the recognition accuracy of LPC cepstral for this series of AWGN tests.

Successful fusion techniques have been demonstrated when differing features can be extracted [87, 115]. Likewise, fusion of classifiers has been demonstrated [24, 123] and may prove more efficient for increased speaker tests. One concern should always be increased dimensionality, which typically increases sparseness within the feature space [91]. Increased recognition was not demonstrated over the best individual classifier. Further analysis on the issue of "user identification" fusion is beginning. This thesis examined fusing information between a speaker model (cepstral representation) and a listener model (auditory features) for recognition. However, the common base between these are the same samples of data. When corrupted, reductions should be seen in both spectral representations. The ability to fuse different representations, such as speech and face imagery, with no common base of information except user identity, could be envisioned as an improved "user identification" system.

Though differenced or delta coefficients were examined within the VQ framework, improved recognition may be evident using models better suited to extract temporal information. These would include recurrent neural networks or the popular Hidden Markov Models. The underlying assumption of this thesis was the evidence of speaker dependent information, available through examination of instantaneous feature vectors or their temporal characteristics. Recent research from AT&T shows instantaneous cepstral providing better recognition than delta cepstral [118]. Based on efforts within this thesis, this transitional information may have characteristics based on speech corpus recording quality or content.

5.2 Preprocessing

Normalization is always an important step in typical neural processing and classification. The effects of statistical normalization, removal of long term averages, insuring each vector has zero mean (across elements) as well as energy normalization have each been examined on the Payton auditory vectors. Using the LBG algorithm, performing a zero mean normalization attained 85% recognition for Payton, and further reduction of vector dimension to 15 coefficients attained 95% recognition.

Liftering provided no significant improvements on the 10 or 26 class KING tests. This procedure, typical of filtering in the cepstral domain, can be regarded as a de-emphasis of certain coefficients. In bandpass liftering, this procedure attenuates the low and high order coefficients. Alternatively, a weighted Euclidean distortion metric could be used. Examination of a form of neural spectral subtraction was performed on the TIMIT AWGN tests, yet no improvements can be reported. A type of emphasis (like band-pass liftering) may be done on the raw speech *before* input into the model to compensate for broad outer ear effects [103, 112]. The Payton coefficients were examined for their saliency [97] to provide inter-speaker separation. Histograms of inter-speaker and intra-speaker codebook distortions were examined, yet coefficients individually provided no class separability. Only when using the average distortion over an ensemble of vectors did separability become evident.

Lastly, temporal filtering on the cepstral vectors may have an analogy when examining the temporal aspects of the nerve firing. This thesis examined the average rate response over windows for speaker dependent information. Likewise, it has been shown in physiological data on cats that synchrony information is a more robust neural representation than average rate response [100, 125]. The *delta* representation examined the temporal aspects of neural firing for speaker identification. Recognition of 95% using delta cepstral and 80% using delta Payton has been shown. Additionally, the final Brachman stage of Payton transduction stage could be developed to provide neural pulse trains, as opposed to the predicted firing rates. Phase synchrony representations of the neural model may provide detailed frequency dependencies among the 20 Payton channels or with various fundamental frequencies.

The drastic drop in classification for the 26 speaker corpus can be explained by several factors. Typically, KING researchers use the entire 45 to 60 second utterances for both training and testing. The effects of training time and testing time greatly effect vector quantization procedures. Due to the described Payton computational complexity, a 15 second window with maximum voicing was extracted for further model processing. The cepstral representation, to be fairly compared with Payton, required equal windowing. However, much of the 15 second window was not voiced speech, since the database is conversational in nature. Training times varied greatly from about 600 to 1500 frames of data, corresponding to about 6 to 15 seconds total, whereas other researchers typically use 90 seconds of training data. Likewise, testing time for a window averaged 379 frames of voiced speech or about 4 seconds, whereas comparable work would could use 30 seconds for testing. For example, a session containing 3993 frames (10.63 msec frame rate) of speech only resulted in 1100 frames with a voicing probability greater than 0.1.

Using a different set of probability of voicing parameters or another means of calculating these values would increase training and test sets. Additionally, the phonetic content of the speech, both in training and testing extraction was limited to high voiced regions, not encompassing a rich phonetic balance. Speaker classification has been shown to be correlated to the phonetic content of the training set [113]. For clean data, such as the TIMIT recordings, perfect classification using cepstral was evident using either VOWELS (high probability of voicing) or non-SILENCE (any speech regions). For degraded signals such as KING, these other phonemes may add additional information.

5.3 Auditory Modeling

The Payton model differs from several other popular models by modeling the biological processes as opposed to their characteristics. This model provides non-linear responses to increased stimulus levels. The background efforts of this thesis have provided the details to fully understand this particular models' parameters, assumptions and limitations. The Payton model, like all others, models a far reduced set of channels than physiologically evident. The approximately 2500-3000 inner hair cells are a measure of spectral resolution. However, many physiological issues remain which should guide future research.

Through nonlinear biological processing, various saturation, rectification and adaptation occur between these inner hair cell depolarizations and the auditory nerves they synapse. Is the vast number of 25,000 - 30,000 auditory nerves for redundancy or to enable further processing? Higher cortical speech processing has begun to be investigated [55]. On the auditory cortex, finer resolution indicates a potential lateral inhibition of neural signals among these auditory nerves. Also, the knowledge that both theories of pitch perception are active for speech based frequencies can guide future work to develop techniques which use both spectral analysis and temporal phase information for the recognition process.

The issue of correct input scale is very necessary and sensitive in auditory modeling [6]. While the ensemble set of auditory nerves have a dynamic range of 120 dB, as evident from Fletcher-Munson curves [80], individual neurons only have a 30 dB range of firing. This thesis has chosen a scale so the average firing for the reference 1 KHz CF neuron is 40 - 50 dB above the model reference level. This puts the model in the overall range of low to moderate speech levels. Instantaneous firing of individual Payton channels still saturate. Such physiological explanations of automatic gain control have been theorized as functionality of the outer hair cells, yet their contribution to the transduction process is still not known.

Payton processing greatly limited the amount of data which could have actually been incorporated. The entire KING database of 51 speakers and 10 sessions per speakers would have taken upwards of 9180 hours or over 12 months to completely process. However, by taking a 15 second window, the results reflect the limitations of this method. Like many other techniques, such as Hidden Markov Models, adequate training data becomes critical. Results for this amount of data on KING, for the 26 speaker tests, provides a relationship to the speaker density function overlap. Additional training data would have enabled improved speaker pdf estimations and additional phonetic content. This would inevitably increased recognition, as evidence from recent published data on KING, using similar codebook design strategies.

The current model trades computation cost (160,000 Fourier-Inverse Fourier Transforms/ second) for physiological precis:on. Engineering dictates trade-offs. Average rate response was examined in this thesis and other models may provide adequate characteristics with much lessing processing. This could allow investigation of further feature preprocessing, such as synchrony, correlations, lateral inhibition, etc. Initial results of auditory modeling, for speech and speaker recognition applications, are still developing. Questions concerning the benefits of non-linear spectral processing and effects of auditory periphery characteristics toward improved recognition need still be addressed.

Appendix A. *Human Auditory Physiology*

For many years, psychoacoustic experimentation was based on simple stimulus, such as single tones and clicks. Only recently has data been published on auditory nerve patterns in response to complex signals such as sums of sinusoids and synthetic speech. Several models have been created which attempt to model this physiological data. Attempts have also been reported using an auditory model as a preprocessor for speech recognition. Such initial research has demonstrated improvements in recognition and pitch tracking, especially with additive noise [38, 25]. Ahn writes [1],

> ...recent study shows that the conventional preprocessors for speech recognizers such as spectral measures (i.e. FFT or LPC, etc) may not be robust against noise and pitch variation.

The research of auditory psychoacoustics incorporates physiology (experimentation of cats), psychoacoustics (human perception), biology and neurology (neural transduction). This chapter reviews the engineering functionality of the peripheral auditory system. It is provided as fundamental background to understanding of the Payton model, the various modeling techniques reported to date, and significant aspects of a specific model, developed by Payton [81, 82].

A.1 Human Physiology

The human ear is a biological transducer. Shown in Figure 38, it first channels sound pressure into the ear canal, via the pinna, to the middle ear. This channeling performs a filtering operation, dependent on sound direction and unique for every pinna, and aids in sound localization [1, 104, 71]. This will not be modeled in this thesis; see AFIT thesis by Scarborough [103]. The impinging sound pressure vibrations are passed through the outer ear canal onto the eardrum, or tympanic membrane. The eardrum resembles a cone or a loudspeaker diaphragm, concentrating sound, into the middle ear cavity. These vibrations are conveyed through a series of middle ear gain-controlling bones called the malleus, the incus, and the stapes. This latter bone is attached to the oval window at the base of

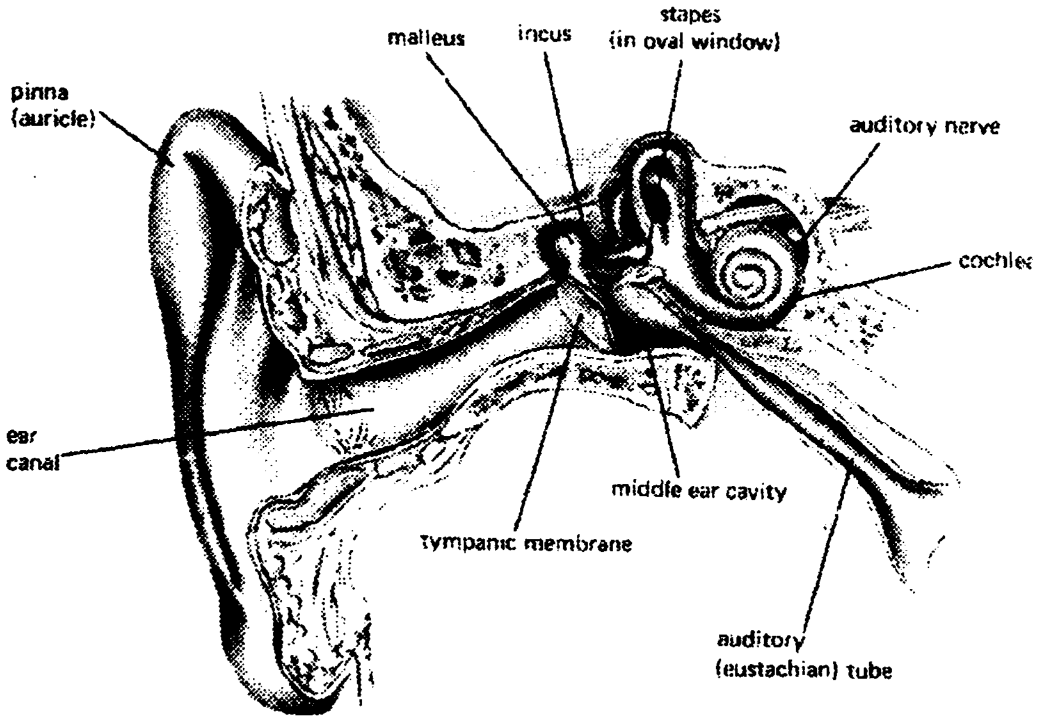

Figure 38. Human Auditory Periphery, showing outer ear, middle ear and inner ear cavities [120]

the cochlea. The cochlea (latin for snail) is a fluid-filled spiral structure which contains three partitions. These partitions are the scalar vestibuli, the scalar tympani, and the scalar media. The first two scalae are separated by the cochlea partition, except at a small opening at the apex called the helicotrema. The major frequency analysis capability of the cochlea, located on the cochlea partition within the scalar media, is performed by the basilar membrane (BM). Resting on this membrane, the Organ of Corti is responsible for the mechanical to electrical transduction process of neural information. The Organ of Corti maintains one row of inner hair cells and three rows of outer hair cells all surrounded by a gelatinous tectorial membrane. Lastly, the hair cells are joined to auditory nerves at junctions called synapses, where electrical neural information is carried to higher auditory brain centers. The layout of cochlea partitions, Organ of Corti and hair cells are shown in Figures 39 and 40.

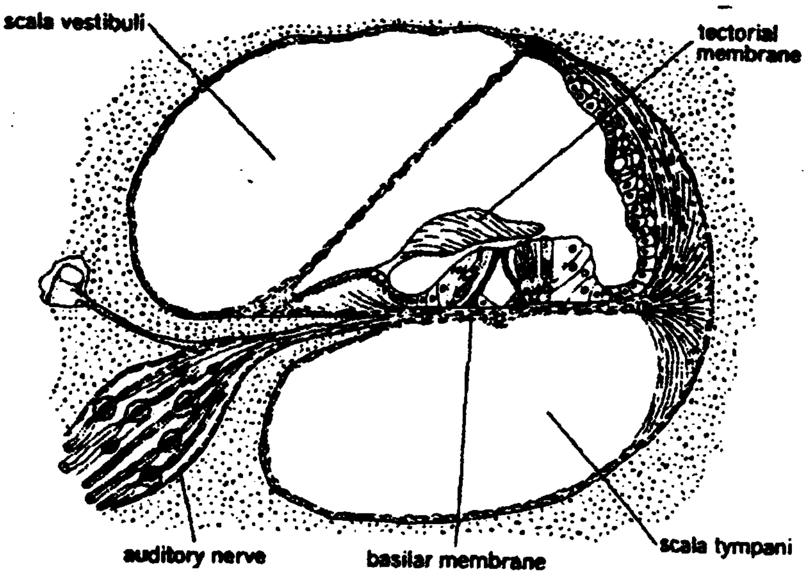

Figure 39. Cochlear Partitions [120].

A.2 Peripheral Functionality/ Quantitative Analysis

The middle ear is stimulated with sound pressure waves at the eardrum and creates displacement of the stapes. The eardrum, itself, will transmit sound waves uniformly up to

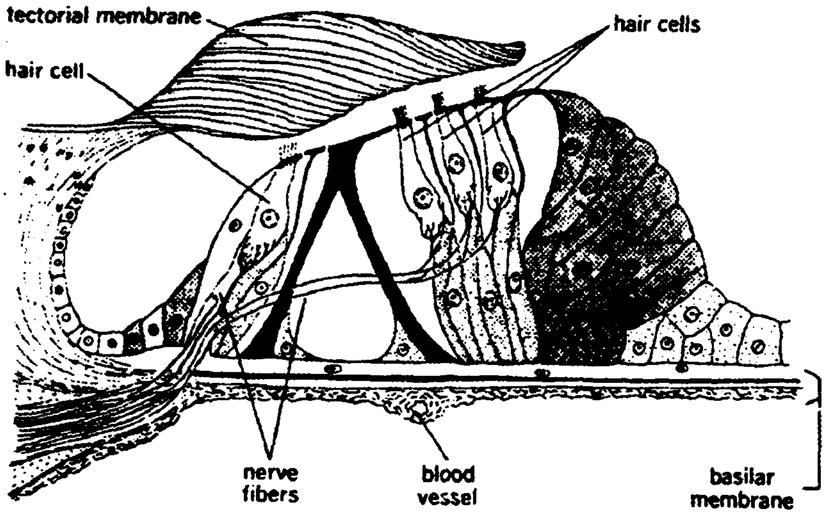

Figure 40. Internal Structures of the Scala Media [120].

about 1500 Hz, and shows decreasing displacement thereafter [104]. At frequencies below 500 Hz, the middle ear generates stapes peak to peak displacements of less than .05 microns [82]. At higher frequencies above 500 Hz, the middle ears bones tend to act nonuniformly creating a response similar to a low pass filter, with resonances at 1 KHz and about 9 KHz [82].

Stapes displacements onto the oval window causes traveling waves propagating down the basilar membrane. The basilar membrane, at the base of the cochlea toward the middle ear, is narrow and relatively stiff , and becomes wider and more elastic toward the apex [120]. At low stimulus levels, the membrane resembles the impulse response of a narrow bandpass filter [71]. Frequency content of the stimulus is evident by the location on the basilar membrane of peak displacement. These curves of basilar membrane displacement as a function of stimulus frequency resemble the "tuning curve" characteristics of both inner hair cell potentials and auditory nerve firing. These curves have been continually developed in the literature [82].

The neural process of transduction translates mechanical BM displacement into neural electrical activity. A row of inner hairs, when displaced, accomplishes this process.

According to Payton, there has been some discourse concerning the transduction process. However, recent evidence suggests that displacement of the basilar membrane conveys a shearing motion of the inner hair cells. This is produced by the inner hair cells affixed to the basilar membrane, yet are surrounded by the tectorial membrane. Recall Figure 40.

There exist approximately 2500-3500 [104, 66] inner hair cells, spaced uniformly along the BM [25], each binding about 40 small hairs called cilia. In contrast, outer hair cells number approximately 25,000. These outer cells protrude about 140 cilia from each. It should be pointed out that the exact function of these outer h ir cells and association with the surrounding tectorial membrane is not fully understood. Experimentation with models strongly suggest their function performs an automatic gain control which aids in frequency selectivity or tuning [66]. The inner hair cells, when sheared, change their internal potential [82, 25, 71]. This internal potential is possibly generated by opening channels allowing ions to flow across the hair-cell membrane [120]. Interestingly, this receptor potential occurs much greater for BM displacement in one direction (positive displacement). This potential causes the hair cells to release a neurotransmitter into the synapse of the the auditory nerves, which lie under the hair cells. This neurotransmitter activates neural receptors which in turn cause the neuron to depolarize. Payton states this neurotransmitter has not yet been identified. The number of afferent (upwards toward brain) auditory nerves is recorded as approximately 30,000 per ear [1] [70]. The inner hair cells account for 95% of these fibers [104]. These numbers reflect each inner hair cell is synapsed by about 20 neurons [71]. The other 5% of the auditory nerves innervate the outer hair cells. These auditory neural responses are typically characterized by the following [71]:

1. Fibers are frequency selective, responding increasingly to certain frequencies.
2. Firings are phase locking, following a particular phase of the waveform.
3. Spontaneous firing rates range from 0 spikes/sec up to 150 spikes/sec.

[1] For contrast, the cat has about 50,000 auditory nerves; the guinea pig has about 25,000 and the porpoise has over 100,000. The reason for quantitative differences can probably be traced to the animals ability to perceive Just Noticeable Difference for different tones. For humans, this number is about one tenth of one percent at 1KHz. Thus, man can detect a 1 Hz change to a 1 KHz tone. However, the size of the basilar membrane and/or the size given to various octaves along the BM may be pertinent [43, 71].

Each of these firing concepts will be further examined. The issue of whether neural information is frequency or temporally coded will be discussed. The importance of this neural coding issue must be reviewed; this could effect the choice of classification later used for speaker identification. This issue also could determine any additional preprocessing of the neural signal before classification. Many characteristics of these neural firing patterns have been evaluated, as discussed in model comparisons [33] in Chapter II.

A.2.1 Frequency Selectivity The theory of place or rate coding, takes the place or region along the basilar membrane as the key representation to higher auditory centers. Basilar membrane displacement, inner hair cell potentials and auditory nerve firing rates are all tuned to a *best* or *characteristic frequency.* These frequencies are ordered, approximately logarithmically [25] along the length of the basilar membrane with points toward the base responding to higher frequencies, and points nearer the apex responding to low frequencies. Typical neural responses for varying intensities are shown in Figure 41. These curves plot the response of various neurons to different pure tones of varying intensity. Figure 41, by Nelson dating back to 1965, shows these responses of several auditory nerves within a single cat. The frequency to which a fiber is most sensitive (i.e. has the lowest threshold) is its characteristic frequency. These curves correspond, especially at low levels, to basilar membrane peak displacement curves. Other information is included in the response of the ensemble of nerves with varying stimulus; shown in Figure 42. This particular example was created with the Payton model and demonstrates the sensitivity of channel 14 to varying degrees of a 1 KHz sinusoid. Channel 14's characteristic frequency is 1133 Hz. Note the subsequent figure (Figure 43), shows the saturation effect when higher levels of stimulus are applied to the membrane.

The place theory can explain how the higher processing centers can determine (perceive) tones. The frequency range of human hearing, 20 Hz to 20 KHz, and would cause maximum firing at the respective location along the basilar membrane. However, when a complex tone is presented which is lacking the fundamental harmonic, humans still perceive this *missing fundamental* tone. Without this tone, the BM should not be maximally displaced at this frequency. Thus, higher processing centers must be using other (non-

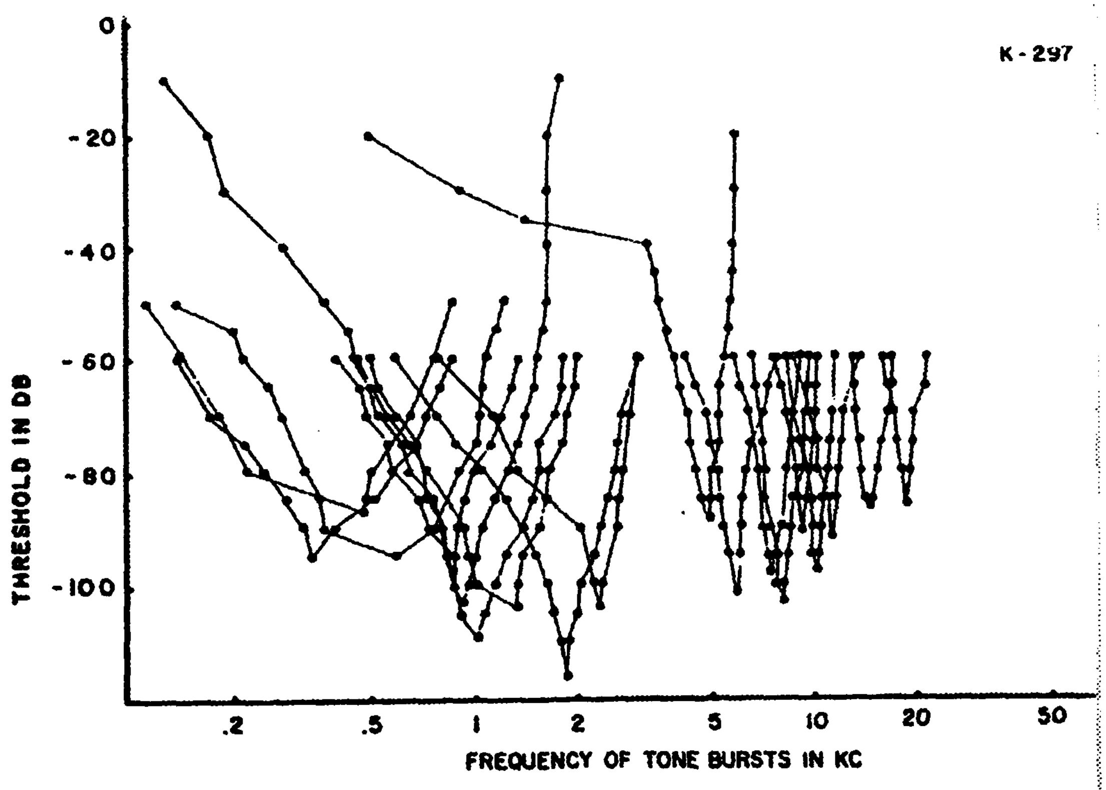

Figure 41. Typical Auditory Tuning Curve. Demonstrates the selectivity of auditory neurons to frequency which vary non-linearly for varying stimulus levels [73].

place) information [18]. So, this coding scheme would extend for all frequencies (20 Hz to 20 KHz) along the basilar membrane.

A.2.2 Phase Synchrony A coding theory based on temporal characteristics of nerve firing, call ***phase synchrony*** may explain the missing fundamental. Information is carried by the temporal firing, or inter-spike timing patterns. However, neurons can not fire near 20 KHz, the highest frequency of human perception. On average, steady state response is usually reported about 250-300 spikes/sec [33]. Coren et al [18] states, "a neuron can only conduct about 1000 impulses/sec." Meddis [33] also states that the upper limit (at onset) is about 1000 spikes/sec "based on the refractory properties of neural spike generation." The ***volley coding*** theory states groups of neurons fire in cooperation. Thus, between several

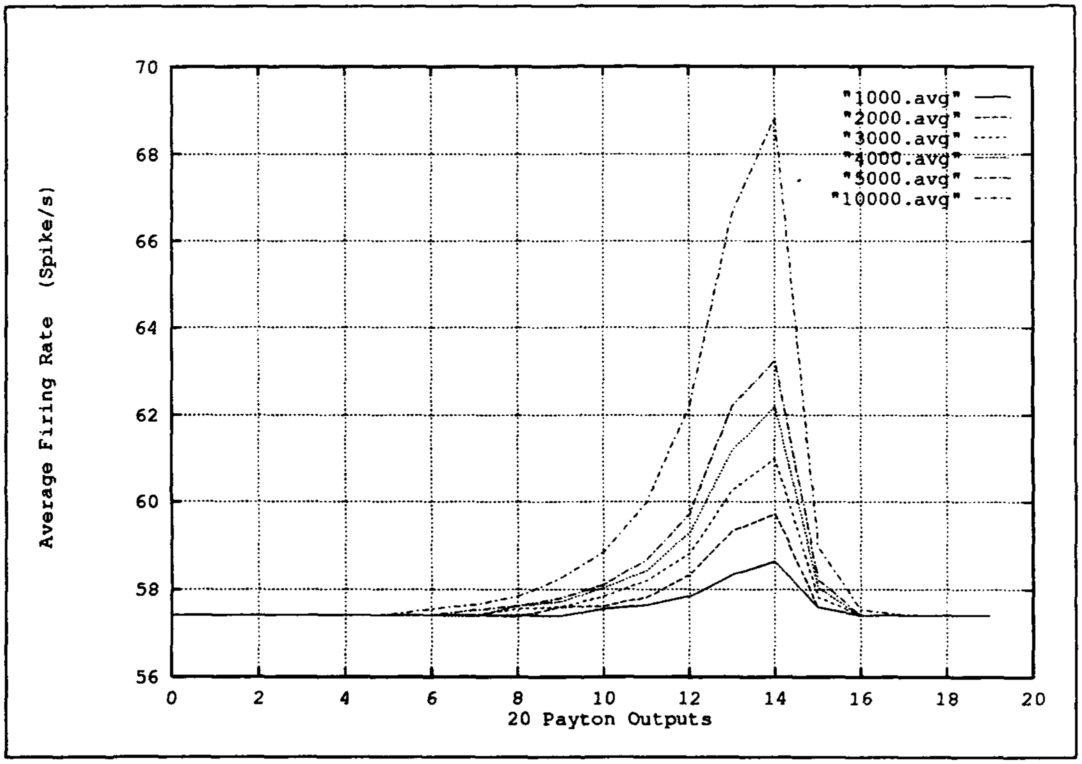

Figure 42. Neuron Characteristic Frequency Selectivity. Channel 14, CF = 1133 Hz, responds maximally to a 1 KHz sinusoid. Note the bandpass filter characteristic with nonsymmetrical bandpass, i.e. small slope on low frequency side, with very sharp high frequency roll-off. This plot was generated with the Payton auditory model.

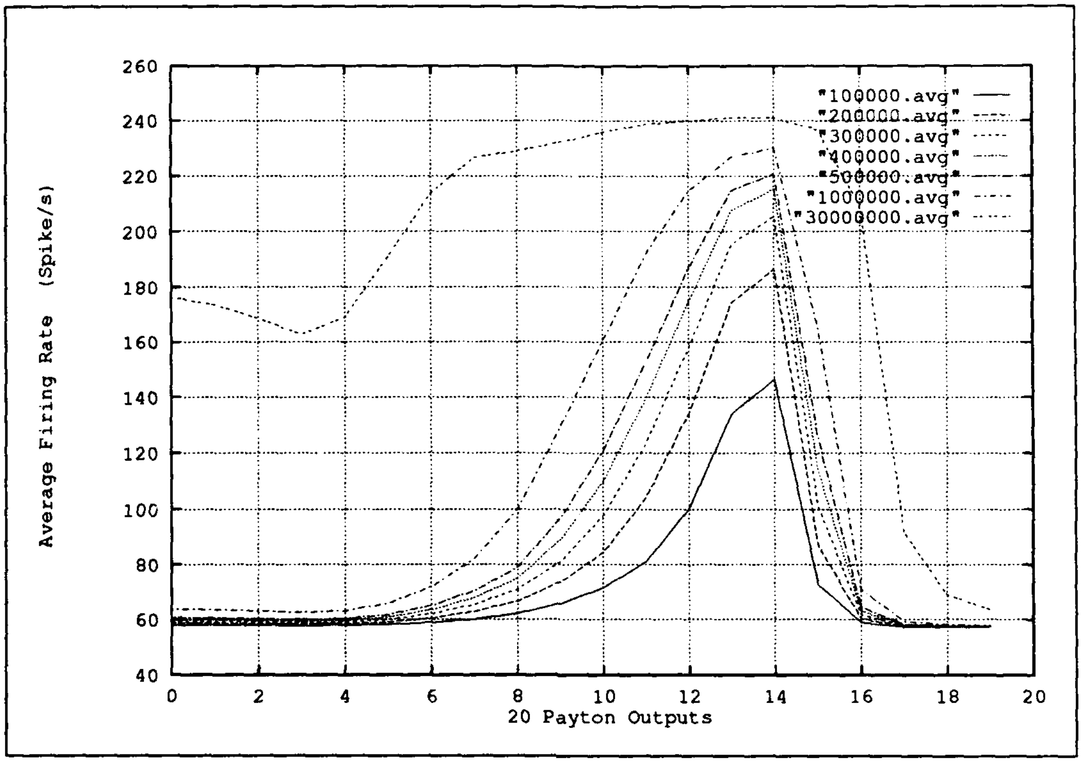

Figure 43. Neuron Characteristic Frequency Selectivity 2. *Note the non-linear distortion at high signal intensities.*

neurons, an impulse will be generated each period of the input stimulus. Moore [71] recently clarifies this theory with referenced data showing inter-spike histograms. Moore states,

> ...information about the period of the stimulating waveform is carried unambiguously in the temporal pattern of firing of a single neurone. Thus, although the neurone does not fire on every cycle of the stimulus, the distribution of time intervals between nerve firing depends closely on the frequency of the stimulating waveform.

Representative neural firing histograms are shown in Figure 44, for a presentation of a several tones. An auditory neuron with CF of 1.6 KHz is depicted in this figure. Note the inter pulse intervals are multiples of the stimulus frequency. However, phase locking of auditory nerves cannot be detected for stimulus frequencies greater than about 4000 -

5000 Hz. This can be explained by the inexact firing of a neuron to the stimulus phase. Since the firing *generally* occurs at the same phase, a "smearing out" effect [71] limits the maximum frequencies of phase locking. So, this temporal coding scheme exists for signals under 4 - 5 KHz, such as speech.

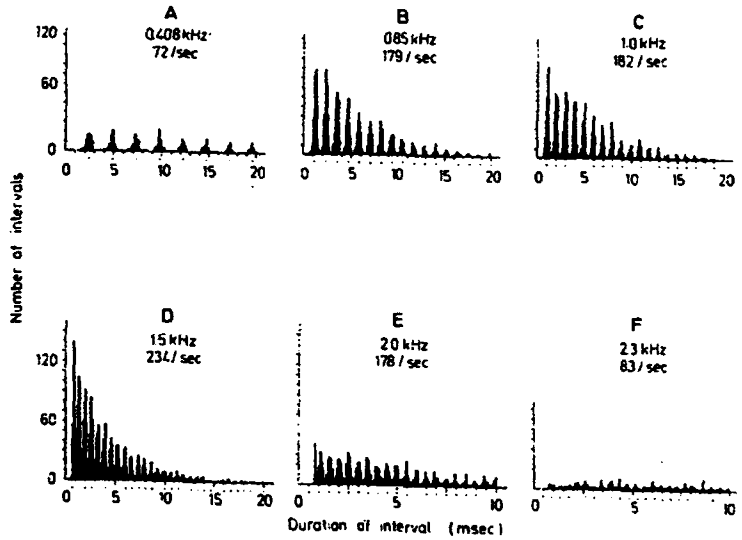

Figure 44. Neural InterSpike Histograms for a single neuron with CF of 1.6 KHz. The top numbers correspond to the stimulus frequency and the bottom number indicates the mean rate firing respond over the stimulus presentation. Notice the spikes occur on integer multiples of the stimulus period, indicated by dots below the abcissa. So in Figure D, the interspike intervals are multiples of .67 msec., [71].

A.2.3 Spontaneous Rate and Thresholds The 20,000 auditory nerves are grouped by their spontaneous rate and threshold characteristics. The literature has concerned itself primarily with modeling the high spontaneous rate (SR), low threshold fibers. Liberman (1982) found various fibers which had low, medium and high spontaneous firing rates. The ratios of each type are referenced [71, 39] as 61% high ($\geq$ 18 spikes/sec and $\leq$ 250 spikes/sec), about 23% show moderate spontaneous rates ($\geq$ .5 $\leq$ 18spikes/sec) and the remainder (about 16%) showed very low or inactive spontaneous firing ($\leq$ .5 spikes/sec).

Each of these fiber types also required various threshold levels of stimulus before firing significantly. There exists an inverse relationship between neural thresholds and spontaneous rate firing. High SR fibers tend to be low thresholds (most sensitive) where some have thresholds close to 0 dB SPL. [2]. Other fibers have been found which have thresholds as high as 80 dB SPL [71].

A.2.4 Nerve Firing Functionality Research by Sachs and Young [100, 125] has presented much physiological data of auditory nerve firing patterns in response to speech-like stimuli (synthesized vowels). Their results show that average firing rate peaks correspond to formant frequencies, at low intensities. At higher levels of stimuli, saturation of neural firing smears these peaks. These authors suggested Averaged Localized Synchrony Rate (ALSR), a measure of the local frequency content based on the temporal aspects of auditory nerve histograms. They demonstrated clear peaks at increasing stimulus level and in the presence of noise. These results indicate temporal coding as a more suitable representation (say, for speech processing) than place coding, or mean rate. However, a conclusion which can be drawn from the frequency ranges of place and temporal coding suggests both are available for the higher brain centers up to 5000 Hz. This implies the brain in making use of both coding schemes for speech-like frequencies.

[2] Sound Pressure Level (SPL) is a measure of sound pressure, relative to .0002 dynes/cm^2.

Vita

Captain John M. Colombi was born on 9 April 1964 in Weymouth, Massachusetts. Captain Colombi graduated from Weymouth South High School in June 1982. He received an ROTC scholarship while attending the University of Lowell, Lowell Massachusetts. He graduated as ROTC Distinguished Graduate with a Bachelor of Science degree in Electrical Engineering Captain Colombi came on active duty to the Communication's Directorate of formerly Rome Air Development Center, Griffiss AFB, New York where he served as a Communication Systems Engineer until April 1991. In May of 1991 he entered the School of Engineering, Air Force Institute of Technology at Wright-Patterson Air Force Base, Ohio, to pursue a Master of Science degree in Electrical Engineering. His primary emphasis lies within the fields of pattern recognition and biological information processing. John is married to Cheryl Anne (Gately) Colombi of Weymouth, Massachusetts and has two children Andrew and Felica.

Permanent address: 30 Westminster Rd.
E. Weymouth, Mass 02189

Bibliography

1. Ahn, Sahng-Gyou and John J. Westerkamp. "Cochlear modeling using a general purpose digital signal processor." *Proceedings of the IEEE 1990 National Aerospace and Electronics Conference*. 57–63. New York: IEEE Press, 1990.

2. Allen, J. B. and M. M. Sondhi. "Cochlear macromechanics: Time domain solutions," *J. Acoust. Soc. Amer.*, *66*(1):123–132 (July 1979).

3. Allen, Jont B. "Cochlear Modeling," *IEEE ASSP Magazine* (January 1985).

4. Anderson, Timothy R. *Speaker independent phoneme recognition using an auditory model and a neural network*. PhD dissertation, University of Dayton, Dayton, OH, 1990.

5. Anderson, Timothy R. "Speaker Independent Phoneme Recognition with an Auditory Model and a Neural Network: A Comparison with Traditional Techniques." *Proceedings of the 1991 International Conference on Acoustics, Speech and Signal Processing*. 149–152. 1991.

6. Anderson, Timothy R. Personal interviews. Dayton, OH, January - September 1992.

7. Anderson, Timothy R., "A Comparison of Auditory Models for Speaker Independent Phoneme Recognition." Proceedings of the 1993 International Conference on Acoustics, Speech, and Signal Processing, August 1992. Submitted for Publication.

8. Atal, B. S. "Effectiveness of linear prediction characteristics of the speech wave for automatic speaker identification and verification," *J. Acoust. Soc. Amer.*, 1304–12 (June 1974).

9. Atal, B. S. and Suzanne L. Hanaufer. "Speech Analysis and Synthesis by Linear Prediction of the Speech Wave," *J. Acoust. Soc. Amer.*, *50*(2):637–655 (April 1971).

10. Atal, Bishnu S. "Automatic Recognition of Speakers From their Voices," *Proc. of the IEEE*, *64(4):460–75* (April *1976*).

11. Bauer, Hans-Ulrich and Klaud R. Pawelzik. "Quantifying the Neighborhood Preservation of Self-Organizing Feature Maps," *IEEE Trans. Neural Networks*, *3*(4):570–579 (July 1992).

12. Bennani, Younes and others. "A Connectionist Approach for Automatic Speaker Identification." *Proceedings of the 1990 International Conference on Acoustics, Speech and Signal Processing1*. 265–268. 1990.

13. Bennani, Younes and Patrick Gallinari. "On the Use of TDNN-Extracted Features Information in Talker Identification." *Proceedings of the 1991 International Conference on Acoustics, Speech and Signal Processing1*. 385–388. 1991.

14. Bezdek, James C. *Self-Organization and Clustering Algorithms*. Report DTIC AN91-21783, Div of Computer Science, University of West Florida, Pensacola, Florida 32514.

15. Buzo, Andres, et al. "Speech Coding Based Upon Vector Quantization," *IEEE Trans. ASSP*, *28*(5):562–574 (October 1980).

16. Childers, D. G., et al. "The Cepstrum: A Guide to Processing," *Proc. of the IEEE*, *65*(10):1428–1443 (October 1977).

17. Cohen, Jordon R. "Application of an auditory model to Speech Recognition," *J. Acoust. Soc. Amer.*, *85*(6):2623–29 (1989).

18. Coren, Stanley, et al. *Sensation and Perception* (Second Edition). New York, New York: Academic Press, Inc, 1986.

19. Davis, Steven B. and Paul Mermelstein. "Comparison of Parametric Representations for Monosyllabic Word Recognition in Continuously Spoken Sentences," *IEEE Trans. ASSP*, *28*(4):357–366 (August 1980).

20. DeSieno, D. "Adding conscience to competitive learning for non-stationary environments," *Proceedings of the 1988 International Conference of Neural Networks*, *1*:117–124 (1988).

21. Devijver, Pierre A. and Josef Kittler. *Pattern Recognition: A Statistical Approach.* London: Prentice-Hall International, Inc., 1982.

22. Furui, Sadaoki. "Cepstral Analysis Techniques for Automatic Speaker Verification," *IEEE Trans. ASSP*, *29*(2):254–72 (April 1981).

23. Gaganelis, D. A. and E. D. Frangoulis. "A novel approach to Speaker Verification." *Proceedings of the 1991 International Conference on Acoustics, Speech and Signal Processing*. 373–376. 1991.

24. Geurts, Capt James F. *Target Recognition Using Remotely Sensed Surface Vibration Measurements.* MS thesis, AFIT/GE/ENG//92D, School of Engineering, Air Force Institute of Technology (AU), Wright-Patterson AFB OH, December 1992.

25. Ghitza, Oded. "Auditory nerve representation as a front-end for speech recognition in a noisy environment," *Computer Speech and Language*, *1*:109–130 (1986).

26. Ghitza, Oded. "Auditory nerve representation Criteria for Speech Analsis/Synthesis," *I.E.E.E. Trans Signal Processing*, *35*(6):736–740 (June 1987).

27. Ghitza, Oded. "Auditory neural feedback as a basis for speech processing." *Proceedings of the 1988 International Conference on Acoustics, Speech, and Signal Processing*. 91–94. New York: IEEE Press, 1988.

28. Grant, P.M. "Speech Recognition Techniques," *Electronics and Communication Engineering Journal*, 37–48 (February 1991).

29. Gray, Robert M. and others. "Distortion Measures for Speech Processing," *I.E.E.E Trans of ASSP*, 367–375 (aug 1980).

30. Gu, Hung-yuan, et al. "Isolated-Utterance Speech Recognition Using hidden markov models with bounded state durations," *IEEE Trans. on Signal Processing*, *39*(8):1743–51 (August 1991).

31. Gulick, W. Lawrence, et al. *Hearing: Physiological Acoustics, Neural Coding and PsychoAcoustics*. N.Y.: Oxford University Press, 1989.

32. Hattori, Hiroaki. "Text-Independent Speaker recognition using Neural Networks." *Proceedings of the 1992 International Conference on Acoustics, Speech and Signal Processing2*. 153–156. 1992.

33. Hewitt, Michael J. and Ray Meddis. "An Evaluation of Eight Computer Models of Mammalian Inner Hair-cell Function," *J. Acoust. Soc. Amer.*, *90*(2):904–917 (August 1991).

34. Higgin, A. and others. *Speaker Identification and Recognition*. Final Report 88-F744200-000, ITT Aerospace/Communications Div, Nov 1991.

35. Higgins, A. L. and L. G. Bahler. "Text-Independent Speaker Verification By Discriminator Counting." *Proceedings of the 1991 International Conference on Acoustics, Speech and Signal Processing1*. 405–408. 1991.

36. Huang, X. D. "Phoneme Classification Using Semicontinuous Hidden Markov Models," *I.E.E.E. Trans on Signal Processing*, *40*(5):1062–1067 (May 1992).

37. Hunt, Melvyn J. and Claude Lefebvre. "Speech recognition using a cochlea model." *Proceedings of the 1986 International Conference on Acoustics, Speech and Signal Processing*. 1979 – 1982. 1986.

38. Hunt, Melvyn J. and Claude Lefebvre. "Speaker dependent and independent speech recognition experiments with an auditory model." *Proceedings of the 1988 International Conference on Acoustics, Speech, and Signal Processing*. 215–218. New York: IEEE Press, 1988.

39. Jenision, Rick L. and others. "A Composite Model of the Auditory Periphery for the Processing of Speech Based on the Filter Response Functions of Single Auditory Nerve Fibers," *J. Acoust. Soc. Amer.*, *90*(1):904–917 (August 1991).

40. Jenison, Rick L. Greeberg, Steven and others. "A Composite Model of the Auditory Periphery for the Processing of Speech Based on the Filter Response Functions of Single Auditory-Nerve Fibers," *J. Acoust. Soc. Amer.*, *90*(2) (August 1991).

41. Jou, Chi-Cheng. "Fuzzy Clustering using fuzzy competitve learning," *IJCNN*, II–714 – II–1719 (1992).

42. Juang, Biing-Hwang, et al. "On the Use of Bandpass Liftering in Speech Recognition," *I.E.E.E Trans of ASSP*, *35*(7) (July 1987).

43. Kabrisky, Matthew. Personal interviews. AFIT, WPAFB OH, January - September 1992.

44. Kangas, Jari, et al. "Variants of Self-Organizing Maps," *IEEE Trans. Neural Networks*, *5*(1):93–94 (March 1990).

45. Kao, Yu-Hung, et al. "Free-Text Identification over long distance telephone channel using hypothesized phonetic segmentation." *Proceedings of the 1992 International Conference on Acoustics, Speech and Signal Processing2*. 177–180. 1992.

46. Kao, Yu-Hung, et al., "Robust Free-Text Speaker Identification Over Long Distance Telephone Channels." Proceedings of the 1993 International Conference on Acoustics, Speech, and Signal Processing, August 1992. Submitted for Publication.

47. Kates, James M. "An Adaptive Digital Cochlear Model." *Proceedings of the 1991 International Conference on Acoustics, Speech and Signal Processing*. 3621–3624. 1991.

48. Kates, James M. "A Time-Domain Digital Cochlear Model," *IEEE Trans. on Signal Processing*, *39*(12) (1991).

49. Kohonen, Teuvo. "The "Neural" Phonetic Typewriter," *IEEE Computer Magazine*, 11–22 (March 1988).

50. Kohonen, Teuvo. "Tutorial/ Self-Organizing Maps," *Proceedings of the 1988 International Conference of Neural Networks*, – (1988).

51. Kohonen, Teuvo. "The Self-Organizing Map," *Proc. of the IEEE*, *78*(9):1464–1479 (September 1990).

52. Kohonen, Teuvo. "Improved Versions of Learning Vector Quantization," *Proceedings of the 1991 International Joint Conference of Neural Networks*, I–545 – I–550 (1991).

53. Kosko, Bart. "Stochastic Competitive Learning," *I.E.E.E. Trans on Neural Networks*, *2*(5):522–529 (September 1991).

54. Krepp, Capt Dennis L. *Face Recognition with Neural Networks*. MS thesis, AFIT/GE/ENG/92D, School of Engineering, Air Force Institute of Technology (AU), Wright-Patterson AFB OH, December 1992.

55. Kurogi, S. "Speech Recognition by an Artificial Neural Network Using Findings on the Afferent Auditory System," *Biol. Cybern.*, *64*:243–249 (1991).

56. Lee, Kai-Fu. "An Overview of the SPHINX Speech Recognition System," *IEEE Trans. ASSP*, *38*(1) (January 1990).

57. Lee, Lt James Kelly. *Application of the Complex Cepstrum and Scanning Electron Microsopy to VLSI Reverse Engineering*. MS thesis, AFIT/GE/ENG//91D-36, School of Engineering, Air Force Institute of Technology (AU), Wright-Patterson AFB OH, December 1991.

58. Levinson, Stephen E. and David B. Roe. "A Perspective on Speaker Recognition," *IEEE Comm. Magazine*, 28–34 (January 1990).

59. Li, Kung-Pu. *Real-Time Speaker and language recognition system : Literature Review on Speaker Recognition and Language Identification*. Final Report F30602-81-C-0134, ITT Defense Communications Div, January 1982.

60. Linde, Yoseph, et al. "An Algorithm for Vector Quantizer Design," *IEEE Trans. on Comm.*, *COM-28*(1):84–94 (January 1980).

61. Lippmann, Richard P., "A Critical Overview of Neural Network Pattern CLassifiers," Sep - Oct 1991.

62. Liu and others. "Study of Line Spectrum Pair Frequencies for Speaker Recognition." *Proceedings of the 1990 International Conference on Acoustics, Speech and Signal Processing 1*. 277–280. 1990.

63. Liu, Weimin, et al. "Voiced-Speech Representations by an Analog Silicon Model of the Auditory Periphery," *I.E.E.E. Trans on Neural Networks*, *3*(3):477–487 (May 1992).

64. Liu, Weimin, et al. "An analog integrated speech front-end based on the auditory periphery." *Proceedings of the IEEE INNS International Joint Conference On Neural Networks, Vol. II*. II–861 - II–864. New York: IEEE Press, 1991.

65. Lyon, Richard F. and Lounette Dyer. "Experiments with a Computational model of the cochlea." *Proceedings of the 1986 International Conference on Acoustics, Speech and Signal Processing*. 1975 - 1978. 1986.

66. Lyon, Richard F. and Carver Mead. "An Analog Electronic Cochlea," *IEEE Trans. ASSP*, *36*(7) (1988).

67. Makhoul, John. "Linear Prediction: A tutorial Review," *Proc. of the IEEE*, *63*(4):561–580 (April 1975).

68. Matsui, Tomoko and Sadaoki Furiui. "Comparison of Text-Independent Speaker recognition methods using VQ Distortion and Discrete/Continuous HMMs." *Proceedings of the 1992 International Conference on Acoustics, Speech and Signal Processing2*. 157–160. 1992.

69. Matsui, Tomoko and Sadaoki Furui. "A Text-Independent Speaker Recognition Method Robust Against Utterance Variations." *Proceedings of the 1991 International Conference on Acoustics, Speech and Signal Processing*. 377–380. 1991.

70. Moller, Aage R. *Auditory Physiology*. New York: Academic Press, 1983.

71. Moore, Brian C. J. *An Introduction to the Psychology of Hearing* (Third Edition). New York: Academic Press, 1989.

72. Naik, Jaynat M. "Speaker Verification: A Tutorial," *IEEE Comm. Magazine*, 42–48 (January 1990).

73. Nelson, et al., "Discharge Patterns of Single Fibers in the Cat's Auditory Nerve." MIT Research Monograph, 1965.

74. NIST. *The DARPA TIMIT Acoustic-Phonetic Continuous Speech Corpus (TIMIT): Training and Test Data and Speech Header Software*, oct 1990.

75. of the Hlesinki University of Technology, LVQ Programming Tean. *LVQ PAK: The Learning Vector Quantization Program Package*. Laboratory of Computer and Information Science, Rakentajanaukio 2 C, SF-02150 Espoo, FINLAND, January 1991. Version 2.0.

76. Oglesby, J. and J. S. Mason. "Optimisation of Neural Models for Speaker Identification." *Proceedings of the 1990 International Conference on Acoustics, Speech and Signal Processing 1*. 261–264. 1990.

77. Oglesby, J. and J. S. Mason. "Radial Basis Function Networks for Speaker Recognition." *Proceedings of the 1991 International Conference on Acoustics, Speech and Signal Processing1*. 393–396. 1991.

78. Paliwal, K. K. "Neural Net classifiers for robust speech recognition under noisy environments." *Proceedings of the 1990 International Conference on Acoustics, Speech, and Signal Processing*. 429–432. New York: IEEE Press, 1990.

79. Parker, Alan and John Shore. *INTRODUCTION TO THE ENTROPIC SIGNAL PROCESSING SYSTEM (ESPS)*. Entropic Research Laboratory, Inc., Washington Research Laboratory, 600 Pennsylvania Ave. S.E., Suite 202, Washington, D.C. 20003, (202)547-1420.

80. Parsons, Thomas W. *Voice and Speech Processing*. McGraw-Hill, Inc., 1987.

81. Payton, Karen L. *Vowel processing by a model of the auditory periphery*. PhD dissertation, The Johns Hopkins University, Baltimore, MD, 1986.

82. Payton, Karen L. "Vowel processing by a model of the auditory periphery: A comparison to eighth-nerve responses," *J. Acoust. Soc. Amer.*, *83*(1):145–162 (1988).

83. Poritz, Alan B. "Linear Prediction of Hidden Markov Models." *Proceedings of the 1982 International Conference on Acoustics, Speech and Signal Processing*. 1291–1294. 1982.

84. Rabiner, L. R. "A Tutorial on Hidden Markov Models and Selected Applications in Speech Recognition," *Proc. of the IEEE*, 77(2) (February 1989).

85. Rabiner, L. R. and B. H. Juang. "An Introduction to Hidden Markov Models," *IEEE ASSP Magazine* (January 1986).

86. Rathbun, Capt Thomas F. *Speech Recognition using Multiple Features and Multiple Recognizers*. MS thesis, AFIT/GE/ENG//91D-7, School of Engineering, Air Force Institute of Technology (AU), Wright-Patterson AFB OH, December 1991.

87. Recla, Capt Wayne F. *A Study in Speech Recognition using a Kohonen Neural Network, Dynamic Programming and Multi-Feature Fusion*. MS thesis, AFIT/GE/ENG/89D-41, School of Engineering, Air Force Institute of Technology (AU), Wright-Patterson AFB OH, December 1989.

88. Reynolds, D. A. and R. C. Rose. "An integrated Speech-background model for Robust Speaker Identification." *Proceedings of the 1992 International Conference on Acoustics, Speech and Signal Processing2*. 185–188. 1992.

89. Ricart, Richard. Personal interviews. Rome, NY, January 1992.

90. Riegelsberger, Edward Lee. *C Implementation of Payton's Model of the Auditory Periphery Users Guide and Programmers Reference*. Armstrong Laboratory (AL/CFBA), August 1990.

91. Rogers, Steven K. and Matthew Kabrisky. *An Introduction to Biological and Artificial Neural Networks*. Bellingham, Washington: SPIE Optical Engineering Press, 1991.

92. Rose, Richard C. and others. "Robust Speaker Identification in Noisy Environments Using Noise Adaptive Speaker Models." *Proceedings of the 1991 International Conference on Acoustics, Speech and Signal Processing1*. 401–404. 1991.

93. Rose, Richard C. and Douglas A. Reynolds. "Text Independent Speaker Identification Using Automatic Acoustic Segmentation." *Proceedings of the 1990 International Conference on Acoustics, Speech and Signal Processing1*. 293–296. 1990.

94. Rosenburg, Aaron E., et al. "Sub-Word Unit Talker Verification Using Hidden Markov Models." *Proceedings of the 1990 International Confeience on Acoustics, Speech and Signal Processing1*. 269–272. 1990.

95. Rosenburg, Aaron E., et al. "Connected Word Talker Verification Using Whole Word Markov Models." *Proceedings of the 1991 International Conference on Acoustics, Speech and Signal Processing1*. 381–384. 1991.

96. Ruck, Dennis W. Personal interviews. Dayton, OH, January - October 1992.

97. Ruck, Dennis W. and others. "Feature Selection Using a Multilayer Perceptron," *Journal on Neural Network Computing*, 40–46 (Fall 1990).

98. Rudasi, Laszlo and Stephen A. Zahorian. "Text-Independent Talker Identification With Neural Networks." *Proceedings of the 1991 International Conference on Acoustics, Speech and Signal Processing1*. 389–392. 1991.

99. Russell, M. J. and L. Sime. *Explicit Modeling of State duration correlation in hidden markov models*. Memorandum 4152, Royal Signals and Radar Establishment, September 1988.

100. Sachs, Murray B. and Eric D. Young. "Encoding of Steady-State Vowels in the Auditory Nerve:Representation in Terms of Discharge Rate," *J. Acoust. Soc. Amer.*, *66*(2):470–479 (August 1979).

101. Savic, M. and J. Sorenson. "Phoneme Based Speaker Verification." *Proceedings of the 1992 International Conference on Acoustics, Speech and Signal Processing2*. 165–168. 1992.

102. Savic, Michael and Sunil K. Gupta. "Variable Parameter Speaker Verification System based on Hidden Markov Models." *Proceedings of the 1990 International Conference on Acoustics, Speech and Signal Processing1*. 281–284. 1990.

103. Scarborough, Eric. *T.B.D.*. MS thesis, School of Engineering, Air Force Institute of Technology (AU), Wright-Patterson AFB OH, December 1992.

104. Scharf, Bertram and Adrianus J. M. Houtsma. "Audition II." *Handbook of Perception and Human Performance, Volume 1, Sensory Processes and Perception* edited by Kenneth R. Boff, et al., New York: Wiley-Interscience, 1986.

105. Schwartz, R. and others. "The application of Probability Density Estimation to Text-Independent Speaker Identification." *Proceedings of the 1982 International Conference on Acoustics, Speech and Signal Processing*. 1649–1652. 1982.

106. Secker-Walker, Hugh E. and Campbell L Searle. "Time-domain Analysis of Auditory-nerve Firing Rates," *J. Acoust. Soc. Amer.*, *88*(3):1427–1436 (September 1990).

107. Secrest, B.G. and G.R. Doddington. "An integrated pitch tracking algorithm for speech systems," *Proceedings of the 1983 International Conference on Acoustics, Speech and Signal Processing*, 1352 – 1355 (1983).

108. Selim, Shokri, Z. "Soft Clustering of Multidimensional Data: A Semi-Fuzzy Approach," *Pattern Recognition*, *17*(5):559–567 (1984).

109. Seneff, S. *Pitch and Spectral Analysis of Speech Based on Auditory Synchrony Model.* PhD dissertation, M.I.T., Cambridge, MA, 1985.

110. Seneff, Stephanie. "Pitch and spectral estimation of speech based on auditory synchrony model." *Proceedings of the 1984 International Conference on Acoustics, Speech, and Signal Processing*. 36.2.1–36.2.4. New York: IEEE Press, 1984.

111. Seneff, Stephanie. "A computational model for the peripheral auditory system: Application to speech recognition research." *Proceedings of the 1986 International Conference on Acoustics, Speech and Signal Processing*. 1983 – 1986. 1986.

112. Seneff, Stephanie. "A joint synchrony/mean-rate model of auditory speech processing," *Journal of Phonetics*, *16*:55 – 75 (1988).

113. Soong, et al. "A Vector Quantization Approach to Speaker Recognition." *Proceedings of the 1985 International Conference on Acoustics, Speech and Signal Processing1*. 387–390. 1985.

114. Soong, Frank K. and Aaron E. Rosenburg. "On the Use of Instantaneous and Transitional Spectral Information in Speaker Recognition," *IEEE Trans. ASSP*, *36*(6):871–79 (June 1988).

115. Stowe, Capt Francis Scott. *Speech Recognition using Kohonen Neural Networks, Dynamic Programming and Multi-Feature Fusion*. MS thesis, AFIT/GE/ENG/90D-59, School of Engineering, Air Force Institute of Technology (AU), Wright-Patterson AFB OH, December 1990.

116. Suarez, Pedro F. *Face Recognition with the Karhunen-Loève Transform*. MS thesis, AFIT/GE/ENG/91D-54. School of Engineering, Air Force Institute of Technology (AU), Wright-Patterson AFB OH, December 1991.

117. Tou, J. T. and R.C. Gonzalez. *Pattern Recognition Principles*. Reading, MA: Addison-Wesley Publishing, 1974.

118. Tseng, Belle, et al. "Continuous Probabilistic Acoustic Map for Speaker Recognition." *Proceedings of the 1992 International Conference on Acoustics, Speech and Signal Processing2*. 161–164. 1992.

119. Turk, Matthew A. and Alex P. Pentland. "Recognition in Face Space," *SPIE Intelligent Robots and Computer Vision IX: Algorithm and Techniques*, 43–54 (1990).

120. Vander, et al., editors. *The Mechanisms of the Human Physiology*. New York: McGraw Hill Book Co., 1980.

121. Weinstein, Clifford J. "Opportunities for Advanced Speech Processing in Militiary Computer-Based Systems," *Proc. of the IEEE*, *79*(11):1627–39 (November 1991).

122. Wu, Nong Liang, et al. "Modeling spectral processing in the central auditory system." *Proceedings of the IEEE ICASSP*. 373-376. New York: IEEE Press, 1982.

123. Xu, Lei, et al. "Methods of Combining Multiple Classifiers and Their Applications to Handwriting Recognition," *I.E.E.E. Trans. on Systems, Man, and Cybernetics*, *22*(3):418 - 435 (1992).

124. Yair, Eyal, et al. "Competitive Learning and Soft Competition for Vector Quantizer Design," *IEEE Trans. Signal Processing*, *40*(2):294–309 (February 1992).

125. Young, Eric D. and Murray B. Sachs. "Representation of Steady-State Vowels in the Temporal Aspects of the Discharge Patterns of Populations of Auditory Nerve Fibers," *J. Acoust. Soc. Amer.*, *66*(5):1381–1403 (November 1979).

126. Zeger, Kenneth, et al. "Globally Optimal Vector Quantization Design by Stochastic Relaxation," *IEEE Trans. Signal Processing*, *40*(2):310–322 (February 1992).

127. Zeger, Kenneth and Vaisey,Jacques and Gersho,Allen. "Globally Optimal Vector Quantization Design by Stochastic Relaxation," *I.E.E.E. Trans on Signal Processing*, *40*(2):310–322 (February 1992).

REPORT

1. AGENCY USE ONLY

December 1992

Master's Thesis

4. TITLE AND SUBTITLE

Cepstral and Auditory Model Features For Speaker Recognition

5. AUTHOR(S)

John M. Colombi, Captain, USAF

7. PERFORMING ORGANIZATION

Air Force Institute of Technology
WPAFB OH 45433-6583

AFIT/GE/ENG/92D-11

9. SPONSORING MONITORING

Capt R. Ricart
RL/IRA
Griffiss AFB NY 13441

11. SUPPLEMENTARY NOTES

12a. DISTRIBUTION

Distribution Unlimited

13. ABSTRACT

The TIMIT and KING databases, as well as a ten day AFIT speaker corpus, are used to compare proven spectral processing techniques to an auditory neural representation for speaker identification. The feature sets compared were Linear Predictive Coding (LPC) cepstral coefficients and auditory nerve firing rates using the Payton model. This auditory model provides for the mechanisms found in the human middle and inner auditory periphery as well as neural transduction. Clustering algorithms were used to generate speaker specific codebooks - one statistically based and the other a neural approach. These algorithms are the Linde-Buzo-Gray (LBG) algorithm and a Kohonen self-organizing feature map (SOFM). The LBG algorithm consistently provided optimal codebook designs with corresponding better classification rates. The resulting Vector Quantized (VQ) distortion based classification indicates the auditory model provides slightly reduced recognition in clean studio quality recordings (LPC 100%, Payton 90%), yet achieves similar performance to the LPC cepstral representation in both degraded environments (both 95%) and in test data recorded over multiple sessions (both over 98%). A variety of normalization techniques, preprocessing procedures and classifier fusion methods were examined on this biologically motivated feature set.

14. SUBJECT TERMS

speaker identification, auditory models, vector quantization, neural networks, user verification

126

17. SECURITY CLASSIFICATION OF REPORT

UNCLASSIFIED

UNCLASSIFIED

UNCLASSIFIED

UL